DSM-Based Design of Cold-Formed Steel Lipped Channel Beams Failing in Distortional Modes under Fire Conditions

Natan Sian das Neves[1], Alexandre Landesmann[1], Dinar Camotim[2]

Abstract

This work reports the findings of a comprehensive numerical investigation on the post-buckling behavior, failure and Direct Strength Method (DSM) design of cold-formed steel (CFS) single-span simply supported lipped channel beams buckling in distortional modes at elevated temperatures (up to 800°C) due to fire conditions. It extends the scope of a previous investigation carried out by Landesmann & Camotim (2016), by analyzing a substantially larger lipped channel beam set, exhibiting various cross-section dimensions and yield stresses, selected to cover wider distortional slenderness ranges. As done before, (i) the beams analyzed display two end support conditions, (ii) the Eurocode 3 (part 1.2) model is adopted to describe the temperature-dependence of the CFS material properties and (iii) the results are obtained by means of ABAQUS shell finite element geometrically and materially non-linear analyses with imperfections (GMNIA). After presenting and discussing the main features of the beam distortional post-buckling behavior, extensive beam failure moment sets are gathered and subsequently used to develop and validate DSM-based design approaches. The methodology followed consists of modifying the most performant available DSM-based design curves, developed by Martins *et al.* (2017) for beams at ambient temperature, which naturally involve the temperature-dependent reduction factors of the CFS material model. A merit assessment procedure shows that the modified DSM-based strength curves efficiently (safely, accurately and reliably) predict the lipped channel beam distortional failure moments, thus constituting an excellent starting point to search for a DSM-based design approach capable of handling arbitrary CFS beams failing in distortional modes at elevated temperatures.

1. Introduction

The versatility and efficiency of cold-formed steel (CFS) structures stem from their exceptional fabrication adaptability and remarkable strength-to-weight ratio. Combined with the increasingly low production and erection costs, these features make CFS structures a highly attractive choice for multi-purpose and cost-effective design solutions. However, due to their inherent slenderness, most open-section thin-walled CFS members are highly prone to various instability phenomena, such as local, distortional or global buckling (as well as to couplings between them). Therefore, the current design specifications incorporate provisions to ensure structural safety against the corresponding failures. In particular, the Direct Strength Method

[1] Programa de Engenharia Civil, COPPE, Universidade Federal do Rio de Janeiro, Brazil. < natan.neves +alandes@coc.ufrj.br>
[2] CERIS, DECivil, Instituto Superior Técnico (IST), Universidade de Lisboa, Portugal. <dcamotim@civil.ist.utl.pt>

(DSM – *e.g.*, Camotim *et al.* 2016, Schafer 2019, and Camotim *et al.* 2023), appearing in the current North-American (AISI 2022), Australian/New Zealand (AS/NZS 2018) and Brazilian (ABNT 2010) specifications for CFS structures, is widely recognized as the most rational approach for the design of such members. Its widespread acceptance stems also from the fact that its application is quite simple and straightforward, requiring only the knowledge of the member yield and buckling stresses. In the context of this investigation, the relevant codified nominal ultimate moment (at room temperature) is the distortional (D) one, termed M_{nD} and given by (AISI 2022)

$$M_{nD} = \begin{cases} M_y + \left(1 - C_{yd}^{-2}\right)\left[M_p - M_y\right] & \lambda_D \leq 0.673 \\ M_y \left[1 - 0.22/\lambda_D\right]/\lambda_D & \lambda_D > 0.673 \end{cases} \quad \text{with} \quad \lambda_D = \sqrt{\frac{M_y}{M_{crD}}} \quad , \quad (1)$$

where, (i) M_{crD} and λ_D are the beam distortional critical buckling moment and slenderness, (ii) M_p and M_y are the yield and plastic moments, and (iii) $C_{yd}=(0.673/\lambda_D)^{0.5}{\leq}3$ is a compression strain factor (parameter involved in the quantification of the cross-section inelastic strength reserve).

As far as lipped channel beam buckling and failing in distortional modes are concerned, the research work available includes experimental investigations (Yu & Schafer 2006, and Wang & Young 2014), numerical simulations (Landesmann & Camotim 2016, Martins *et al.* 2017, and Yu & Schafer 2007) and the development of DSM-based design proposals (Martins *et al.* 2017, Yu & Schafer 2007, Schafer & Peköz 1998, and Schafer 2008). Note that Eq. (1) was calibrated on the basis of the experimental failure moment data obtained by Yu & Schafer (2006), covering only beams with small-to-moderate distortional slenderness values (0.68≤λ_D≤1.53). In order to assess the accuracy of this curve, Martins *et al.* (2017) investigated the behavior of simply supported uniformly bent CFS beams failing in "pure" distortional modes – the beams analyzed consisted of (i) lipped channels under major-axis bending, (ii) hat-sections under major and minor-axis bending) and (iii) zed-sections under skew bending causing uniform flange compression (worst case). These beams exhibited (i) two support conditions, denoted as SCA and SCB (see Figs. 1(a)-(b) – further details are provided in Section 2), (ii) several yield stresses and (iii) various cross-section dimension ratios and lengths. Based on the numerical distortional failure moment data obtained, Martins *et al.* (2017) concluded that the codified DSM distortional design curve is unable to predict adequately the failure moments of many simply supported beams. They showed that Eq. (1) provides excessively unsafe estimates for non-stocky beams, thus confirming and extending the findings reported by Landesmann & Camotim (2016), for lipped channel beams (LCB) under major-axis bending. After investigating the mechanics of D buckling and failure in CFS beams, Martins *et al.* (2017) proposed novel DSM-based design curves, which perform much better than Eq. (1) for simply supported beams. These strength curves, cast in the "Winter-type" format, incorporate three parameters (*a*, *b*, *c*), dependent on the beam cross-section shape bending axis and support conditions (SCA or SCB), and read

$$M_{nD} = \begin{cases} M_y + \left(1 - C_{yd}^{-2}\right)\left[M_p - M_y\right] & \lambda_D \leq 0.673 \\ M_y \left[1 - a/\lambda_D^b\right]/\lambda_D^c & \lambda_D > 0.673 \end{cases} \quad \text{with} \quad \lambda_D = \sqrt{\frac{M_y}{M_{crD}}} \quad . \quad (2)$$

Note that (i) the initial (λ_D≤0.673) branch of Eq.(1) remains unchanged and, for <u>lipped channel beams under major-axis bending</u>, (ii) the parameters *a*, *b* and *c* equal, respectively, 0.25, 1.75 and 1.75 (SCA), or 0.23, 1.55 and 1.45 (SCB).

Landesmann & Camotim (2016) investigated the distortional post-buckling behavior, ultimate strength and DSM design of CFS single-span simply supported (SCA and SCB) lipped channel beams uniformly

bent about the major-axis under elevated temperatures. They gathered failure moment data concerning beams with (i) five cross-section shapes, (ii) several room-temperature yield stresses and (iii) various uniform temperatures (up to 800 °C). To establish preliminary guidelines for the design of lipped channel beams under fire conditions, the numerical distortional failure moment data gathered were used to assess how Eq. (1) (modified to reflect the temperature effects – see Section 5) predicts the simply supported beam failure moments – virtually all beams under elevated temperature had their distortional failure moments overestimated (the few exceptions concerned stocky beams at T=200 °C).

While the DSM-based strength curve set proposed by Martins *et al.* (2017) succeeded in achieving a high-quality failure moment prediction for simply supported CFS beams, its applicability under elevated temperatures remains an open question – recall the substantial alteration of the steel constitutive law, namely its Young's modulus, yield strength and amount of non-linearity. Hence, it is necessary to assess whether the above strength curve set can be adopted (with more or less modifications) in high-temperature scenarios. Furthermore, even if research has been devoted to CFS beams at elevated temperatures (*e.g.*, Kankanamge & Mahendran 2012, Laím *et al.* 2016, Laím & Rodrigues 2018, and Santiago *et al.* 2021), the authors are not aware of any investigation on the DSM-based design of CFS beams against distortional failures at elevated temperatures carried out by other researchers. Thus, this work aims at providing a first contribution towards filling this gap, by presenting and discussing the available results of an ongoing numerical investigation on the post-buckling behavior, ultimate strength and DSM-based design of CFS simply supported LCB uniformly bent about the major-axis and failing in distortional modes at uniform elevated temperatures. The beams analyzed (i) display a wide variety of geometries (cross-section dimensions and lengths) and room-temperature yield stresses (selected to cover wide critical slenderness ranges), and (ii) are subjected to several uniform elevated temperatures, up to 800°C. It should be noted that some results concerning beams at room and elevated temperatures were already reported by Martins *et al.* (2017) (room temperature) and Landesmann & Camotim (2016) (elevated temperatures) – the former are shown here for comparison purposes.

The paper begins with the beam geometry selection (Section 2) – the selected beams exhibit D critical buckling moments significantly lower than their local and global counterparts, both at room and elevated temperatures. Next, in Section 3, the ABAQUS (2014) shell finite element model used to perform the geometrically and materially non-linear analyses with imperfections (GMNIA) is briefly described. Then, Section 4 addresses the influence of the temperature on the beam elastic-plastic post-buckling behavior, failure moment and associated DSM-based estimation – several room-temperature yield stresses are considered, covering wide distortional slenderness ranges. The model prescribed in part 1-2 of Eurocode 3 (EC3:1-2, 2005) is employed to describe the temperature dependence of the CFS material properties. Then, the numerical D failure moment data concerning LCB at room temperature, obtained in this work and reported by Landesmann & Camotim (2016) and Martins *et al.* (2017), are used in Section 5 to reassess the merits of the DSM-based distortional strength curves proposed by Martins *et al.* (2017) for SCA and SCB beams. Finally, the D failure moment data also obtained in this work and reported by Landesmann & Camotim (2016), but for LCB at elevated temperatures, are used in Section 6 to assess the merits of the most performant DSM-based strength curves at room temperature, modified to account for the elevated temperatures – since they are shown not to be adequate for non-slender beams, modifications are proposed for the low and moderate slenderness range. These modifications visibly improve the D failure moment prediction quality, both for the SCA and SCB lipped channel beams.

2. Beam Geometry Selection – Buckling Behavior

As done in previous studies (*e.g.*, Landesmann & Camotim 2016 and Martins *et al.* 2017), the first task of this work consists of selecting the geometries (cross-section dimensions and lengths) of the single-span CFS lipped channel beams to be analyzed. Two end support conditions are considered, denoted here SCA and SCB (Martins *et al.* 2017), both simply supported with respect to major and minor-axis bending, and having the end cross-section torsional rotations prevented – the difference resides in the fact that the end cross-section warping and local displacements and rotations are either free (SCA beams – unrestrained end cross-sections) or fully prevented (SCB beams – rigid plates attached to their end cross-sections) – Figs. 1(a)-(b) depict and show the differences between these two support conditions. The selection procedure involves sequences of buckling analyses, performed by means of the code GBTUL (Bebiano *et al.* 2018) (based on Generalized Beam Theory – GBT) or ABAQUS SFEA and intended to identify beams buckling and failing in "pure" distortional modes – *i.e.*, such that their D (critical) buckling moments are well below their local and global bifurcation moments.
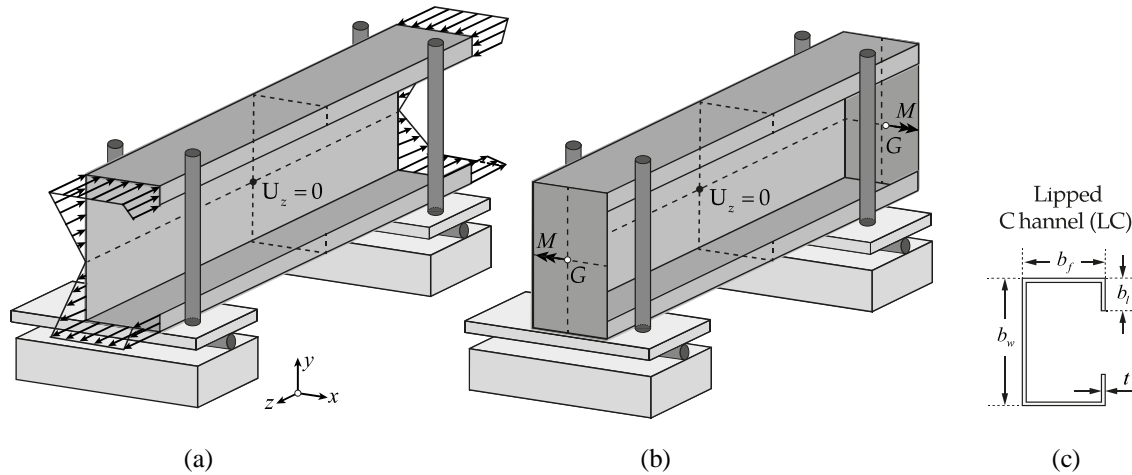
Figure 1. (a) SCA and (b) SCB lipped channel beams end support and loading conditions, and (c) LC geometry and dimensions.

The end product of the lipped channel beam selection procedure are the 30 cross-section dimensions (b_w, b_f, b_l and t – see Fig. 1(c)) given in Table 1 – their web-to-flange width ratios range from 1.25 to 3.0. This table also provides, for each beam cross-section geometry, (i) the length associated with critical distortional buckling (L_D), (ii) the corresponding critical (distortional) buckling moment at room temperature (M_{crD}) and (iii) its ratios with respect to the lowest local (M_{crL}) and global (M_{crG}) buckling moments – all these buckling moments were calculated for E_{20}=210 GPa (steel Young's modulus at room temperature) and v=0.3 (Poisson's ratio, deemed not to vary with the temperature). Note that the first "non-distortional" buckling moment is always local and that M_{crL}/M_{crD} varies between 2.2 and 2.8 (SCA beams), and 1.6 and 3.0 (SCB beams). The first global (lateral-torsional) buckling moment is much higher – M_{crG}/M_{crD} varies from 23 to 106 (SCA beams) and from 23 to 93 (SCB beams).

The $M_{crD.T}$ vs. L curves depicted in Fig. 2(a)-(b) provide the variation of the critical distortional buckling moment at temperature with the length L (logarithmic scale) and temperature T, for SCA and SCB beams with the LC19 cross-section (note that the vertical scales are different in Figs. 2(a) and 2(b)) – (i) four temperatures are considered (20/100°C, 400°C, 600°C and 800°C), and (ii) the EC3-1.2 (2005) constitutive model, presented in Section 3, is adopted. Also shown are the critical (distortional) buckling modes of the SCA beam with L_D=30 cm and SCB beam with L_D=55 cm. It should be pointed out that any given buckling

Table 1: Selected SCA and SCB LC beams failing in "pure" distortional modes: geometries (b_w, b_f, b_l, t, L_D – values in mm), critical distortional buckling moments ($kNcm$) and local-to-distortional and global-to-distortional critical moment ratios.

Beam	Cross-Section Dimensions				SCA				SCB			
	b_w	b_f	b_l	t	L_D	M_{crD}	$\dfrac{M_{crL}}{M_{crD}}$	$\dfrac{M_{crG}}{M_{crD}}$	L_D	M_{crD}	$\dfrac{M_{crL}}{M_{crD}}$	$\dfrac{M_{crG}}{M_{crD}}$
LC1	120	75	10	3	320	1788	2.7	39	500	2580	2	25
LC2	150	120	10	3.5	420	1905	2.8	106	550	2857	3	93
LC3	160	100	10	2.2	460	842	2.2	86	700	1236	1.6	57
LC4	200	100	10	2.5	450	1393	2.5	82	700	2013	1.9	53
LC5	210	70	9	2.5	340	1954	2.2	44	550	2750	2.3	27
LC6	210	110	10	2.5	500	1314	2.5	95	800	1883	1.8	32
LC7	150	95	10	2.5	400	1126	2.3	79	700	1620	1.8	40
LC8	150	100	10	2.5	450	1062	2.4	75	750	1528	1.7	42
LC9	150	75	10	2.5	400	1468	2.4	34	600	2090	1.8	24
LC10	150	80	10	2.5	400	1359	2.5	43	600	1960	1.8	30
LC11	130	80	10	3	350	1803	2.6	42	500	2619	2	32
LC12	130	80	10	3	400	1848	2.5	32	550	2583	2	27
LC13	140	90	10	2.5	350	1145	2.3	81	650	1617	1.8	38
LC14	145	90	10	2.45	450	1115	2.4	52	675	1594	1.7	36
LC15	150	100	10	2.5	450	1062	2.4	75	725	1531	1.8	45
LC16	120	80	10	2.5	350	1101	2.4	71	600	1593	1.7	28
LC17	130	80	10	2.5	400	1193	2.4	41	600	1716	1.8	28
LC18	130	80	10	2.5	500	1331	2.2	23	550	1735	1.7	33
LC19	135	75	10	2.7	300	1602	2.4	52	550	2262	1.9	25
LC20	135	85	10	2.8	350	1493	2.6	58	600	2143	1.9	31
LC21	135	90	10	2.8	450	1453	2.3	41	650	2013	1.9	35
LC22	125	80	10	2.9	300	1639	2.4	58	500	2345	2	33
LC23	125	80	10	2.9	400	1655	2.4	32	550	2309	1.9	28
LC24	160	90	10	2.5	400	1267	2.5	66	700	1824	1.8	34
LC25	165	85	10	2.4	400	1261	2.5	58	675	1821	1.8	32
LC26	250	100	12	2.8	500	2591	2.4	56	850	3713	1.8	31
LC27	275	110	13	3	550	3204	2.4	58	600	5502	2.2	65
LC28	265	105	13	3	550	3253	2.4	49	650	5144	2.4	50
LC29	215	80	10	2.8	400	2477	2.5	42	625	3489	2	27
LC30	225	90	12	2.9	450	2845	2.5	44	775	4079	1.8	23

curve can be obtained through a "vertical translation" of the top one, with a magnitude depending solely on the Young's modulus erosion stemming from the temperature rise. Moreover, the critical distortional moment $M_{crD.T}$ corresponds to the same length (L_D) for all temperature values.

3. Numerical Model

The beam post-buckling equilibrium paths and failure moments were determined through ABAQUS (2014) SFE GMNIAs, employing models already validated and used by the authors in the past (*e.g.*, Landesmann & Camotim 2016 and Martins *et al.* 2017)[3]. The beams were discretized into fine S4 element (ABAQUS nomenclature – 4-node general-purpose SFE with six degrees of freedom per node and full integration) meshes. The analyses (i) were performed by means of an incremental-iterative technique, combining Newton-Raphson's method with an arc-length control strategy, and (ii) simulate the response of beams subjected to constant uniform temperature distributions (*i.e.*, the beams are deemed engulfed in flames, thus sharing the temperature with the surrounding air) and subsequently acted by an increasing uniform major-axis bending moment up to failure – steady-state structural analyses providing failure moments. Note that, in the context of the distortional ultimate strength of CFS columns, it has been shown in the past (*e.g.*, Landesmann & Camotim 2011) that the failure loads provided by steady-state analyses match the more realistic failure temperatures obtained through the "corresponding" transient analyses – axially compressed columns heated up to failure. It is assumed here that the above finding can be extended to beams, *i.e.*, that the failure moments provided by steady-state analyses match the failure temperatures obtained from the transient analyses.
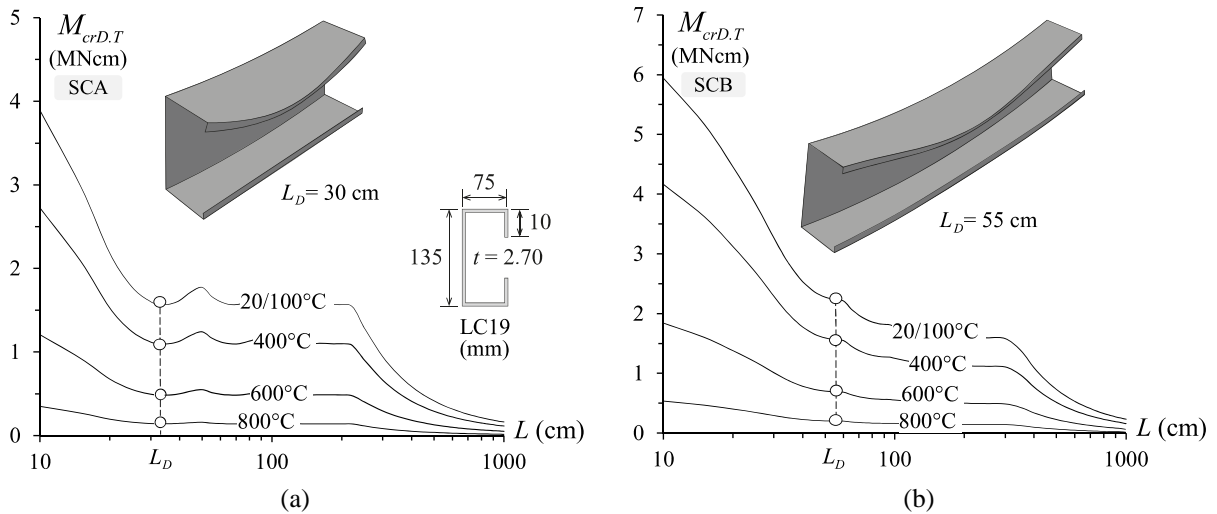
Figure 2. Variation of $M_{crD.T}$ with L and T=20/100, 400, 600 and 800 °C for (a) SCA and (b) SCB LC19 beams, adopting the EC3-1.2 (2005) CFS constitutive model.

As mentioned earlier, the simply supported beams analyzed exhibit two end support conditions, denoted SCA and SCB (see Figs. 1(a)-(b)) – the SCB beams are modelled by attaching rigid plates to their end cross-sections. In order to preclude the occurrence of rigid-body motions, the longitudinal displacement at the mid-span cross-section mid-web point was prevented in all the beams analyzed (see Figs. 1(a)-(b)). The uniform bending moment diagram is applied by means of either (i) sets of concentrated forces acting on the nodes of both end cross-sections (SCA beams – see Fig. 1(a)) or (ii) two concentrated moments acting on the rigid end-plates (SCB beams – see Fig. 1(b)). This loading procedure was previously adopted by the authors in the SFE analysis of CFS beams at ambient (Martins *et al.* 2017) and elevated (Landesmann

---

[3] Since the authors are unaware of any previous investigation (numerical or experimental) on the distortional behavior and strength of CFS beams at elevated temperatures, no specific validation of the SFE model employed in this work could be carried out. However, it should be noted that the authors (Landesmann & Camotim 2016) validated this SFE model in the context of ambient temperature and using numerical results taken from Yu & Schafer (2007), which had been validated against test results reported by Yu & Schafer (2006).

& Camotim 2016) temperatures. The force/moment application is always imposed in small increments, by means of the ABAQUS automatic loading stepping procedure. All the beams analyzed contain critical-mode (distortional) initial geometrical imperfections involving inward compressed flange-lip motions (the most detrimental, in the sense that they lead to lower post-buckling strengths (Landesmann & Camotim 2016 and Martins *et al.* 2017) and having small amplitudes $(0.1t)$[4]. The beam critical buckling mode shapes were obtained through preliminary ABAQUS buckling analyses, performed with the same SFE mesh subsequently employed to carry out the GMNIA – this procedure makes it easy to "transform" the buckling analysis output into a GMNIA input. It is still worth noting that strain-hardening, residual stress and rounded corner strength effects were disregarded in this work, since it has been shown (*e.g.*, Ellobody & Young 2005) that their joint influence on the failure moments is negligible.

3.1 Steel Material Behavior

The multi-linear stress-strain curve available in ABAQUS is adopted to model the steel material behaviors associated with the several yield stresses considered. The CFS constitutive law at elevated temperature adopted in this work is that prescribed in EC3-1.2 (2005), which was previously adopted in the numerical simulations reported by Landesmann & Camotim (2016) and Arrais *et al.* (2021)[5]. Fig. 3(a) makes it possible to assess the temperature dependence of the reduction factors applicable to the CFS Young's modulus ($k_E = E_T/E_{20}$), nominal yield stress ($k_y = \sigma_{y.T}/\sigma_{y.20}$) and proportionality limit stress ($k_p = \sigma_{p.T}/\sigma_{y.20}$), which are tabulated in EC3:1-2. As for Fig. 3(b), it illustrates the qualitative differences between the stress-strain curves prescribed in EC3:1-2 for room and elevated temperatures – plots $\sigma_T/\sigma_{y.20}$ *vs.* ε, where the applied stress at a given temperature (σ_T) is normalized with respect to the room temperature yield stress $\sigma_{y.20}$. Note that the stress-strain curve non-linearity increases significantly with the temperature (for $T=20/100$°C, the constitutive law is bi-linear – elastic-perfectly plastic material). The stress-strain curves prescribed in EC3:1-2 are divided into three regions, associated with distinct strain ranges. It is clear that the stress-strain curve proportionality limit strain ($\varepsilon_{p.T} = \sigma_{p.T}/E_T$) and non-linear shape are considerably influenced by the temperature.

At elevated temperatures, the first part of the well-defined yield plateau exhibited by the $T=20/100$°C curve is replaced by a strain-hardening region that becomes gradually more pronounced as the temperature rises. The stress-strain curve (i) is linear elastic, with slope E_T ($E_{20}=210$ GPa), up to the proportionality limit stress $\sigma_{p.T}$, then (ii) becomes elliptic in the transition between the elastic and plastic ranges, up to the effective yield stress $\sigma_{y.T}$, occurring at $\varepsilon_{y.T}$ ($\sigma_{y.T}$ is taken as the 0.2% proof strength) and accounting for kinematic strain-hardening, and (iii) ends with a perfectly flat yield plateau, up to the limit strain $\varepsilon_{u.T}=0.15$ – in all cases, Prandtl-Reuss's plasticity model (von Mises yield criterion and associated flow rule) is adopted.

---

[4] The authors have been considering these distortional initial geometrical imperfections for quite a long time (about two decades) – for instance, Landesmann & Camotim (2011, 2016, 2019) and Martins *et al.* (2017), all dealing with the distortional behavior of cold-formed steel members (columns or beams). Moreover, in the context of cold-formed steel fixed-ended columns, Landesmann & Camotim (2013) showed that the failure loads obtained with distortional initial geometrical imperfections exhibiting inward flange-lip motions and $0.1t$ amplitudes (like those considered in this work) are accurately predicted by the currently codified DSM design curve.

[5] In the context of a numerical study on the distortional behavior and failure of CFS fixed-ended lipped channel columns at elevated temperatures, Landesmann & Camotim (2015) found that changing the temperature-dependent steel constitutive model adopted does influence significantly the failure load prediction quality provided by an available DSM-based design approach. Thus, this work is based on the temperature-dependent constitutive model currently prescribed by EC3-1.2 (2005) for cold-formed steel. Naturally, the adoption of a different model will entail the need to re-calibrate the proposed DSM-based design approach, after having performed the corresponding numerical parametric study – however, the general concepts and procedures used in this work will remain the same.
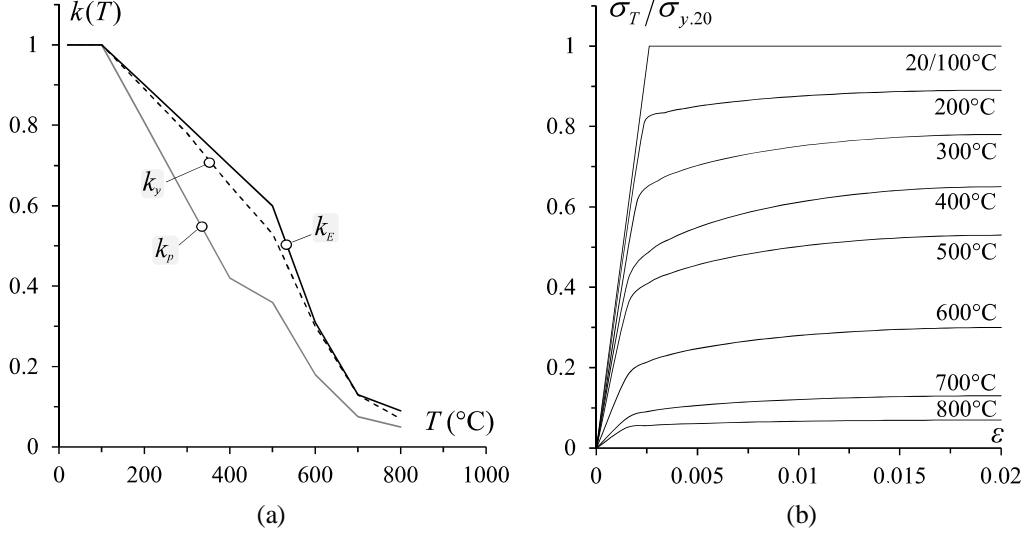
Figure 3. (a) Variation of the reduction factors k_E, k_y, k_p with the temperature for $T \leq 800\,°C$ and (b) CFS stress-strain curves $\sigma_T/\sigma_{y.20}$ vs. ε ($\varepsilon \leq 2\%$) for $T=20/100\text{-}300\text{-}500\text{-}600\text{-}800\,°C$ – as prescribed by the EC3-1.2 (2005) model.

Finally, since the distortional post-buckling analyses carried out may involve large inelastic strains, the nominal (engineering) static stress-strain curve is replaced by the relation between the true stress and the logarithmic plastic strain, given by

$$\sigma_T = \begin{cases} \varepsilon \cdot E_T & \varepsilon \leq \varepsilon_{p.T} \\ \sigma_{p.T} - c + (b/a)\left[a^2 - \left(\varepsilon_{y.T} - \varepsilon\right)^2\right]^{0.5} & \varepsilon_{p.T} < \varepsilon < \varepsilon_{y.T} \\ \sigma_{y.T} & \varepsilon_{y.T} \leq \varepsilon \leq \varepsilon_{u.T} \end{cases} \quad , \quad (3)$$

$$a^2 = \left(\varepsilon_{y.T} - \varepsilon_{p.T}\right)\left(\varepsilon_{y.T} - \varepsilon_{p.T} + c/E_T\right),\ b^2 = c\left(\varepsilon_{y.T} - \varepsilon_{p.T}\right)E_T + c^2,\ c = \frac{\left(\sigma_{y.T} - \sigma_{p.T}\right)^2}{\left(\varepsilon_{y.T} - \varepsilon_{p.T}\right)E_T - 2\left(\sigma_{y.T} - \sigma_{p.T}\right)}$$

where it should be noted that parameters a, b and c have nothing to do with those appearing in Eq. (2).

4. Distortional Response under Elevated Temperatures

4.1 Elastic-Plastic Post-Buckling Behavior

The influence of the (elevated) temperature on the distortional elastic-plastic post-buckling behavior and failure moment of selected CFS lipped channel beams is addressed in this section. The investigation deals with SCA and SCA beams exhibiting the LC19 geometry (see Table 1) and adopts the EC3-based temperature-dependent steel constitutive model described in Section 3.1 – the results presented and discussed constitute a representative sample of the whole set of beams dealt with in this work. Figs. 4(a)-(b) show equilibrium paths M/M_{crD} vs. $|v|/t$, where t is the wall thickness and $|v|$ is the absolute value of the beam maximum vertical displacement, occurring at the mid-height compressed (top) flange-lip corner, of beams with $\lambda_D=1.2$ (yield stress $\sigma_{y.20}$ equal to 600 MPa and 840 MPa, respectively for the SCA and SCB support conditions) under temperatures $T=20/100\text{-}200\text{-}300\text{-}400\text{-}500\text{-}600\text{-}700\text{-}800\,°C$. The white circles identify the failure moments $M_{u.T}$ and the room temperature elastic curves are also shown, for comparison purposes. As for Fig. 5, it displays the deformed configurations and von Mises stress contours, at collapse

8
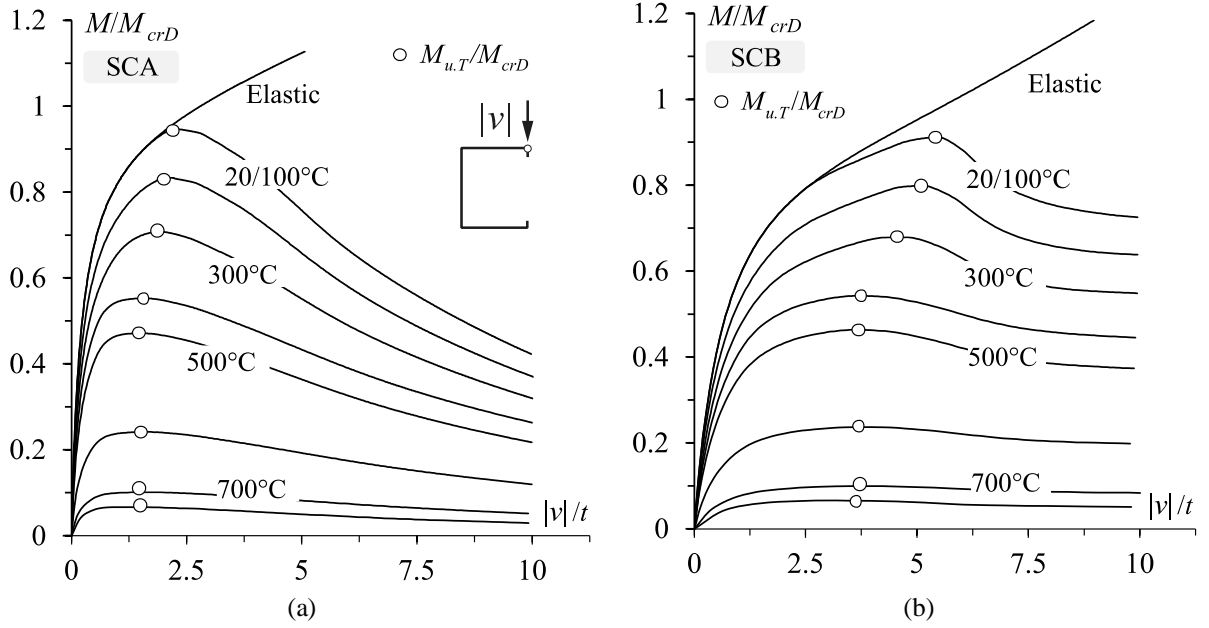
Figure 4. Distortional post-buckling equilibrium paths M/M_{crD} vs. $|v|/t$ of the (a) SCA and (b) SCB LC19 beams with $\lambda_D=1.2$ and under temperatures $T=20/100$-200-300-400-500-600-700-800°C.
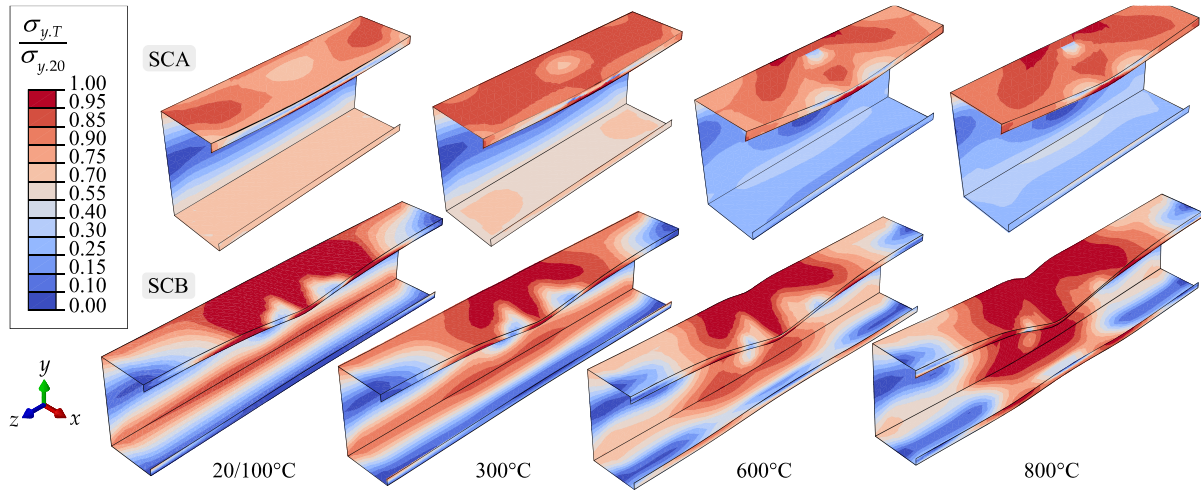
Figure 5. Deformed configurations and von Mises stress contours, at collapse, of the SCA and SCB LC19 beams with $\lambda_D=1.2$ and under temperatures $T=20/100$-300-600-800 °C.

($M=M_{u.T}$), of the beams under temperatures $T=20/100$-300-600-800°C. The observation of these post-buckling results prompts the following remarks:

(i) As expected, and regardless of the end support conditions considered (SCA or SCB), the beam normalized strength and failure moment decrease as the temperature T rises. The drop is mostly perceptible between 500 and 600°C.

(ii) The equilibrium paths of the beams under temperatures $T{\geq}600$°C fall clearly below the remaining ones, thus reflecting the sudden increase in the rate of the steel material behavior erosion occurring between 500 and 600 °C. This erosion is felt mostly via the proportionality limit strain and the smoothness of the elliptic transition between the elastic and plastic ranges (see Figs. 3(a)-(b)). For $T{>}600$°C, the steel stress-strain curve exhibits again a well-defined yield plateau.

9

(iii) Concerning the beam failure modes (deformed configurations at collapse), it is worth noting that, since the thermal action effects are negligible (uniform temperature and free-to-deform beams), they do not vary with the temperature – indeed, they are virtually identical for all the beams analyzed (Fig. 5 makes it possible to compare the SCA and SCB beam failure modes). This is also true for the corresponding von Mises stress contours – for both support conditions, the beams always collapse after the full yielding of the top (compressed) web-flange corners and lip free edge at the mid-span region, leading to the formation of a "distortional plastic hinge" – similar observations were reported by Landesmann & Camotim (2016) and Martins *et al.* (2017). In quantitative terms, the stresses obviously decrease as the temperature rises and continuously erodes the steel material behavior.

(iv) No clear trend was detected concerning the influence of the temperature, geometry and/or steel grade on the amount of elastic-plastic strength reserve and ductility prior to failure. Moreover, all the beams analyzed exhibit quite similar post-collapse behaviors (equilibrium path descending branches), regardless of the temperature, even if the post-failure strength displayed by the SCB beams is a bit higher (slightly lower negative slopes).

4.2 Failure Moment Data

This section reports the output of a parametric study carried out to gather the failure moment data that will subsequently be used to develop and assess the merits of DSM-based design approaches intended to handle lipped channel beams buckling and failing in distortional modes at elevated temperatures. This parametric study involves a total of 2400 beams, corresponding to all possible combinations of (i) the 30 geometries (cross-section dimensions and lengths) given in Table 1, (ii) the 2 end support conditions dealt with (SCA and SCB), (iii) 8 uniform temperatures (T=20/100-200-300-400-500-600-700-800 °C) and (iv) 5 yield stresses at room temperature, which enable covering wide distortional slenderness ranges (between 0.3 and 3.75). The whole set of numerical results obtained is given, in tabular form, in Annexes A to C. The tables also include several values related to the DSM-based prediction of the numerical failure moments, which will be addressed in Sections 5 and 6. Figure 6 shows plots $M_{u.T}/M_{y.T}$ *vs.* $\lambda_{D.T}$ for the various temperatures considered in this work, each of them (i) concerning both SCA and SCB beams, and (ii) including, for comparison purposes, the elastic buckling curves $\lambda_{D.T}^{-2} - M_{u.T}$, $M_{y.T}$ and $\lambda_{D.T}=(M_{y.T}/M_{crD.T})^{0.5}$ are the beam distortional failure moments, yield moments and slenderness values, respectively. Besides the failure moment data obtained in this work, Fig. 6 includes also 630 and 1020 numerical distortional failure moments reported by Martins *et al.* (2017) (room temperature) and by Landesmann & Camotim (2016) (elevated temperatures), respectively. The joint observation of these plots leads to the following comments:

(i) Regardless of the temperature, the $M_{u.T}/M_{y.T}$ *vs.* $\lambda_{D.T}$ "clouds" follow the trend of "Winter-type" strength curves, even if there exists some "vertical dispersion" along the whole slenderness ranges considered, thus reflecting the influence of the beam end support conditions and/or cross-section geometry on the beam distortional post-critical strength reserve – this feature was also observed and discussed by Martins *et al.* (2017), in the context of beams at room temperature.

(ii) It is quite interesting to notice that, for $\lambda_{D.T} \geq 1.5$ and regardless of the temperature, the elastic buckling strength curves provide lower bounds for all the $M_{u.T}/M_{y.T}$ values – moreover, these lower bounds are quite accurate estimates for the $M_{u.T}/M_{y.T}$ values of the SCA beams.

(iii) All the $M_{u.T}/M_{y.T}$ values concerning stocky beams at temperatures T>200°C are well below 1.0, in clear contrast with what happens for $T \leq 200$°C – the differences tend to increase with the temperature and the elastic buckling curves provide a useful reference to quantify these differences. In the moderate and high slenderness ranges ($\lambda_{D.T}$>0.673), this very striking distinction between the $M_{u.T}/M_{y.T}$ values concerning the beams at T>200°C and $T \leq 200$°C ceases to occur.
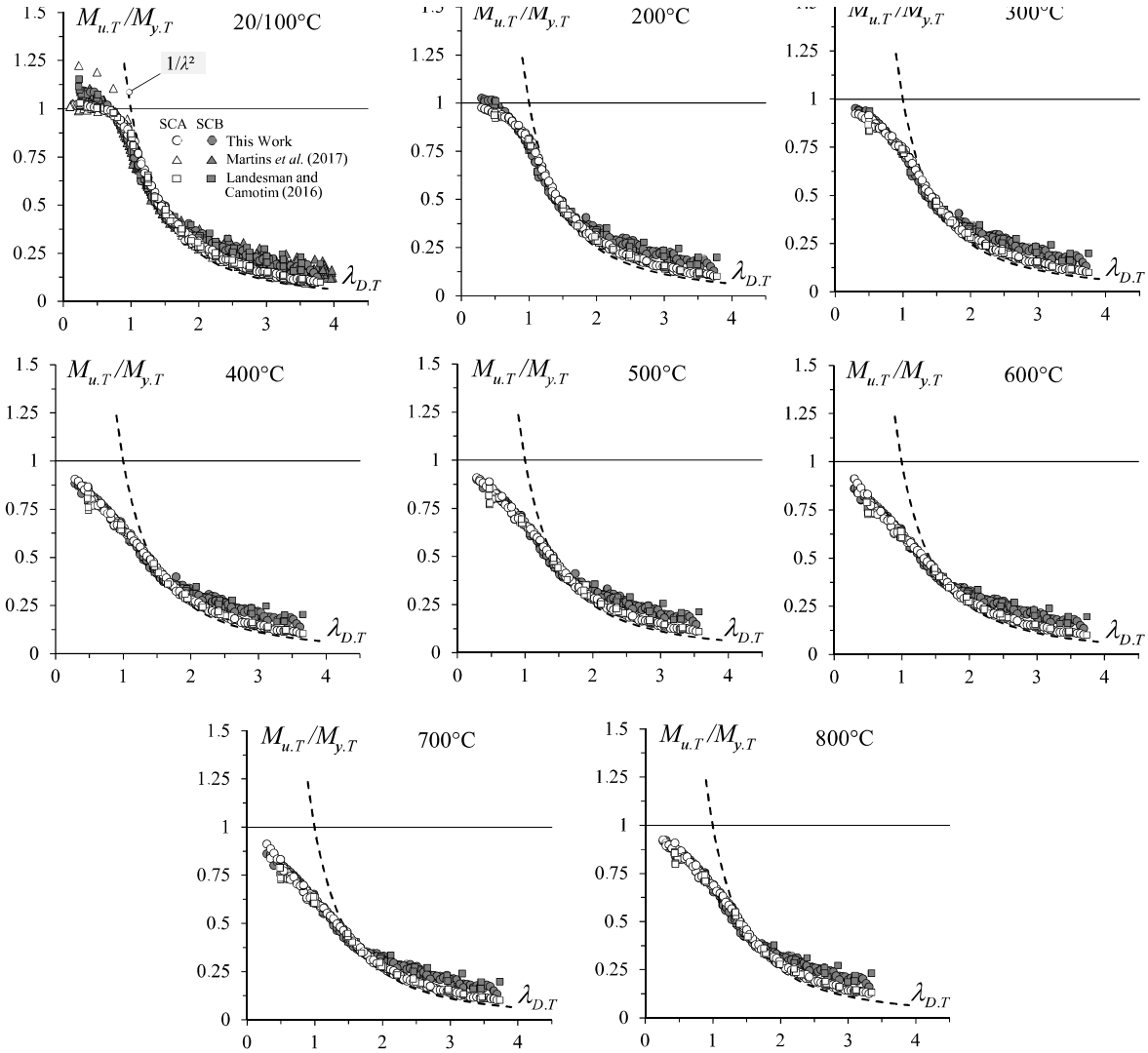
Figure 6. $M_{uT}/M_{y.T}$ *vs.* $\lambda_{D.T}$ values concerning all the SCA and SCB LC beams under room and elevated temperatures analyzed in this work, and the elastic buckling curves (*T*=20/100-200-300-400-500-600-700-800 ℃).

(iv) Concerning the stocky beams at *T*>200℃, note that their $M_{u.T}/M_{y.T}$ values are aligned along clearly descending curve branches (no "almost plateau" exists, like for *T*≤200℃) that transition fairly smoothly to those associated with the beams exhibiting moderate and high slenderness values (invariably located slightly below the elastic buckling curve). Moreover, note that these "stocky beam $M_{u.T}/M_{y.T}$ curves" originate at points ($M_{p.T}$) not ordered according to the temperature value – this stems from the fact that the k_p/k_y values prescribed for CFS in EC3-1.2 are not "logically ordered", since they are equal to 1-0.907-0.786-0.646-<u>0.679</u>-0.6-0.577-<u>0.714</u> for *T*=20/100-200-300-400-500-600-700-800℃ (the "out of order" values are underlined).

(v) Although the results displayed in Fig. 6 provide promising indications on the possibility of developing an efficient (safe, accurate and reliable) DSM-based design approach to predict distortional failure moments of simply supported CFS lipped channel beams under elevated temperatures, they also clearly show that the failure moment predictions for beams at *T*>200℃ and *T*≤200℃ must be handled separately in the low-to-moderate slenderness range (at least when the EC3-based CFS constitutive model is adopted). The quantification of these qualitative assertions is addressed in the next section.

11

5. DSM Design at Room Temperature

The DSM-based prediction of D failure moments of CFS simply supported lipped channel beams at room temperature (20/100ºC), exhibiting the two support conditions considered (SCA and SCB), is addressed in this section. In particular, it is intended to reassess the prediction quality provided by Eq. (2), proposed earlier by Martins *et al.* (2017), for the beam D failure moments obtained in the previous section and reported by Landesmann & Camotim (2016) or Martins *et al.* (2017). Figures 7(a)-(b), dealing with the LCB analyzed in this work and reported by Landesmann & Camotim (2016) or Martins *et al.* (2017), show the M_u/M_{nD} *vs.* λ_D plots, thus enabling a quick and visual quantitative assessment of the quality (accuracy and safety) of the failure moment predictions provided by the DSM-based strength curves proposed by Martins *et al.* (2017). The M_u/M_{nD} statistical indicators (averages, standard deviations and maximum-minimum values) are given in Table 2, which also includes the numbers of failure moment predictions such that $M_u/M_{nD}<0.95$, deemed "clearly unsafe" and denoted "*Uns*" in the above table. The observation of the results presented in these figures and table prompts the following comments:

(i) Virtually all the DSM-based beam failure moment predictions of the SCA LCB at room temperature are safe and accurate. Their M_u/M_{nD} averages, standard deviations and maximum/minimum values for the lipped channel beams in this work, reported by Landesmann & Camotim (2016) and Martins *et al.* (2017), and all together read, respectively (see Table 2), 1.05-0.05-1.23-0.93, 1.03-0.04-1.16-0.94, 1.05-0.05-1.17-0.95 and 1.05-0.05-1.23-0.93. Thus, it is confirmed that Eq. (2) predicts quite well the failure moments of the SCA LCB at room temperature.

(ii) Although the M_u/M_{nD} statistical indicators of the SCB LCB at room temperature, which read (see Table 2) 1.02-0.06-1.52-0.85, 1.06-0.08-1.47-0.90, 1.03-0.05-1.26-0.90 and 1.02-0.05-1.52-0.85 (respectively for the beams analyzed in this work, reported by Landesmann & Camotim (2016) and Martins *et al.* (2017), and all together), are strikingly similar to their SCA beam counterparts, the failure moment prediction quality clearly differs for the SCA and SCB beams, which is due to their distinct post-critical strength reserves, as discussed by Landesmann & Camotim (2016). Indeed, the DSM-based beam failure moment predictions of the SCB LCB at room temperature are only generally safe for $\lambda_D \leq 1.0$ and $\lambda_D > 2.5$ – for $1.0 < \lambda_D \leq 2.5$, the vast majority of failure moments (120 out of 314) are overestimated, even if often by fairly small amounts (never exceeding 15%). In addition, a number of quite considerable failure moment underestimations occur in the high slenderness range, particularly for the LCB analyzed by Landesmann & Camotim (2016) and Martins *et al.* (2017) – such underestimations may reach about 50%.
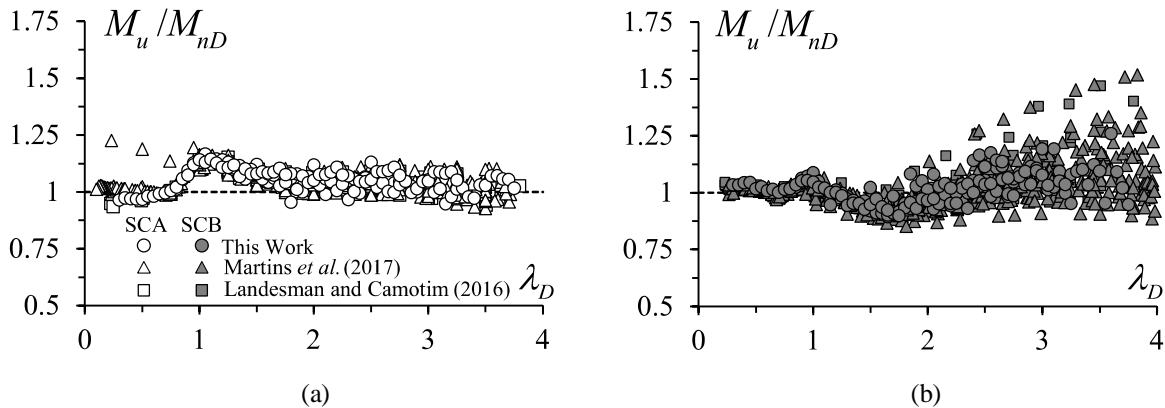
Figure 7. M_u/M_{nD} *vs.* λ_D plots concerning the (a) SCA and (b) SCB lipped channel beams at room temperature analyzed in this work and reported by Landesmann & Camotim (2016) and Martins *et al.* (2017).

Table 2: M_u/M_{nD} statistical indicators concerning the SCA and SCB lipped channel beams at room temperature analyzed in this work, reported by Landesmann & Camotim (2016) and Martins *et al.* (2017), and all together.

		Martins *et al.* (2017)			Landesmann & Camotim (2016)			This Work			All Beams		
		$\lambda_D \leq 1$	$1<\lambda_D<2.5$	$\lambda_D \geq 2.5$	$\lambda_D \leq 1$	$1<\lambda_D<2.5$	$\lambda_D \geq 2.5$	$\lambda_D \leq 1$	$1<\lambda_D<2.5$	$\lambda_D \geq 2.5$	$\lambda_D \leq 1$	$1<\lambda_D<2.5$	$\lambda_D \geq 2.5$
SCA	*n*	90	168	152	16	32	22	20	82	48	126	282	222
	Avr	1.06	1.07	1.02	1.03	1.07	1.04	0.99	1.06	1.03	1.04	1.07	1.03
	SD	0.06	0.04	0.04	0.06	0.04	0.04	0.04	0.05	0.04	0.06	0.04	0.04
	Max	1.23	1.16	1.12	1.14	1.17	1.13	1.14	1.16	1.09	1.23	1.17	1.13
	Min	0.98	0.99	0.93	0.97	0.95	0.95	0.94	0.99	0.94	0.94	0.95	0.93
	Uns	0	0	3	0	0	0	2	0	1	2	0	5
SCB	*n*	104	204	202	17	28	25	20	82	48	141	314	275
	Avr	1.01	0.97	1.08	1.04	0.98	1.07	1.03	1.00	1.15	1.02	0.97	1.08
	SD	0.02	0.06	0.11	0.02	0.05	0.06	0.02	0.08	0.15	0.02	0.06	0.11
	Max	1.07	1.27	1.52	1.09	1.17	1.26	1.08	1.26	1.47	1.09	1.27	1.52
	Min	0.97	0.85	0.89	1.00	0.90	0.95	1.00	0.90	0.96	0.97	0.85	0.89
	Uns	0	85	13	0	27	0	0	8	0	0	120	14

(iii) In view of the content of the previous item, it is concluded that the performance of Eq. (2), in predicting the failure moments of LCB at room temperature, can be improved. Thus, an alternative (slightly modified) DSM-based strength curve set is proposed, in the next section, for SCB beams at room temperature − the modification merely consists of small alterations in parameters *a*, *b* and *c*.

5.1 Modification of the available DSM-based design curves at room temperature (SCB beams)

In order to improve the failure moment prediction quality concerning the SCB LCB at room temperature, namely by reducing the number and amounts of the failure moment overestimations (mostly for beams such that $1.0<\lambda_D \leq 2.5$ – see Fig. 7(b)), the DSM-based design curve developed by Martins *et al.* (2017) (see Eq. (2)) is slightly modified. The format of Eq. (2) is retained and, as mentioned above, the modification merely consists of tiny alterations in parameters *a*, *b* and *c*, which change from *a*=0.23, *b*=1.55 and *c*=1.45 to *a*=0.25, *b*=1.51 and *c*=1.52. Figures 8(a)-(b) make it possible to compare the plots M_u/M_{nD} *vs.* λ_D and $M_u/M_{nD.mod}$ *vs.* λ_D ($M_{nD.mod}$ are the failure moment estimates obtained with the modified parameters) and, therefore, qualitatively assess the failure moment prediction quality improvement achieved with the modification. The $M_u/M_{nD.mod}$ statistical indicators are given in Table 3 and the comparison with their M_u/M_{nD} counterparts (see the bottom part of Table 2) enables a quantitative assessment of the above failure moment prediction quality improvement. Although the M_u/M_{nD} *vs.* λ_D and $M_u/M_{nD.mod}$ *vs.* λ_D "clouds" do not differ substantially, the latter exhibits much less failure moment overestimations exceeding 5% (31 *vs.* 133, *i.e.*, 4% *vs.* 18% of the total number of beams analyzed in this work and reported by Landesmann & Camotim (2016) and Martins *et al.* (2017) – the drop is particularly visible in the slenderness range $1.0<\lambda_D \leq 2.5$ (31 *vs.* 120, *i.e.*, 10% *vs.* 38%), as reflected in the mean value increase from 0.97 to 1.02. Naturally, on the downside, the failure moment underestimations increase for beams with $\lambda_D>2.5$ (the mean value increases from 1.08 to 1.18, and the maximum underestimation grows from 52% to 67%) – however, the major contribution to this underestimation increase comes from the most slender beams, less common in practice. The overall statistical indicators (for the whole set of SCB LCB assembled) change from 1.02-0.09-1.52-0.85 to 1.08-0.12-1.67-0.90 – recall that, for all the SCA LCB gathered, these indicators read 1.05-0.05-1.23-0.93. Finally, it should still be note that the M_u/M_{nD} and $M_u/M_{nD.mod}$ values concerning all the SCB LCB analyzed in this work and reported by Landesmann & Camotim (2016) and Martins *et al.* (2017) are provided, in tabular form, in Annex A.
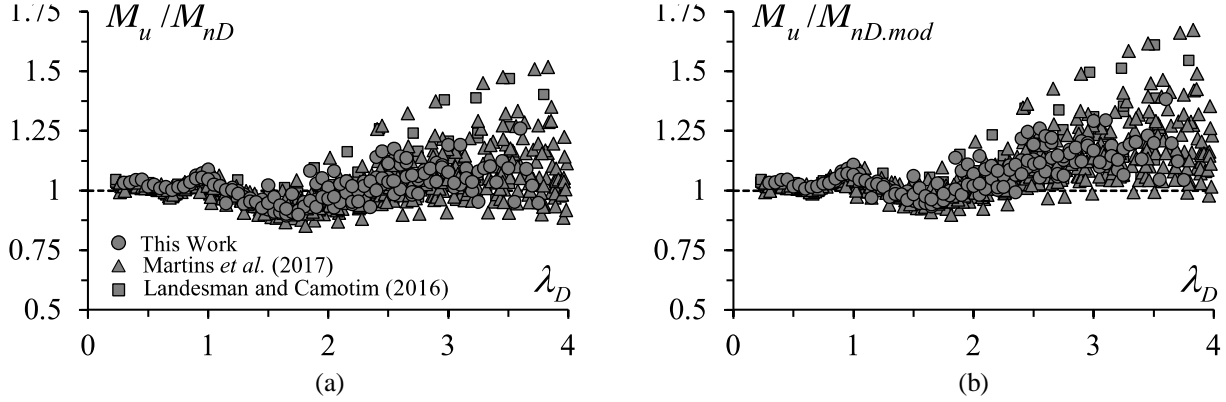
Figure 8. (a) M_u/M_{nD} vs. λ_D and (b) $M_u/M_{nD.mod}$ vs. λ_D plots concerning the SCB LCB at room temperature analyzed in this work and reported by Landesmann & Camotim (2016) and Martins *et al.* (2017).

Table 3: $M_u/M_{nD.mod}$ statistical indicators for the SCB lipped channel beams at room temperature analyzed in this work, reported by Landesmann & Camotim (2016) and Martins *et al.* (2017), and all together.

<table>
<tr><td rowspan="2" colspan="2"></td><td colspan="3">Martins <i>et al.</i> (2017)</td><td colspan="3">Landesmann & Camotim (2016)</td><td colspan="3">This Work</td><td colspan="3">All Beams</td></tr>
<tr><td>$\lambda_D \le 1$</td><td>$1 < \lambda_D < 2.5$</td><td>$\lambda_D \ge 2.5$</td><td>$\lambda_D \le 1$</td><td>$1 < \lambda_D < 2.5$</td><td>$\lambda_D \ge 2.5$</td><td>$\lambda_D \le 1$</td><td>$1 < \lambda_D < 2.5$</td><td>$\lambda_D \ge 2.5$</td><td>$\lambda_D \le 1$</td><td>$1 < \lambda_D < 2.5$</td><td>$\lambda_D \ge 2.5$</td></tr>
<tr><td rowspan="6"><i>SCB (modified)</i></td><td>n</td><td>104</td><td>204</td><td>202</td><td>17</td><td>28</td><td>25</td><td>20</td><td>82</td><td>48</td><td>141</td><td>314</td><td>275</td></tr>
<tr><td>Avr</td><td>1.03</td><td>1.02</td><td>1.17</td><td>1.03</td><td>1.05</td><td>1.24</td><td>1.05</td><td>1.03</td><td>1.16</td><td>1.03</td><td>1.02</td><td>1.18</td></tr>
<tr><td>SD</td><td>0.02</td><td>0.07</td><td>0.13</td><td>0.02</td><td>0.09</td><td>0.17</td><td>0.03</td><td>0.06</td><td>0.07</td><td>0.02</td><td>0.07</td><td>0.13</td></tr>
<tr><td>Max</td><td>1.09</td><td>1.36</td><td>1.67</td><td>1.11</td><td>1.35</td><td>1.61</td><td>1.11</td><td>1.25</td><td>1.38</td><td>1.11</td><td>1.36</td><td>1.67</td></tr>
<tr><td>Min</td><td>0.99</td><td>0.90</td><td>0.97</td><td>1.01</td><td>0.94</td><td>1.03</td><td>1.01</td><td>0.93</td><td>1.04</td><td>0.99</td><td>0.90</td><td>0.97</td></tr>
<tr><td>Uns</td><td>0</td><td>25</td><td>0</td><td>0</td><td>2</td><td>0</td><td>0</td><td>4</td><td>0</td><td>0</td><td>31</td><td>0</td></tr>
</table>

6. DSM Design at Elevated Temperatures

The DSM-based prediction of the distortional failure moments gathered in Section 4.2, concerning CFS simply supported lipped channel beams with the two support conditions considered (SCA and SCB) at elevated temperatures, is addressed in this section. The first step consists of assessing the adequacy of the most performant DSM-based design approaches available to handle beam distortional failures at room temperature, namely Eq. (2) with the values of parameters *a*, *b* and *c* (i) proposed by Martins *et al.* (2017) (SCA beams) and (ii) proposed in Section 5.1 (SCB beams). Naturally, these strength curves must be appropriately adapted to include the temperature effects associated with the EC3-1.2 (2005) material model, via the distortional buckling ($M_{crD.T}$), yield ($M_{y.T}$) and plastic ($M_{P.T}$) moments, which implies that λ_D and C_{yd} will also vary with *T* (they become $\lambda_{D.T}$ and $C_{yd.T}$). It should be noted that this approach was already explored by other authors (*e.g.*, Bandula Heva & Mahendran (2012) and Bicelli *et al.* (2021), for columns buckling and failing in flexural-torsional modes, and Landesmann *et al.* (2019), for columns buckling and failing in distortional modes). These studies involved solely the then most performant column DSM global and distortional design curves available (either codified or not). Therefore, the nominal estimates of the beam distortional failure moments at elevated temperatures are provided by

$$M_{nD.T} = \begin{cases} M_{y.T} + \left(1 - C_{yd.T}^{-2}\right)\left[M_{P.T} - M_{y.T}\right] & \lambda_{D.T} \le 0.673 \\ M_{y.T}\left[1 - a/\lambda_{D.T}^{b}\right]/\lambda_{D.T}^{c} & \lambda_{D.T} > 0.673 \end{cases} \quad \text{with} \quad \lambda_{D.T} = \sqrt{\frac{M_{y.T}}{M_{crD.T}}} \quad , \quad (4)$$

14

where it should be noted that, with respect to Eq. (2), (i) the compression strain factor C_{yd} (quantifying the cross-section inelastic strength reserve) becomes temperature-dependent ($C_{yd.T}=(0.673/\lambda_{D.T})^{0.5}\leq3$) and (ii) the values of parameters a, b and c, either proposed by Martins *et al.* (2017) (SCA beams) or determined in Section 5.1 (SCB beams), are deemed not to vary with the temperature.

Figures 9 and 10, concerning the lipped channel beams analyzed in this work and reported by Landesmann & Camotim (2016), respectively, show the $M_{u.T}/M_{nD.T}$ *vs.* $\lambda_{D.T}$ plots, thus enabling a quick and visual qualitative assessment of the quality (accuracy and safety) of the failure moment predictions provided by the DSM-based strength curves given by Eq. (4). The $M_{u.T}/M_{nD.T}$ statistical indicators (averages, standard deviations and maximum/minimum values) are given in Tables 4 and 5, respectively for SCA and SCB beams at elevated temperatures (recall that, for the SCA and SCB beams at room temperature – 20/100°C –, those indicators were already given in Tables 2 and 3) – as before, the failure moment predictions such that $M_{u.T}/M_{nD.T}<0.95$ are deemed "clearly unsafe" and denoted "*Uns*". Moreover, the tables appearing in Annexes B and C include the failure moment ratios $M_{u.T}/M_{y.T}$ and $M_{u.T}/M_{nD.T}$ for all the SCA and SCB beams analyzed in this work and reported by Landesmann & Camotim (2016). The observation of the results presented in these figures and tables prompts the following comments:

(i) As for the beams under room temperature, the performance of Eq. (4) is again clearly different for the SCA and SCB lipped channel beams at elevated temperatures ($T\geq200$°C), as can be attested   by the observation of Figs. 9 and 10, and Tables 4 and 5. It is still worth pointing out the similarity between the patterns and statistical indicators of the failure moment predictions provided by Eq. (4) for the SCA and SCB beams analyzed in this work and reported by Landesmann and Camotim (2016) – thus, the comments included in the next items apply equally to the two lipped channel beam sets.
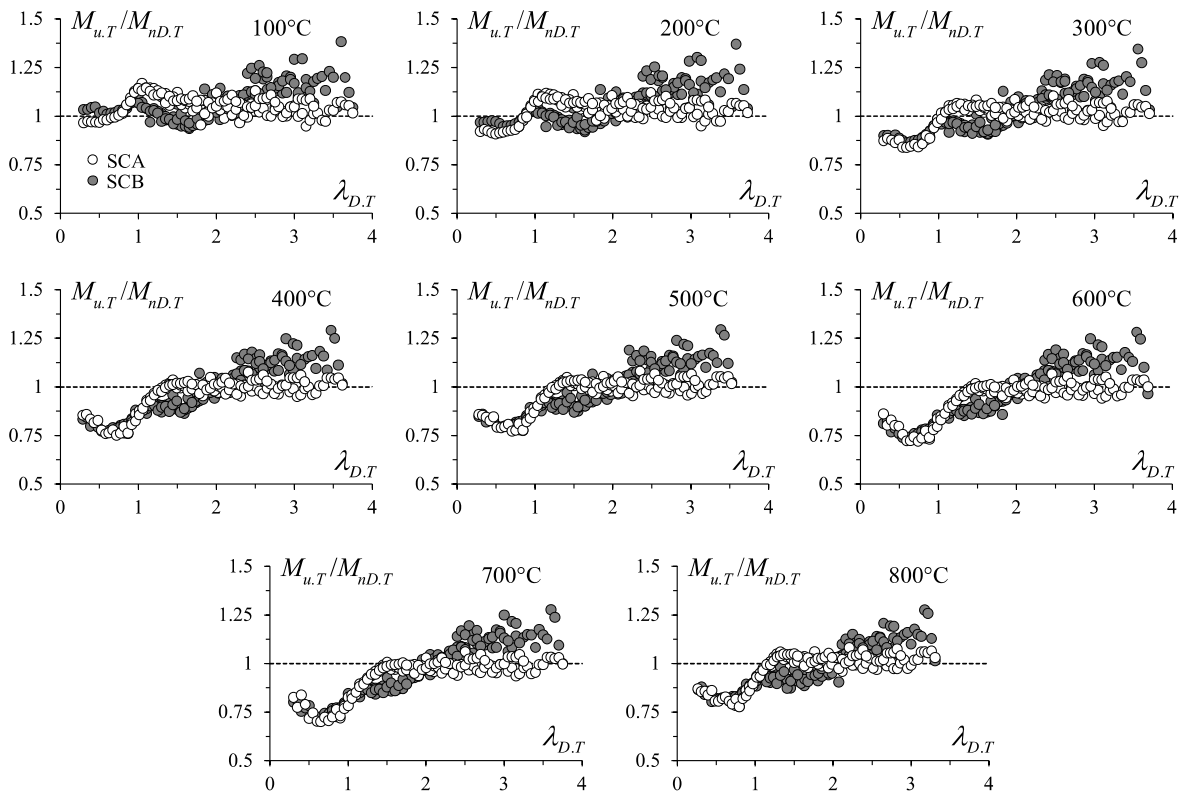
Figure 9. $M_{u.T}/M_{nD.T}$ *vs.* $\lambda_{D.T}$ plots for the SCA and SCB LCB analyzed in this work ($T=20/100$°C to $T=800$°C).

15
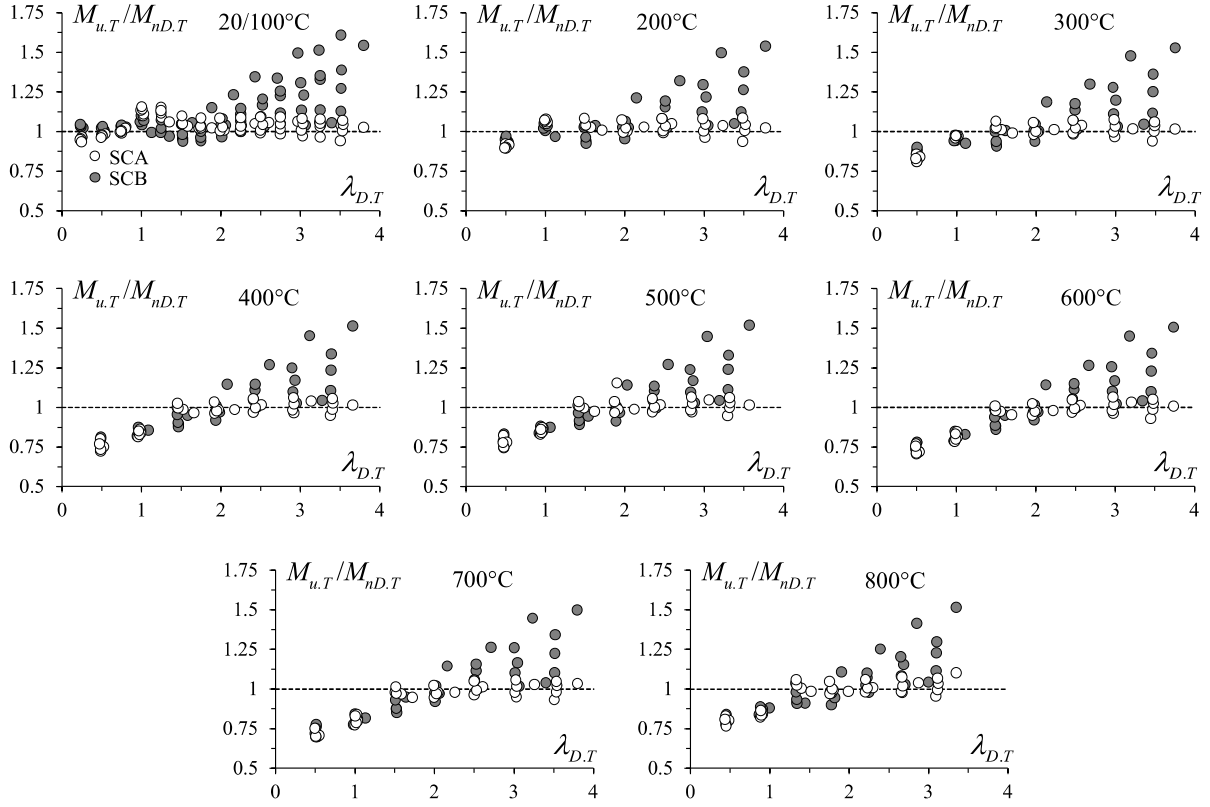
**Figure 10.** $M_{u.T}/M_{nD.T}$ vs. $\lambda_{D.T}$ plots for the SCA and SCB LCB reported by Landesmann and Camotim (2016) (T=20/100 °C to T=800 °C).

Table 4: $M_{u.T}/M_{nD.T}$ statistical indicators concerning the SCA lipped channel beams analyzed in this work, reported by Landesmann and Camotim (2016) and all together, at $200 \leq T \leq 800$°C.

T (°C)	$\lambda_{D.T}$	Landesmann & Camotim (2016)						This Work						All Beams					
		n	Avr	SD	Max	Min	Uns	n	Avr	SD	Max	Min	Uns	n	Avr	SD	Max	Min	Uns
200	≤1.0	7	0.95	0.07	1.07	0.89	5	20	0.97	0.06	1.08	0.91	12	27	0.96	0.06	1.08	0.89	17
	>1.0	28	1.03	0.04	1.09	0.94	1	130	1.05	0.03	1.12	0.95	0	158	1.05	0.04	1.12	0.94	1
300	≤1.0	8	0.88	0.07	0.97	0.81	5	20	0.89	0.04	0.99	0.84	18	28	0.89	0.04	0.99	0.81	23
	>1.0	27	1.01	0.03	1.08	0.94	1	130	1.03	0.03	1.10	0.95	0	157	1.03	0.03	1.10	0.94	1
400	≤1.5	13	0.85	0.10	1.03	0.72	10	48	0.90	0.10	1.04	0.75	28	61	0.89	0.10	1.04	0.72	38
	>1.5	22	1.00	0.03	1.06	0.95	0	102	1.00	0.03	1.08	0.95	0	124	1.00	0.03	1.08	0.95	0
500	≤1.5	14	0.87	0.10	1.04	0.75	10	48	0.91	0.09	1.05	0.77	27	62	0.90	0.09	1.05	0.75	37
	>1.5	21	1.01	0.05	1.15	0.95	1	102	1.01	0.03	1.08	0.96	0	123	1.01	0.03	1.15	0.95	1
600	≤1.5	13	0.82	0.10	1.01	0.71	10	45	0.87	0.10	1.02	0.72	31	58	0.86	0.10	1.02	0.71	41
	>1.5	22	1.00	0.03	1.06	0.93	1	105	0.99	0.03	1.07	0.94	3	127	0.99	0.03	1.07	0.93	4
700	≤1.5	10	0.77	0.05	0.84	0.70	10	45	0.85	0.10	1.01	0.70	34	55	0.84	0.10	1.01	0.70	44
	>1.5	25	0.99	0.03	1.06	0.93	3	105	0.99	0.03	1.06	0.94	7	130	0.99	0.03	1.06	0.93	10
800	≤1.5	14	0.88	0.10	1.06	0.77	10	57	0.94	0.10	1.06	0.78	27	71	0.93	0.10	1.06	0.77	37
	>1.5	21	1.01	0.04	1.10	0.96	0	93	1.02	0.03	1.08	0.96	0	114	1.02	0.03	1.10	0.96	0

Table 5: $M_{u.T}/M_{nD.T}$ statistical indicators concerning the SCB LCB analyzed in this work, reported by Landesmann and Camotim (2016) and all together, at $200 \leq T \leq 800\,°C$.

T (°C)	$\lambda_{D.T}$	Landesmann & Camotim (2016)						This Work						All Beams					
		n	Avr	SD	Max	Min	Uns	n	Avr	SD	Max	Min	Uns	n	Avr	SD	Max	Min	Uns
200	≤2.5	21	1.00	0.07	1.21	0.93	4	105	1.01	0.06	1.23	0.92	13	126	1.01	0.06	1.23	0.92	17
	>2.5	14	1.23	0.16	1.54	1.02	0	45	1.16	0.07	1.37	1.04	0	59	1.17	0.08	1.54	1.02	0
300	≤2.5	23	0.98	0.09	1.19	0.84	12	105	0.98	0.08	1.21	0.86	41	128	0.98	0.08	1.21	0.84	53
	>2.5	12	1.23	0.16	1.53	1.01	0	45	1.14	0.07	1.34	1.03	0	57	1.16	0.07	1.53	1.01	0
400	≤2.5	24	0.92	0.11	1.15	0.75	14	108	0.94	0.10	1.18	0.77	65	132	0.93	0.10	1.18	0.75	79
	>2.5	11	1.23	0.15	1.51	1.03	0	42	1.12	0.06	1.29	1.01	0	53	1.15	0.06	1.51	1.01	0
500	≤2.5	24	0.93	0.10	1.14	0.77	15	114	0.95	0.09	1.19	0.79	66	138	0.95	0.09	1.19	0.77	81
	>2.5	11	1.23	0.15	1.52	1.03	0	36	1.13	0.07	1.29	1.01	0	47	1.15	0.07	1.52	1.01	0
600	≤2.5	23	0.90	0.13	1.15	0.71	15	105	0.92	0.10	1.17	0.74	68	128	0.91	0.10	1.17	0.71	83
	>2.5	12	1.21	0.16	1.51	1.00	0	45	1.12	0.07	1.28	0.97	0	57	1.14	0.07	1.51	0.97	0
700	≤2.5	20	0.86	0.11	1.14	0.70	15	105	0.91	0.10	1.17	0.72	67	125	0.90	0.11	1.17	0.70	82
	>2.5	15	1.19	0.15	1.50	1.00	0	45	1.12	0.07	1.28	0.99	0	60	1.14	0.07	1.50	0.99	0
800	≤2.5	25	0.94	0.11	1.25	0.79	16	122	0.95	0.08	1.15	0.80	74	147	0.95	0.08	1.25	0.79	90
	>2.5	10	1.21	0.15	1.52	1.03	0	28	1.13	0.06	1.27	1.01	0	38	1.15	0.06	1.52	1.01	0

(ii) Regarding the SCA LCB, a distinction must be made between the beams at $T \leq 300\,°C$ and $T \geq 400\,°C$. For the former, the failure moment predictions provided by Eq. (4) are (ii$_1$) safe and accurate for $\lambda_{D.T} > 1.0$ (only a few slightly unsafe predictions and all underestimations below 9%) and (ii$_2$) consistently unsafe for $\lambda_{D.T} \leq 1$, even if the overestimations never exceed 19% — they become more pronounced for $T = 300\,°C$. For the beams under $T \geq 400\,°C$, the distortional slenderness threshold separating the safe and unsafe failure moment estimates moves from $\lambda_{D.T} = 1.0$ to $\lambda_{D.T} = 1.5$. Regardless of the temperature, (ii$_1$) the "safe slenderness range" continues to be characterized by only a few slightly unsafe failure moment estimates and fairly small underestimations (all below 15%, with most of them not exceeding 10%), while (ii$_2$) the "unsafe slenderness range" now exhibits visibly larger failure moment overestimations, which can be as high as 30%.

(iii) With respect to the SCB LCB, it can be generally said that the failure moment predictions provided by Eq. (4) are (iii$_1$) safe and reasonably accurate for $\lambda_{D.T} > 2.5$ (very few slightly unsafe predictions and all underestimations below 54%), (iii$_2$) virtually all unsafe for $\lambda_{D.T} \leq 2.0$, with the overestimations reaching 30%, and (iii$_3$) mostly safe and fairly accurate for $2.0 < \lambda_{D.T} \leq 2.5$. Moreover, it should be noted that the "unsafe slenderness range" pattern gradually changes as the temperature rises, mostly due to the failure moment overestimation growth occurring for $\lambda_{D.T} \leq 1.5$.

(iv) In view of the contents of the previous items, it can be concluded that the $M_{nD.T}$ DSM-based strength curve set predicts quite satisfactorily the failure moments of the SCA beams in the moderate-to-high slenderness range ($\lambda_{D.T} > 1.0$ or $\lambda_{D.T} > 1.5$, respectively for $T \leq 300\,°C$ and $T \geq 400\,°C$). Concerning the failure moments of the SCB beams, they can be deemed satisfactorily estimated by the $M_{nD.T}$ DSM-based strength curve for $\lambda_{D.T} > 2.0$, regardless of the temperature, even if it provides several slight failure moment overestimations for beams such that $2.0 < \lambda_{D.T} \leq 2.5$ (particularly for $T \geq 400\,°C$).

(v) Therefore, it is clear that, in order to improve the failure moment prediction quality provided by the $M_{nD.T}$ DSM-based strength curves for lipped channel beams under elevated temperatures, these strength curves need to be modified/lowered in the low-to-moderate slenderness range (more so in the

case of the SCB beams). Such modifications are proposed in the next section, which also includes the assessment of the failure moment prediction quality they entail – the reliability of the modified DSM-based design approach is also addressed.

6.1 Modification of the available DSM-based design curves at elevated temperatures

In order to improve the failure moment prediction quality provided by Eq. (4) for the lipped channel beams exhibiting low and moderate slenderness values, the strategy previously employed by other authors (*e.g.*, Bandula Heva & Mahendran 2012, and Bicelli *et al.* 2021) is adopted in this work. It consists of modifying/lowering Eq. (4) through the incorporation of the reduction factor ratios k_p and k_y, shown earlier to play a key role in the steel constitutive law temperature-dependence prescribed by the EC3-1.2 (2005) model (see Section 4.2). The modification consists of (i) replacing $M_{y.T}$ (yield moment at elevated temperatures) by $M_{y.20} \cdot k_p$, where it should be recalled that $k_p = \sigma_{p.T}/\sigma_{y.20}$ ($\sigma_{p.T}$ is the proportionality limit stress at temperature T), (ii) the coefficient $(k_p/k_y)^{2.5}$ is included in the first branch of the design curve (see the first expression in Eq. (5)), (iii) the parameter a is replaced by $[a \cdot (k_y/k_p)]$ in the second branch of the design curve (see the second expression in Eq. (5)), and (iv) the distortional slenderness transition value 0.673 is replaced by $0.673/\eta$, where $\eta \leq 1.0$ is a coefficient calculated to ensure continuity of the design curves – Table 6 gives its values for the two support conditions (SCA and SCB) and eight temperatures considered in this work (the η values at intermediate temperatures can be obtained via linear interpolation). The modified/lowered DSM-based design curves, denoted $M_{nD.T*}$, are given by the expressions

$$M_{nD.T*} = \begin{cases} \left(M_{y.20} \cdot k_p\right) + \dfrac{\left(1 - C_{yd.T}^{-2}\right)}{\left(k_p/k_y\right)^{2.5}}\left[M_{p.T} - M_{y.T}\right] & \lambda_{D.T} \leq 0.673/\eta \\ M_{y.T}\left[1 - a \cdot \left(k_y/k_p\right)/\lambda_{D.T}^b\right]/\lambda_{D.T}^c & \lambda_{D.T} > 0.673/\eta \end{cases} \quad \text{with} \quad \lambda_{D.T} = \sqrt{\dfrac{M_{y.T}}{M_{crD.T}}} \quad , \quad (5)$$

where (i) $C_{yd.T} = (0.673\eta^{-1}/\lambda_{D.T})^{0.5} \leq 3$, (ii) k_p and k_y are the proportional limit and yield stress reduction factors prescribed in EC3-1.2 (2005) (see Fig. 3(a)), and (iii) the values of parameters a, b and c are those proposed by Martins *et al.* (2017) (SCA beams) or in Section 5.1 (SCB beams), deemed not to vary with the temperature.

Table 6: Values of η appearing in the $M_{nD.T*}$ expressions for SCA and SCB for LCB at room and elevated temperatures.

T (ºC)	20/100	200	300	400	500	600	700	800
SCA	1.00	0.92	0.84	0.74	0.75	0.70	0.69	0.78
SCB	1.00	0.95	0.87	0.78	0.82	0.73	0.71	0.83

Figures 11(a)-(b) display the DSM-based design curves defined by Eq. (5), respectively for the SCA and SCB lipped channel beams – they include zoomed views of the transition between the pairs of design curve branches. It is worth noting that (i) the design curves remain unchanged for the room/mildly elevated temperature ($T \leq 100°C – \eta = k_p = k_y = 1$) and (ii) the modifications of the design curves concerning the elevated temperatures are only felt in the low-to-moderate slenderness range ($\lambda_{D.T} \leq 0.673/\eta$) – the failure moment predictions concerning LCB such that $\lambda_{D.T} > 0.673/\eta$ remain practically unaltered. Since the design curve modifications stem essentially from the incorporation of the ratio k_p/k_y, it is just logical to expect the temperature-dependence of this ratio to be directly reflected in the design curve variation with the temperature. Indeed, this is the case: as clearly shown in Figs. 11(a)-(b), the modified design curves are ordered like the k_p/k_y values – sequence T=20/100-200-300-800-500-400-600-700°C.
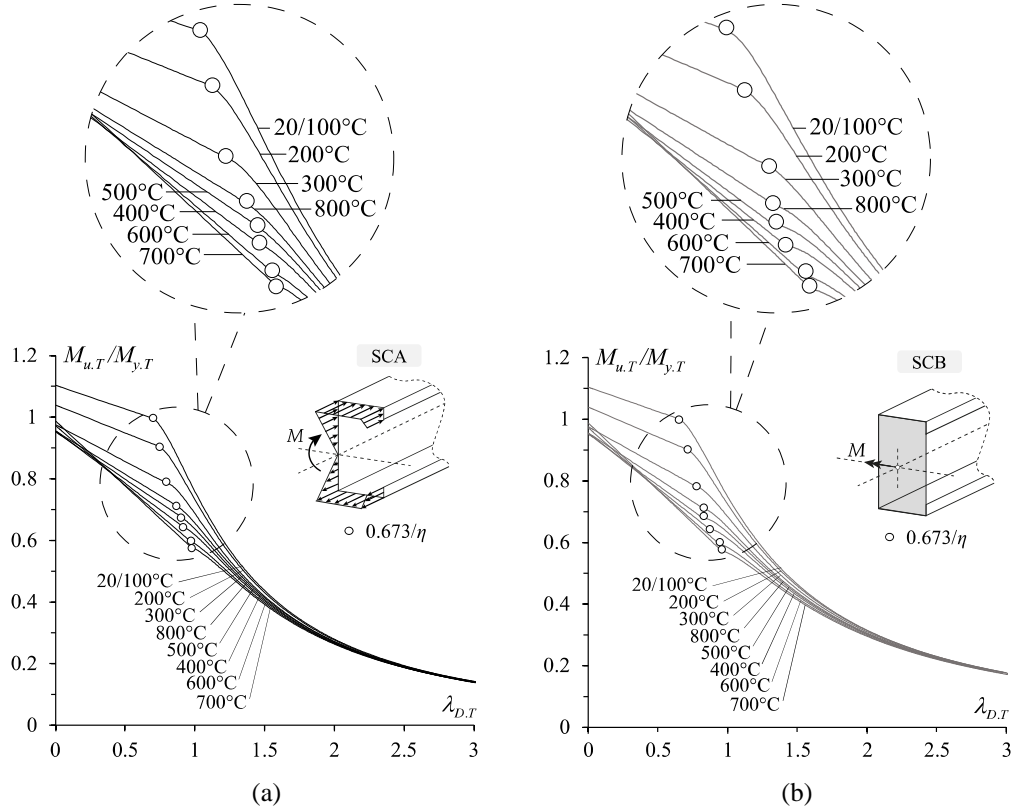
Figure 11. $M_{nD.T*}$ DSM-based D strength curves for (a) SCA and (b) SCB LCB under elevated temperatures ($T \leq 800$°C).

In order to enable the qualitative assessment of the failure moment prediction quality provided by Eq. (5), Fig. 12 shows the $M_{u.T}/M_{nD.T*}$ *vs.* $\lambda_{D.T}$ plots concerning the whole set of LCB analyzed in this work and by Landesmann & Camotim (2016) – the associated statistical indicators are shown in Table 7. Moreover, the full set of $M_{u.T}/M_{nD.T*}$ values for the above lipped channel beams are given, in tabular form, in Annexes B (SCA) and C (SCB). The observation and analysis of the results shown in Fig. 12 and Table 7, as well as their comparison with those shown earlier in Figures 9-10 and Tables 4-5, prompt the following remarks:

(i) It is clear that the proposed modification of Eq. (4), leading to Eq. (5), considerably improves the failure moment prediction for both the SCA and SCB lipped channel beams with low and moderate slenderness values (*i.e.*, such that $\lambda_{D.T} \leq 0.673/\eta$) subjected to elevated temperatures. Moreover, it is also very clear that, regardless of the slenderness and temperature values, Eq. (5) yields quite good failure moment estimates for all the SCA and SCB lipped channel beams considered, *i.e.*, either analyzed in this work or reported by Landesmann & Camotim (2016).

(ii) The $M_{u.T}/M_{nD.T*}$ statistical indicators given in Table 7, which are similarly good for the full set of temperatures considered, confirm the above assertion – the averages, standard deviations and maximum/minimum values for LCB with $\lambda_{D.T} \leq 0.673/\eta$ vary from (ii$_1$) 0.97 to 1.06, 0.01 to 0.05, 0.99 to 1.20, and 0.89 to 0.97 (SCA beams), and (ii$_2$) 1.02 to 1.10, 0.01 to 0.12, 1.05 to 1.61 and 0.92 to 1.02 (SCB beams). Moreover, the numbers of "clearly unsafe" failure moment estimates concerning the SCA and SCB beams with $\lambda_{D.T} \leq 0.673/\eta$ are now quite small – 14 (out of 160 – 8.8%), for the SCA beams, and 7 (out of 154 – 4.5%), for the SCB beams. For the SCA and SCB beams with $\lambda_{D.T} > 0.673/\eta$, these numbers are much smaller: they read 5 (out of 1355 – 0.4%), for the SCA beams, and 20 (out of 1361 – 1.5%), for the SCB beams. On the other hand, it should also be noted that the maximum and minimum predicted-to-numerical failure moment ratios read 1.20 and 0.90, for the SCA beams,

19
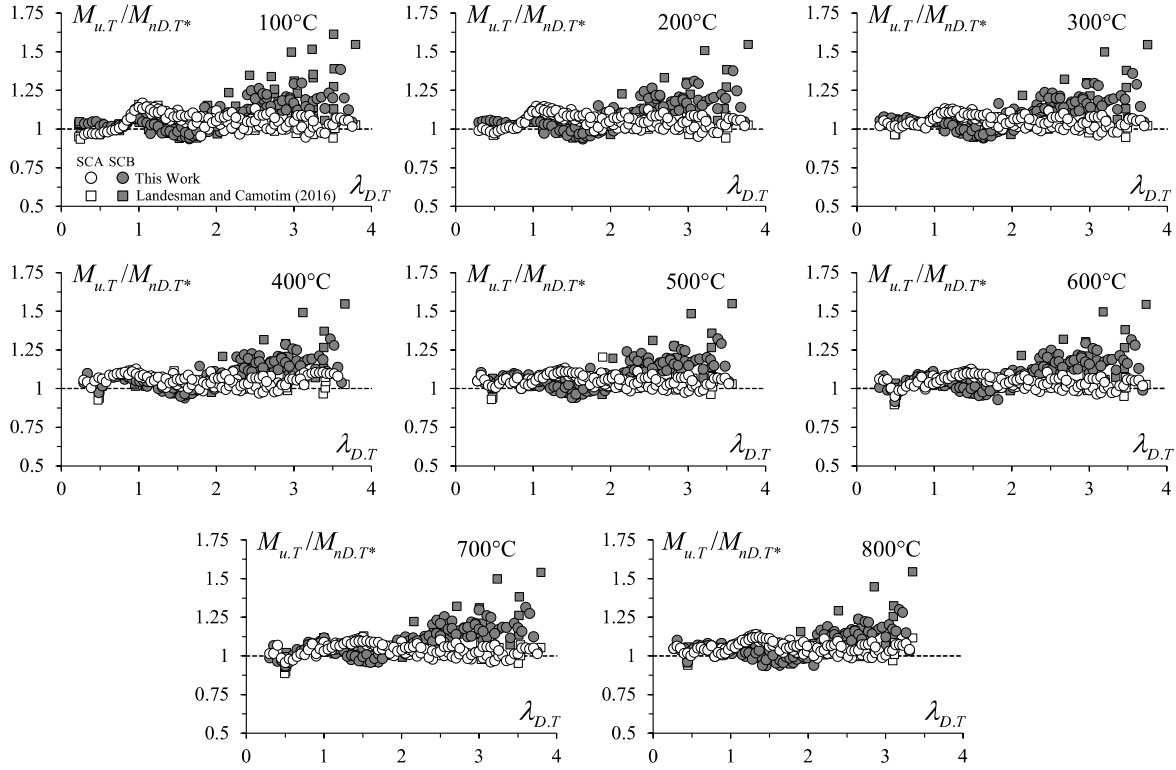
Figure 12. $M_{u.T}/M_{nD.T*}$ vs. $\lambda_{D.T}$ plots for the SCA and SCB LCB beams analyzed in this work and by Landesmann & Camotim (2016) (T=20/100-800 °C).

Table 7: $M_{u.T}/M_{nD.T*}$ statistical indicators for the SCA and SCB beams analyzed in this work, and by Landesmann & Camotim (2016) (T=20/100-800 °C).

T (°C)		100		200		300		400		500		600		700		800		All beams	
$\lambda_{D.T}\leq0.673/\eta$ or $\lambda_{D.T}>0.673/\eta$		$\leq$	$>$	$\leq$	$>$	$\leq$	$>$	$\leq$	$>$	$\leq$	$>$	$\leq$	$>$	$\leq$	$>$	$\leq$	$>$	$\leq$	$>$
SCA	*n*	18	202	14	171	17	168	21	164	21	164	23	162	23	162	23	162	160	1355
	Avr	0.97	1.06	0.99	1.06	1.02	1.05	1.02	1.05	1.02	1.05	1.01	1.05	1.00	1.05	1.02	1.06	1.01	1.05
	SD	0.01	0.04	0.02	0.04	0.03	0.04	0.04	0.03	0.04	0.04	0.05	0.03	0.05	0.04	0.03	0.04	0.04	0.04
	Min	0.94	0.94	0.96	0.94	0.96	0.95	0.93	0.97	0.93	0.96	0.90	0.95	0.89	0.95	0.94	0.97	0.89	0.94
	Max	0.99	1.17	1.01	1.15	1.05	1.13	1.11	1.13	1.09	1.20	1.08	1.12	1.08	1.13	1.07	1.14	1.11	1.20
	Uns	2	2	0	1	0	1	3	0	2	0	3	1	3	0	1	0	14	5
SCB	*n*	17	203	13	172	15	170	21	164	21	164	23	162	23	162	21	164	154	1361
	Avr	1.03	1.09	1.04	1.09	1.05	1.09	1.05	1.09	1.06	1.09	1.03	1.09	1.02	1.10	1.04	1.07	1.04	1.09
	SD	0.01	0.12	0.01	0.10	0.02	0.10	0.04	0.10	0.03	0.10	0.05	0.10	0.06	0.10	0.03	0.09	0.04	0.10
	Min	1.01	0.94	1.02	0.93	1.02	0.94	0.97	0.94	1.00	0.94	0.92	0.93	0.93	0.96	0.96	0.94	0.92	0.93
	Max	1.05	1.61	1.06	1.55	1.08	1.55	1.10	1.55	1.10	1.55	1.09	1.54	1.09	1.54	1.10	1.54	1.10	1.61
	Uns	0	4	0	3	0	3	0	2	0	2	3	1	4	0	0	5	7	20

and 1.61 and 0.93, for the SCB beams – as can be clearly observed in Fig. 12, the failure moments of several slender ($\lambda_{D.T}\geq2.5$) SCB beams are visibly underestimated.

(iii) The very good performance of Eq. (5) in predicting the failure moments of both the SCA and SCB lipped channel beams provides encouragement to proceed along this path in the search for an efficient

20

DSM-based design approach capable of handling the distortional failures of arbitrary cold-formed steel beams subjected to elevated temperatures.

6.2 Reliability Assessment

Next, the reliability of the failure moment predictions provided by the proposed DSM-based design approaches is assessed, through the determination of the LRFD (Load and Resistance Factor Design) resistance factors ϕ associated with the numerical failure moments obtained for the CFS LC beams analyzed in this work and by Landesmann & Camotim (2016). In particular, it is intended to check whether values equal to or higher than ϕ_b=0.90 are achieved – this is the limit value prescribed by the current North American Specification (AISI 2022) for members under bending. According to this specification (Chapter K – Section K2.1.1), ϕ can be determined by means of the expression

$$\phi = C_\phi \left(M_m\, F_m\, P_m \right) e^{-\beta_0 \sqrt{V_M^2 + V_F^2 + C_P V_P^2 + V_Q^2}} \qquad \text{with} \qquad C_P = \left(1 + \frac{1}{n} \right) \frac{m}{m-2} \qquad , \quad (6)$$

where (i) C_ϕ is a calibration coefficient (C_ϕ=1.52 for LRFD), (ii) M_m=1.10 and F_m=1.00 are the mean values of the material and fabrication factors, respectively, (iii) β_0 is the target reliability index (β_0=2.5 for structural members in LRFD), (iv) V_M=0.10, V_F=0.05 and V_Q=0.21 are the coefficients of variation of the material factor, fabrication factor and load effect, respectively, (v) C_P is a correction factor depending on the numbers of tests (n) and degrees of freedom (m=n−1), and (vi) P_m and V_P are the mean and coefficient of variation of the "exact"-to-predicted failure moment ratios $M_{u.T}/M_{nD.T*}$[6].

Table 8 shows the n, C_P, P_m, V_P and ϕ values associated with the $M_{nD.T*}$ values concerning the whole set of numerical failure moments assembled in this study (either obtained in this work or reported by Landesmann & Camotim 2016) for SCA and SCB lipped channel beams at temperatures T=20/100-200-300-400-500-600-700-800°C. The observation of the ϕ values obtained leads to the following conclusions:

Table 8: LRFD ϕ values obtained from the $M_{u.T}/M_{nD.T*}$ distortional failure moment predictions of SCA and SCB lipped channel beams at temperatures T=20/100-200-300-400-500-600-700-800°C.

T (°C)		20/100	200	300	400	500	600	700	800	All Beams
SCA	n	630	185	185	185	185	185	185	185	1925
	m	629	184	184	184	184	184	184	184	1924
	C_P	1.005	1.016	1.016	1.016	1.016	1.016	1.016	1.016	1.002
	P_m	1.047	1.052	1.050	1.047	1.050	1.042	1.053	1.040	1.048
	V_P	0.053	0.043	0.037	0.037	0.038	0.039	0.038	0.040	0.044
	ϕ	0.952	0.961	0.961	0.959	0.961	0.954	0.964	0.951	0.956
SCB	n	730	185	185	185	185	185	185	185	2025
	m	729	184	184	184	184	184	184	184	2024
	C_P	1.004	1.016	1.016	1.016	1.016	1.016	1.016	1.016	1.001
	P_m	1.083	1.084	1.085	1.086	1.083	1.086	1.067	1.087	1.083
	V_P	0.117	0.102	0.099	0.095	0.093	0.098	0.088	0.099	0.104
	ϕ	0.933	0.948	0.952	0.956	0.955	0.953	0.946	0.954	0.946

---

[6] The target reliability used in this work is the same for distortional failures at room and elevated temperatures members – this has been done in the past, also by several other researchers (*e.g.*, Kankanamge & Mahendran 2012, and Bandula & Mahendran 2012). The authors are not aware of any investigation aimed at identifying the most adequate target reliability for distortional failures at elevated temperatures.

(i) The ϕ values obtained from the $M_{nD.T*}$ failure moment estimates concerning the SCA and SCB lipped channel beams are not far apart from each other, regardless of the temperature considered – indeed, they read 0.952-0.961-0.961-0.959-0.961-0954-0.961-0.964 (SCA beams) and 0.933-0.948-0.952-0.956-0.955-0.953-0.954-0.946 (SCB beams). Moreover, it should be noted that all of these ϕ values are visibly above that prescribed in AISI (2022) for members in bending (ϕ_b=0.90).

(ii) If the $M_{nD.T*}$ failure moment estimates concerning all the temperature values considered are put together, the ϕ values obtained are 0.956 (SCA beams), 0.946 (SCB beams) and 0.949 (SCA and SCB beams) – naturally, these values are also visibly above ϕ_b=0.90.

(iii) In view of the contents of the previous items, it seems fair to conclude that the proposed DSM-based design approach ($M_{nD.T*}$) can handle reliably cold-formed steel SCA and SCB lipped channel beams failing in distortional modes, both at room and elevated temperatures.

7. Concluding Remarks

This paper reported the most recent results of an investigation, initiated a few years ago (Landesmann & Camotim 2016 and Martins *et al.* 2017), on the post-buckling behavior, ultimate strength and DSM design of cold-formed steel single-span simply supported lipped channel beams buckling in distortional modes at room and elevated temperatures, typically caused by fire conditions. After addressing the beam geometry selection and the influence of the temperature on the beam distortional post-buckling behavior, numerical failure moment data were obtained for 2400 beams, corresponding to (i) 30 geometries (cross-section dimensions and lengths), (ii) two end support conditions, denoted as SCA and SCB (end cross-section warping and local displacement/rotations free or fully prevented, respectively), (iii) five room temperature yield stresses, chosen to enable covering wide distortional slenderness ranges (0.30≤$\lambda_{D.T}$≤3.75), and (iv) eight uniform temperatures (T=20/100-200-300-400-500-600-700-800°C) – the model prescribed in part 1-2 of Eurocode 3 (EC3-1.2 2005) was employed to describe the temperature dependence of the cold-formed steel material properties. The numerical distortional failure moments obtained in this work, together with those previously reported by Landesmann & Camotim (2016) and Martins *et al.* (2017), were subsequently used to propose contributions towards the development of an efficient DSM-based design approach for cold-formed steel beams failing in distortional modes at room and elevated temperatures. Out of the various findings reported in this work, the following ones deserve to be specially mentioned:

(i) On the basis of the room temperature SCB beam failure moments obtained in this work, it was found that the prediction quality provided by the DSM-based distortional strength curve proposed by Martins *et al.* (2017) could be improved – a visible improvement was achieved by slightly altering the values of *a*, *b* and *c* (parameters appearing in Eq. (2)), thus leading to a more performant DSM-based distortional design curve. Conversely, it was also found that, for SCA beams, the DSM-based distortional strength curve proposed by Martins *et al.* (2017) predicts quite well the failure moments obtained in this work.

(ii) It was shown that incorporating the temperature dependence of the critical distortional buckling ($M_{crD.T}$), yield ($M_{y.T}$) and plastic ($M_{p.T}$) moments in the DSM-based design curves proposed by Martins *et al.* (2017) (including the slight alteration/improvement for the SCB beams – see the previous item), does not lead to an acceptable failure moment prediction quality for SCA or SCB beams at elevated temperatures. Indeed, regardless of the temperature, safe and reasonably accurate failure moment estimates are only obtained for beams with a fairly high slenderness – in the low and moderate slenderness range, several SCA and SCB beam failure moments are clearly overestimated, thus providing ample evidence that the above DSM-based design curves need to be modified.

(iii) The DSM-based distortional design curves addressed in the previous item were modified through the inclusion of (iii_1) the temperature-dependent ratio k_p/k_y, where k_p and k_y are reduction factors prescribed by EC3-1.2 (2005), and (iii_2) the coefficient η, calculated to ensure continuity between the branches of the two (modified) design curves. In spite of its simplicity, this modification led to a quite considerable improvement in failure moment prediction quality for SCA and SCB beams exhibiting low and moderate distortional slenderness at elevated temperatures.

(iv) The failure moment predictions provided by the (modified) DSM-based distortional design curves proposed, for the SCA and SCB lipped channel beams at room and elevated temperatures analyzed in this work and by Landesmann & Camotim (2016) and Martins *et al.* (2017), lead to LRFD resistance factors never below 0.946, *i.e.*, well above the value prescribed in AISI for members in bending – ϕ_b=0.90. The proposed DSM-based design approaches for both room and elevated temperatures, considered individually (each temperature or end support condition) or together (all temperatures, both end support conditions), lead to LRFD resistance factors visibly above ϕ_b=0.90, the value prescribed in AISI (2022) for members in bending.

It should still be pointed out that the authors are currently (i) investigating how the temperature-dependent steel material model influences of the beam distortional failure moments and their DSM-based prediction, (ii) preparing a test campaign involving lipped channel beams failing in distortional modes at both room and elevated temperatures, and (iii) looking for additional experimental and numerical failure moment data available in the literature – this last task is quite time consuming since, to the authors' best knowledge, the number of works dealing solely with beam distortional failures under elevated temperature is very scarce (the available failure moments are expected to be dispersed among studies with different focuses). The outputs of these research efforts should provide either further evidence on the adequacy of the proposed DSM-based strength curves or guidelines on how to improve them.

Finally, just two words to mention that the final goal of this ongoing investigation is to find an efficient DSM-based design approach for arbitrary beams exhibiting distortional failures at elevated temperatures. The results obtained so far provide encouragement that this goal can be achieved by proceeding along the path that has been followed up to now.

9. References

ABAQUS (2014). Analysis User's Manual-Version 6.14-1. ABAQUS Inc., USA.

ABNT (Brazilian Standards Association) (2010). *Brazilian Standard on Design of Cold-Formed Steel Structures*, (ABNT NBR 14762:2010, Rio de Janeiro. (Portuguese).

AISI (American Iron and Steel Institute) (2022). *North American Specification (NAS) for the Design of Cold-Formed Steel Structural Members* (2016 edition reaffirmed in 2020 with Supplement 3), AISI-S100-16 w/S3-22, Washington DC.

Arrais F., Lopes N., Real P.V. (2021). "Fire design of slender cold-formed lipped channel and sigma section members with uniform temperature under compression", *Fire Safety Journal*, **122**(June), paper 103340 (17 pages).

AS/NZS (Standards of Australia and Standards of New Zealand) (2018). *Cold-Formed Steel Structures*, AS/NZS 4600:2018 (3rd ed.), Sydney-Wellington.

Bandula Heva Y., Mahendran M. (2012). "Flexural-torsional buckling tests of cold-formed steel compression members at elevated temperatures", *Steel and Composite Structures*, **14**(3), 205-227.

Bebiano R., Camotim D., Gonçalves R. (2018). "GBTUL 2.0 – a second-generation code for the GBT-based buckling and vibration analysis of thin-walled members", *Thin-Walled Structures*, **124**(March), 235-257.

Bicelli A.A., Landesmann A., Camotim D., Dinis P.B. (2021). "Flexural-torsional failure and DSM design of fixed-ended cold-formed steel columns at elevated temperatures", *Thin-Walled Structures*, **169**(December), paper 108362 (16 pages).

Camotim D., Dinis P.B., Martins A.D. (2016). "Direct Strength Method (DSM) – a general approach for the design of cold-formed steel structures", *Recent Trends in Cold-Formed Steel Construction*, C. Yu (ed.), Woodhead Publishing (Series in Civil and Structural Engineering), Amsterdam, 69-105.

Camotim D., Martins A.D., Dinis P.B. (2023). "Towards the next generation design of cold-formed steel structures: the Direct Strength Method (DSM)", *Recent Trends in Cold-Formed Steel Construction* (2nd ed.), C. Yu (ed.), Woodhead Publishing (Series in Civil and Structural Engineering), Elsevier, Cambridge (MA – USA) and Kidlington (UK), 101-173.

CEN (Comité Européen de Normalisation) (2005). *Eurocode 3: Design of Steel Structures – Part 1.2: General Rules – Structural Fire Design*, EN 1993-1-2, Brussels.

Ellobody E., Young B. (2005). "Behavior of cold-formed steel plain angle columns", *Journal of Structural Engineering* (ASCE), **131**(3), 469-478.

Kankanamge N.D., Mahendran M. (2012). "Behaviour and design of cold-formed steel beams subject to lateral–torsional buckling at elevated temperatures", *Thin-Walled Structures*, **61**(December), 213-228.

Laím L., Rodrigues J.P.C. (2018). Fire design methodologies for cold-formed steel beams made with open and closed cross-sections, *Engineering Structures*, **171**(September), 759-778.

Laím L., Rodrigues J.P.C., Craveiro H.D. (2016). "Flexural behaviour of axially and rotationally restrained cold-formed steel beams subjected to fire", *Thin-Walled Structures*, **98A**(January), 39-47.

Landesmann A., Camotim D. (2011). "On the distortional buckling, post-buckling and strength of cold-formed steel lipped channel columns under fire conditions", *Journal of Structural Fire Engineering*, **2**(1), 1-19.

Landesmann, A., Camotim, D. (2013). "On the Direct Strength Method (DSM) design of cold-formed steel columns against distortional failure", *Thin-Walled Structures*, **67**(June), 168-187.

Landesmann A., Camotim D. (2015). "DSM to predict distortional failures in cold-formed steel columns exposed to fire: effect of the constitutive law temperature-dependence", *Computers & Structures*, **147**(1), 47-67.

Landesmann A., Camotim D. (2016). "Distortional failure and DSM design of cold-formed steel lipped channel beams under elevated temperatures", *Thin-Walled Structures*, **98A**(January), 75-93.

Landesmann A., Camotim D., Silva F.C.M. (2019). "DSM design of cold-formed steel columns failing in distortional modes at elevated temperatures", *International Journal of Steel Structures*, **19**(3), 1023-1041.

Martins A.D., Landesmann A., Camotim D., Dinis P.B. (2017). "Distortional failure of cold-formed steel beams under uniform bending: behaviour, strength and DSM design", *Thin-Walled Structures*, **118**(September), 196-213.

Santiago I.B., Rodrigues J.P.C., Rodrigues F.C., Oliveira R.L.G. (2021). "Numerical analysis of cold-formed steel sigma-shaped beams in fire conditions". *Architecture, Structures and Construction*, **1**(September), 53-63.

Schafer B.W., Peköz T. (1998), "Direct strength prediction of cold-formed steel members using numerical elastic buckling solutions, *Proceedings of 14th International Specialty Conference on Cold-Formed Steel Structures* (St. Louis, 15-16/10), W.W. Yu, R. Laboube (eds.), 69-76.

Schafer B.W. (2008), "Review: the direct strength method of cold-formed member design", *Journal of Constructional Steel Research*, **64**(7-8) (2008), 766-778.

Schafer B.W. (2019). "Advances in the Direct Strength Method of cold-formed steel design", *Thin-Walled Structures*, **140**(July), 533-541.

Wang L., Young B. (2014). "Design of cold-formed steel channel with stiffened webs subjected to bending", *Thin-Walled Structures*, **85**(December), 81-92. https://doi.org/10.1016/j.tws.2014.08.002

Yu C., Schafer B.W. (2006). "Distortional buckling tests on cold-formed steel beams", *Journal of Structural Engineering* (ASCE), **132**(4), 515-528.

Yu C., Schafer B.W. (2007). "Simulation of cold-formed steel beams in local and distortional buckling with applications to the direct strength method", *Journal of Constructional Steel Research*, **63**(May), 581-590.

Annex A: Data Concerning the SCB Lipped Channel Beams at Room Temperature

This annex includes three tables (A1 to A3), concerning SCB lipped channel beams at room temperature, and displays the whole set of numerical failure moments (i) obtained in this work (Table A1) and (ii) reported by Landesmann & Camotim (2016) and Martins et $al.$ (2017) (Tables A2 and A3). Each table provides, for the various lipped channel beams analyzed, (i) the distortional slenderness value (λ_D), (ii) the ratio between the failure and yield moments (M_u/M_y), and (iii) the numerical-to-predicted failure moment ratios obtained with Eq. (2), namely M_u/M_{nD} (a=0.23, b=1.55, c=1.45 – proposed by Martins et $al.$ 2017), and $M_u/M_{nD.mod}$ (a=0.25, b=1.51, c=1.52 – proposed in Section 5.1).

Table A1: Data concerning the SCB lipped channel beams at room temperature analysed in this work.

Beam	λ_D	$\dfrac{M_u}{M_y}$	$\dfrac{M_u}{M_{nD}}$	$\dfrac{M_u}{M_{nD.mod}}$	Beam	λ_D	$\dfrac{M_u}{M_y}$	$\dfrac{M_u}{M_{nD}}$	$\dfrac{M_u}{M_{nD.mod}}$
LC 1	0.300	1.021	1.034	1.033	LC 16	1.05	0.804	1.025	1.046
	0.800	0.945	1.020	1.034		1.55	0.440	0.912	0.948
	1.300	0.590	0.984	1.014		2.05	0.277	0.929	0.983
	1.800	0.316	0.935	0.981		2.55	0.193	0.984	1.055
	2.300	0.216	0.960	1.023		3.05	0.141	1.014	1.100
LC 2	0.350	1.014	1.034	1.034	LC 17	1.1	0.769	1.020	1.042
	0.850	0.938	1.026	1.040		1.6	0.428	0.911	0.949
	1.350	0.549	0.950	0.980		2.1	0.274	0.951	1.007
	1.850	0.327	1.084	1.139		2.6	0.191	1.006	1.081
	2.350	0.229	0.932	0.994		3.1	0.139	1.025	1.114
LC 3	0.400	1.011	1.045	1.044	LC 18	1.15	0.715	1.003	1.027
	0.900	0.923	1.064	1.080		1.65	0.406	0.903	0.942
	1.400	0.523	0.950	0.982		2.15	0.261	0.992	1.052
	1.900	0.311	1.029	1.083		2.65	0.178	1.058	1.137
	2.400	0.215	1.142	1.220		3.15	0.126	1.093	1.189
LC 4	0.450	1.009	1.046	1.046	LC 19	1.2	0.665	1.003	1.029
	0.950	0.900	1.073	1.090		1.7	0.371	0.911	0.952
	1.450	0.498	0.963	0.998		2.2	0.242	0.954	1.013
	1.950	0.307	1.053	1.110		2.7	0.172	0.995	1.071
	2.450	0.215	1.165	1.246		3.2	0.127	0.998	1.087
LC 5	0.500	1.008	1.017	1.017	LC 20	1.25	0.628	0.987	1.015
	1.000	0.861	1.089	1.109		1.75	0.360	0.916	0.959
	1.500	0.490	1.023	1.062		2.25	0.240	0.998	1.061
	2.000	0.313	1.011	1.067		2.75	0.172	1.061	1.144
	2.500	0.221	1.056	1.131		3.25	0.128	1.080	1.178
LC 6	0.550	1.004	1.026	1.026	LC 21	1.3	0.601	0.945	0.973
	1.050	0.830	1.050	1.071		1.8	0.357	0.934	0.980
	1.550	0.445	0.942	0.980		2.3	0.239	1.020	1.087
	2.050	0.285	1.082	1.144		2.8	0.170	1.072	1.157
	2.550	0.203	1.176	1.261		3.3	0.125	1.094	1.194
LC 7	0.600	0.993	1.010	1.009	LC 22	1.35	0.544	0.955	0.986
	1.100	0.769	1.019	1.041		1.85	0.320	0.957	1.006
	1.600	0.413	0.916	0.954		2.35	0.217	1.040	1.110
	2.100	0.256	1.022	1.083		2.85	0.157	1.093	1.181
	2.600	0.189	1.109	1.192		3.35	0.118	1.103	1.204
LC 8	0.650	0.995	1.016	1.015	LC 23	1.4	0.532	0.952	0.985
	1.150	0.726	0.947	0.970		1.9	0.325	0.932	0.981
	1.650	0.401	0.896	0.935		2.4	0.219	1.001	1.070
	2.150	0.262	1.039	1.102		2.9	0.155	1.038	1.123
	2.650	0.187	1.118	1.202		3.4	0.114	1.036	1.133
LC 9	0.700	0.992	1.002	1.018	LC 24	1.45	0.495	0.927	0.961
	1.200	0.684	1.013	1.039		1.95	0.304	0.973	1.026
	1.700	0.390	0.917	0.959		2.45	0.211	1.053	1.126
	2.200	0.256	0.944	1.003		2.95	0.156	1.097	1.188
	2.700	0.179	0.984	1.059		3.45	0.118	1.124	1.231
LC 10	0.750	0.977	1.015	1.029	LC 25	1.5	0.472	0.948	0.984
	1.250	0.641	0.998	1.026		2	0.294	0.966	1.020
	1.750	0.370	0.915	0.959		2.5	0.206	1.037	1.111
	2.250	0.246	0.998	1.062		3	0.152	1.078	1.168
	2.750	0.175	1.047	1.128		3.5	0.115	1.095	1.200
LC 11	0.800	0.953	1.018	1.032	LC 26	1.55	0.453	0.972	1.011
	1.300	0.594	0.972	1.002		2.05	0.290	0.974	1.030
	1.800	0.351	0.953	1.000		2.55	0.206	1.041	1.117
	2.300	0.235	1.038	1.106		3.05	0.153	1.033	1.121
	2.800	0.167	1.086	1.172		3.55	0.117	0.954	1.046
LC 12	0.850	0.941	1.036	1.051	LC 27	1.6	0.429	0.938	0.977
	1.350	0.568	0.968	0.999		2.1	0.279	1.028	1.089
	1.850	0.342	0.931	0.979		2.6	0.200	1.143	1.228
	2.350	0.229	0.999	1.066		3.1	0.149	1.192	1.295
	2.850	0.162	1.036	1.119		3.6	0.114	1.261	1.384
LC 13	0.900	0.907	1.052	1.068	LC 28	1.65	0.412	0.924	0.964
	1.400	0.510	0.947	0.980		2.15	0.271	1.040	1.103
	1.900	0.303	0.962	1.013		2.65	0.194	1.137	1.222
	2.400	0.208	1.055	1.127		3.15	0.144	1.053	1.145
	2.900	0.153	1.116	1.207		3.65	0.110	1.092	1.199
LC 14	0.950	0.894	1.055	1.072	LC 29	1.7	0.399	0.986	1.031
	1.450	0.504	0.940	0.974		2.2	0.267	1.020	1.083
	1.950	0.311	0.967	1.020		2.7	0.191	1.065	1.147
	2.450	0.215	1.027	1.099		3.2	0.141	1.037	1.129
	2.950	0.156	1.108	1.200		3.7	0.107	1.021	1.123
LC 15	1.000	0.860	1.048	1.067	LC 30	1.75	0.372	0.899	0.988
	1.500	0.470	0.922	0.957		2.25	0.249	0.955	1.016
	2.000	0.294	1.014	1.071		2.75	0.179	0.986	1.063
	2.500	0.206	1.115	1.194		3.25	0.133	0.953	1.067
	3.000	0.152	1.192	1.292		3.75	0.101	0.949	1.044

Table A2: Data concerning the SCB lipped channel beams at room temperature reported by Landesmann & Camotim (2016).

λ_D	$\dfrac{M_u}{M_y}$	$\dfrac{M_u}{M_{nD}}$	$\dfrac{M_u}{M_{nD.\mathrm{mod}}}$
0.510	1.037	1.012	1.012
1.005	0.778	1.023	1.042
1.519	0.439	0.919	0.955
2.010	0.306	0.915	0.967
2.548	0.235	0.963	1.033
3.063	0.182	0.959	1.041
3.398	0.158	0.966	1.056
0.255	1.093	1.026	1.026
0.750	0.959	1.002	1.016
1.248	0.586	0.971	0.998
1.749	0.360	0.899	0.942
2.247	0.271	0.940	1.000
2.752	0.213	0.973	1.049
3.246	0.170	0.972	1.059
0.266	1.076	1.024	1.024
0.806	0.931	1.016	1.030
1.350	0.519	0.941	0.971
1.887	0.398	1.094	1.151
2.430	0.327	1.259	1.346
2.969	0.273	1.380	1.495
3.509	0.230	1.470	1.610
0.531	1.025	1.007	1.007
1.127	0.657	0.972	0.994
1.638	0.441	1.012	1.056
2.159	0.354	1.163	1.234
2.710	0.278	1.242	1.337
3.233	0.244	1.389	1.514
3.795	0.197	1.402	1.545
0.241	1.098	1.030	1.030
0.748	0.973	1.015	1.030
1.242	0.588	0.968	0.995
1.745	0.370	0.921	0.965
2.248	0.301	1.044	1.111
2.749	0.250	1.138	1.227
3.248	0.213	1.221	1.331
0.520	1.036	1.013	1.013
0.982	0.811	1.043	1.062
1.521	0.431	0.904	0.939
2.060	0.319	0.985	1.042
2.523	0.269	1.089	1.167
3.042	0.217	1.134	1.230
3.513	0.182	1.162	1.273
0.230	1.116	1.034	1.034
0.740	0.982	1.019	1.034
1.247	0.600	0.993	1.021
1.749	0.383	0.957	1.002
2.249	0.311	1.077	1.146
2.748	0.256	1.165	1.255
3.249	0.216	1.241	1.352
0.498	1.055	1.023	1.023
1.030	0.779	1.049	1.070
1.516	0.453	0.944	0.981
2.016	0.341	1.024	1.082
2.523	0.278	1.125	1.206
3.003	0.235	1.207	1.309
3.518	0.198	1.266	1.388
0.232	1.154	1.046	1.046
0.750	0.983	1.027	1.041
1.247	0.631	1.044	1.073
1.749	0.396	0.989	1.036
2.249	0.289	1.003	1.067
2.748	0.228	1.036	1.117
3.249	0.182	1.044	1.138
0.509	1.073	1.034	1.034
0.997	0.828	1.081	1.100
1.506	0.487	1.008	1.047
2.000	0.332	0.986	1.041
2.504	0.255	1.021	1.094
3.013	0.203	1.046	1.135
3.510	0.161	1.030	1.128

Table A3: Data concerning the SCB lipped channel beams at room temperature reported by Martins *et al.* (2017).
(*to be continued*)

λ_D	$\frac{M_u}{M_y}$	$\frac{M_u}{M_{nD}}$	$\frac{M_u}{M_{nD.\text{mod}}}$	λ_D	$\frac{M_u}{M_y}$	$\frac{M_u}{M_{nD}}$	$\frac{M_u}{M_{nD.\text{mod}}}$	λ_D	$\frac{M_u}{M_y}$	$\frac{M_u}{M_{nD}}$	$\frac{M_u}{M_{nD.\text{mod}}}$
0.638	1.001	0.995	0.995	0.267	1.064	0.994	0.994	0.300	1.090	1.031	1.031
0.654	0.996	0.993	0.993	0.562	1.040	1.020	1.020	0.464	1.048	1.015	1.015
1.018	0.767	1.014	1.041	0.654	1.012	1.008	1.008	0.647	1.003	0.999	0.999
1.024	0.758	1.008	1.035	0.808	0.960	1.061	1.061	0.871	0.886	1.014	1.039
1.109	0.690	0.997	1.027	1.111	0.693	1.003	1.033	1.046	0.743	1.010	1.038
1.116	0.684	0.996	1.026	1.521	0.448	0.935	0.976	1.314	0.544	0.952	0.987
1.528	0.437	0.917	0.957	1.625	0.412	0.935	0.979	1.466	0.468	0.932	0.972
1.774	0.353	0.896	0.943	1.772	0.384	0.972	1.023	1.999	0.326	0.966	1.023
2.701	0.220	0.977	1.054	2.096	0.335	1.057	1.123	2.153	0.303	0.991	1.055
2.866	0.203	0.980	1.061	2.284	0.312	1.102	1.177	2.216	0.295	1.002	1.068
2.874	0.202	0.979	1.060	2.552	0.282	1.160	1.247	2.407	0.270	1.026	1.099
2.908	0.200	0.983	1.065	2.669	0.271	1.186	1.279	2.700	0.237	1.054	1.137
3.103	0.182	0.981	1.067	2.889	0.253	1.231	1.334	3.008	0.208	1.070	1.162
3.178	0.176	0.979	1.067	3.247	0.226	1.293	1.411	3.236	0.188	1.073	1.171
3.246	0.171	0.977	1.066	3.477	0.210	1.323	1.451	3.506	0.167	1.068	1.171
3.751	0.136	0.952	1.048	3.579	0.203	1.333	1.464	3.818	0.146	1.052	1.160
3.794	0.133	0.947	1.044	3.861	0.185	1.352	1.492	3.938	0.139	1.042	1.151
0.321	1.078	1.032	1.032	0.333	1.075	1.023	1.023	0.295	1.080	1.021	1.021
0.450	1.046	1.017	1.017	0.411	1.066	1.025	1.025	0.436	1.053	1.016	1.016
0.660	0.988	0.986	0.986	0.638	1.009	1.004	1.004	0.702	0.983	0.977	1.003
0.780	0.944	0.994	1.018	0.732	0.979	0.994	1.019	0.978	0.809	1.029	1.055
1.082	0.687	0.968	0.996	1.024	0.771	1.025	1.053	1.145	0.668	0.999	1.030
1.385	0.504	0.938	0.975	1.531	0.432	0.909	0.949	1.385	0.511	0.951	0.989
1.552	0.458	0.980	1.024	1.608	0.403	0.903	0.945	1.547	0.434	0.925	0.966
1.739	0.422	1.044	1.098	1.958	0.332	0.956	1.012	1.906	0.331	0.923	0.975
2.015	0.380	1.138	1.206	2.010	0.326	0.971	1.029	2.104	0.299	0.949	1.008
2.410	0.331	1.259	1.348	2.445	0.273	1.057	1.134	2.323	0.270	0.977	1.044
2.449	0.327	1.273	1.365	2.589	0.257	1.077	1.159	2.546	0.243	0.997	1.071
2.663	0.304	1.325	1.428	2.879	0.229	1.112	1.204	2.866	0.210	1.011	1.095
2.895	0.281	1.375	1.490	3.122	0.209	1.134	1.234	3.082	0.190	1.014	1.103
3.292	0.249	1.452	1.586	3.341	0.192	1.147	1.254	3.246	0.177	1.012	1.104
3.454	0.236	1.476	1.617	3.546	0.178	1.154	1.266	3.677	0.146	0.997	1.097
3.720	0.218	1.510	1.662	3.645	0.172	1.157	1.272	3.776	0.140	0.991	1.092
3.831	0.210	1.518	1.674	3.826	0.161	1.157	1.276	3.930	0.131	0.979	1.082
0.340	1.075	1.023	1.023	0.276	1.078	1.019	1.019	0.262	1.090	1.027	1.027
0.513	1.038	1.013	1.013	0.445	1.043	1.010	1.010	0.476	1.048	1.018	1.018
0.664	0.996	0.994	0.994	0.582	1.017	1.003	1.003	0.729	0.976	0.988	1.013
0.797	0.953	1.019	1.043	0.714	0.983	0.985	1.011	0.953	0.837	1.038	1.065
1.093	0.711	1.012	1.042	0.942	0.848	1.040	1.066	1.187	0.624	0.971	1.002
1.528	0.423	0.888	0.927	1.397	0.500	0.940	0.978	1.411	0.491	0.934	0.972
1.611	0.399	0.895	0.937	1.621	0.399	0.901	0.944	1.652	0.388	0.897	0.941
1.812	0.364	0.950	1.001	1.803	0.356	0.923	0.972	1.892	0.337	0.929	0.981
2.065	0.323	0.998	1.059	2.012	0.327	0.976	1.035	2.131	0.304	0.979	1.042
2.264	0.297	1.038	1.107	2.444	0.275	1.066	1.143	2.212	0.294	0.998	1.064
2.546	0.271	1.110	1.193	2.564	0.262	1.083	1.165	2.583	0.253	1.058	1.138
2.878	0.241	1.169	1.266	2.874	0.232	1.123	1.216	2.828	0.229	1.083	1.172
3.004	0.232	1.194	1.297	3.095	0.213	1.143	1.243	3.061	0.209	1.101	1.197
3.178	0.219	1.220	1.330	3.139	0.210	1.147	1.249	3.291	0.191	1.113	1.216
3.564	0.195	1.271	1.395	3.537	0.181	1.168	1.282	3.534	0.174	1.124	1.233
3.751	0.182	1.273	1.402	3.706	0.170	1.172	1.290	3.731	0.161	1.122	1.235
3.836	0.178	1.288	1.421	3.809	0.163	1.169	1.289	3.986	0.146	1.114	1.232
0.401	1.092	1.041	1.041	0.263	1.102	1.027	1.027	0.396	1.059	1.016	1.016
0.539	1.040	1.016	1.016	0.402	1.078	1.028	1.028	0.657	1.000	0.998	0.998
0.583	1.029	1.013	1.013	0.559	1.028	1.007	1.007	0.740	0.974	0.994	1.019
0.774	0.970	1.017	1.042	0.685	0.994	0.979	1.007	0.817	0.941	1.024	1.048
1.111	0.709	1.026	1.057	0.832	0.926	1.022	1.046	1.132	0.680	1.005	1.036
1.368	0.526	0.965	1.002	1.353	0.530	0.961	0.998	1.352	0.522	0.944	0.980
1.554	0.438	0.939	0.982	1.535	0.439	0.926	0.968	1.556	0.422	0.907	0.948
1.747	0.391	0.971	1.022	1.734	0.366	0.901	0.948	1.874	0.338	0.919	0.970
1.943	0.358	1.022	1.081	1.965	0.311	0.901	0.954	2.023	0.316	0.951	1.008
2.416	0.294	1.124	1.204	2.256	0.266	0.926	0.988	2.382	0.272	1.019	1.090
2.561	0.278	1.149	1.235	2.447	0.243	0.943	1.012	2.551	0.254	1.042	1.120
2.859	0.250	1.203	1.302	2.654	0.220	0.955	1.029	2.832	0.226	1.072	1.160
2.955	0.242	1.219	1.322	2.883	0.197	0.960	1.039	3.031	0.208	1.085	1.178
3.274	0.217	1.260	1.375	3.136	0.176	0.959	1.044	3.174	0.197	1.092	1.190
3.454	0.204	1.274	1.396	3.379	0.158	0.954	1.044	3.413	0.179	1.102	1.206
3.635	0.192	1.286	1.413	3.573	0.145	0.947	1.040	3.602	0.167	1.105	1.213
3.858	0.177	1.292	1.426	3.794	0.131	0.933	1.028	3.866	0.151	1.105	1.219
0.392	1.111	1.043	1.043	0.321	1.082	1.021	1.021	0.343	1.080	1.031	1.031
0.611	1.041	1.026	1.026	0.402	1.065	1.018	1.018	0.706	0.986	0.983	1.009
0.732	0.990	1.005	1.030	0.580	1.025	1.009	1.009	0.807	0.949	1.023	1.048
0.795	0.962	1.026	1.051	0.740	0.978	0.998	1.023	1.009	0.783	1.026	1.053
1.094	0.748	1.065	1.096	0.969	0.826	1.040	1.067	1.100	0.702	1.006	1.036
1.504	0.487	1.003	1.047	1.125	0.690	1.012	1.043	1.431	0.476	0.921	0.959
1.621	0.443	1.001	1.049	1.360	0.524	0.955	0.992	1.634	0.392	0.894	0.937
1.860	0.366	0.986	1.041	1.855	0.338	0.908	0.958	1.827	0.356	0.938	0.989
2.012	0.333	0.996	1.056	2.018	0.312	0.936	0.992	1.930	0.340	0.963	1.018
2.257	0.291	1.014	1.083	2.194	0.287	0.963	1.026	2.304	0.293	1.049	1.120
2.451	0.265	1.030	1.104	2.343	0.269	0.984	1.052	2.452	0.276	1.075	1.153
2.709	0.234	1.046	1.128	2.673	0.231	1.010	1.089	2.876	0.236	1.144	1.239

Table A3: Data concerning the SCB lipped channel beams at room temperature reported by Martins *et al.* (2017).
(*continuation*)

λ_D	$\dfrac{M_u}{M_y}$	$\dfrac{M_u}{M_{nD}}$	$\dfrac{M_u}{M_{nD.\text{mod}}}$	λ_D	$\dfrac{M_u}{M_y}$	$\dfrac{M_u}{M_{nD}}$	$\dfrac{M_u}{M_{nD.\text{mod}}}$	λ_D	$\dfrac{M_u}{M_y}$	$\dfrac{M_u}{M_{nD}}$	$\dfrac{M_u}{M_{nD.\text{mod}}}$
2.902	0.215	1.052	1.140	2.918	0.207	1.024	1.110	3.063	0.220	1.163	1.264
3.142	0.193	1.057	1.151	3.103	0.191	1.029	1.120	3.301	0.202	1.181	1.290
3.404	0.171	1.048	1.148	3.363	0.172	1.034	1.131	3.483	0.189	1.194	1.309
3.675	0.151	1.031	1.134	3.748	0.146	1.024	1.128	3.750	0.171	1.198	1.319
3.860	0.136	0.994	1.096	3.892	0.138	1.017	1.122	3.875	0.163	1.197	1.321
0.270	1.096	1.035	1.035	0.400	1.054	1.014	1.014	0.565	1.038	1.015	1.015
0.638	0.999	0.994	0.994	0.436	1.058	1.023	1.023	0.626	1.017	1.007	1.007
0.826	0.930	1.021	1.045	0.864	0.905	1.029	1.054	0.961	0.849	1.061	1.088
1.051	0.739	1.009	1.037	1.028	0.710	0.948	0.974	1.035	0.781	1.051	1.080
1.116	0.665	0.968	0.997	1.119	0.687	1.002	1.032	1.318	0.569	0.999	1.036
1.441	0.472	0.921	0.960	1.379	0.509	0.944	0.981	1.386	0.530	0.988	1.027
1.569	0.408	0.885	0.926	1.715	0.373	0.907	0.952	1.696	0.394	0.944	0.991
1.882	0.319	0.874	0.922	1.827	0.350	0.921	0.971	1.881	0.343	0.937	0.990
2.090	0.289	0.908	0.965	2.087	0.311	0.977	1.038	2.106	0.304	0.964	1.024
2.263	0.266	0.930	0.992	2.322	0.281	1.017	1.087	2.345	0.272	0.996	1.066
2.544	0.234	0.957	1.029	2.475	0.264	1.040	1.115	2.512	0.252	1.013	1.088
2.719	0.217	0.971	1.048	2.686	0.242	1.066	1.149	2.816	0.218	1.027	1.111
2.904	0.199	0.976	1.057	2.981	0.214	1.090	1.183	2.943	0.207	1.035	1.123
3.156	0.179	0.986	1.074	3.302	0.187	1.098	1.200	3.342	0.177	1.053	1.151
3.408	0.161	0.984	1.077	3.455	0.176	1.100	1.205	3.514	0.165	1.054	1.157
3.668	0.145	0.983	1.081	3.580	0.168	1.102	1.210	3.601	0.159	1.053	1.157
3.888	0.132	0.970	1.071	3.898	0.148	1.093	1.207	3.962	0.137	1.039	1.148
0.300	1.078	1.019	1.019	0.408	1.058	1.017	1.017	0.618	1.014	1.002	1.002
0.577	1.017	1.002	1.002	0.518	1.036	1.012	1.012	0.681	0.987	0.970	0.998
0.798	0.943	1.009	1.033	0.905	0.859	1.016	1.041	0.936	0.816	0.994	1.019
1.116	0.692	1.007	1.038	1.034	0.750	1.007	1.035	1.024	0.732	0.973	0.999
1.219	0.612	0.981	1.014	1.275	0.566	0.957	0.991	1.299	0.526	0.907	0.940
1.464	0.465	0.926	0.965	1.386	0.502	0.935	0.972	1.471	0.451	0.904	0.942
1.706	0.367	0.884	0.929	1.715	0.374	0.908	0.954	1.730	0.387	0.951	1.000
1.775	0.346	0.878	0.924	1.908	0.338	0.941	0.994	1.838	0.367	0.973	1.026
2.071	0.295	0.916	0.972	2.162	0.300	0.987	1.050	2.181	0.313	1.042	1.110
2.406	0.253	0.959	1.028	2.284	0.285	1.007	1.075	2.434	0.283	1.090	1.169
2.604	0.232	0.981	1.056	2.610	0.246	1.043	1.123	2.537	0.272	1.108	1.191
2.674	0.224	0.982	1.059	2.795	0.227	1.058	1.143	2.779	0.247	1.142	1.234
2.961	0.198	0.999	1.084	3.079	0.201	1.070	1.164	2.993	0.229	1.173	1.274
3.168	0.181	1.003	1.093	3.241	0.188	1.072	1.169	3.374	0.200	1.206	1.319
3.467	0.160	1.005	1.101	3.495	0.169	1.071	1.174	3.461	0.194	1.216	1.332
3.579	0.152	1.000	1.098	3.619	0.160	1.066	1.171	3.620	0.183	1.221	1.341
3.889	0.134	0.989	1.092	3.920	0.140	1.047	1.156	3.968	0.162	1.225	1.355
0.307	1.055	0.998	0.998	0.452	1.051	1.017	1.017	0.661	1.005	1.002	1.002
0.519	1.038	1.014	1.014	0.534	1.028	1.007	1.007	0.710	0.984	0.983	1.009
0.810	0.931	1.007	1.031	0.908	0.857	1.016	1.041	0.995	0.790	1.020	1.047
1.152	0.656	0.987	1.018	1.082	0.718	1.010	1.040	1.046	0.745	1.012	1.040
1.274	0.568	0.958	0.992	1.328	0.533	0.944	0.979	1.142	0.661	0.987	1.017
1.516	0.436	0.907	0.947	1.446	0.475	0.931	0.969	1.487	0.456	0.926	0.966
1.598	0.402	0.892	0.934	1.625	0.400	0.908	0.951	1.774	0.378	0.959	1.009
1.921	0.328	0.922	0.975	1.829	0.343	0.905	0.954	1.923	0.350	0.986	1.042
2.010	0.314	0.937	0.993	2.159	0.289	0.948	1.009	2.096	0.323	1.019	1.083
2.391	0.265	0.998	1.068	2.433	0.255	0.981	1.052	2.363	0.288	1.068	1.142
2.558	0.246	1.017	1.093	2.471	0.250	0.985	1.057	2.645	0.258	1.116	1.202
2.754	0.226	1.033	1.116	2.771	0.218	1.005	1.085	2.690	0.254	1.123	1.211
3.049	0.200	1.051	1.142	2.928	0.203	1.008	1.093	2.951	0.230	1.154	1.251
3.193	0.189	1.060	1.155	3.318	0.171	1.010	1.104	3.353	0.199	1.191	1.303
3.424	0.172	1.061	1.162	3.434	0.163	1.008	1.104	3.517	0.184	1.177	1.291
3.757	0.150	1.055	1.162	3.683	0.146	0.999	1.099	3.781	0.163	1.156	1.274
3.891	0.142	1.047	1.156	3.949	0.131	0.983	1.087	3.969	0.151	1.142	1.262
0.325	1.094	1.034	1.034	0.479	1.043	1.011	1.011	0.421	1.092	1.035	1.035
0.431	1.063	1.022	1.022	0.536	1.032	1.010	1.010	0.560	1.043	1.018	1.018
0.819	0.929	1.013	1.037	0.867	0.905	1.032	1.057	0.992	0.826	1.065	1.093
1.109	0.701	1.013	1.043	1.018	0.746	0.986	1.013	1.060	0.766	1.055	1.085
1.243	0.598	0.981	1.015	1.151	0.625	0.940	0.970	1.234	0.626	1.019	1.054
1.462	0.468	0.929	0.969	1.419	0.468	0.898	0.935	1.506	0.465	0.959	1.001
1.710	0.372	0.900	0.945	1.645	0.377	0.868	0.910	1.656	0.420	0.976	1.023
1.914	0.322	0.902	0.953	1.813	0.327	0.853	0.899	1.905	0.350	0.973	1.028
2.117	0.289	0.924	0.982	2.082	0.278	0.870	0.924	2.246	0.290	1.004	1.071
2.258	0.269	0.937	0.999	2.281	0.250	0.882	0.942	2.347	0.277	1.016	1.087
2.466	0.244	0.956	1.025	2.619	0.211	0.899	0.968	2.509	0.256	1.028	1.104
2.730	0.215	0.968	1.045	2.760	0.197	0.903	0.975	2.806	0.223	1.045	1.129
3.048	0.186	0.974	1.058	2.988	0.178	0.909	0.987	2.996	0.205	1.049	1.139
3.219	0.172	0.971	1.059	3.332	0.153	0.909	0.994	3.356	0.173	1.039	1.137
3.435	0.156	0.966	1.058	3.506	0.142	0.907	0.995	3.451	0.166	1.037	1.136
3.677	0.140	0.951	1.047	3.779	0.127	0.900	0.992	3.794	0.144	1.022	1.127
3.893	0.127	0.935	1.032	3.959	0.117	0.886	0.979	3.976	0.132	1.006	1.113
0.266	1.098	1.034	1.034	0.541	1.034	1.011	1.011	0.476	1.064	1.022	1.022
0.450	1.054	1.019	1.019	0.674	0.998	0.978	1.006	0.552	1.046	1.020	1.020
0.869	0.902	1.031	1.055	1.001	0.806	1.047	1.075	0.875	0.909	1.045	1.070
1.057	0.740	1.016	1.045	1.052	0.748	1.024	1.052	1.013	0.801	1.053	1.081
1.230	0.604	0.980	1.013	1.295	0.566	0.974	1.009	1.348	0.552	0.995	1.033
1.479	0.461	0.930	0.969	1.490	0.460	0.936	0.976	1.461	0.488	0.970	1.010
1.610	0.407	0.912	0.955	1.693	0.381	0.910	0.956	1.668	0.402	0.942	0.988
1.787	0.354	0.905	0.953	1.872	0.335	0.912	0.962	1.824	0.352	0.926	0.976
1.926	0.328	0.927	0.980	2.177	0.292	0.968	1.031	2.082	0.296	0.927	0.984
2.382	0.267	1.001	1.072	2.444	0.260	1.009	1.081	2.266	0.268	0.939	1.003
2.539	0.250	1.020	1.096	2.516	0.251	1.014	1.089	2.484	0.240	0.953	1.022
2.766	0.226	1.039	1.122	2.695	0.232	1.028	1.109	2.701	0.216	0.961	1.037
2.908	0.213	1.048	1.135	3.085	0.198	1.056	1.148	2.933	0.194	0.964	1.046
3.184	0.189	1.055	1.150	3.217	0.188	1.062	1.158	3.196	0.171	0.958	1.044
3.423	0.171	1.056	1.156	3.442	0.172	1.068	1.170	3.461	0.152	0.952	1.043
3.706	0.152	1.049	1.154	3.687	0.155	1.064	1.170	3.791	0.131	0.933	1.028
3.895	0.141	1.041	1.149	3.962	0.139	1.053	1.164	3.981	0.121	0.919	1.016

Annex B: Data Concerning the SCA Lipped Channel Beams at Room and Elevated Temperatures

This annex includes two table sets (B1 and B2), concerning SCA lipped channel beams at room and elevated temperatures, and displays the whole set of numerical failure moments (i) obtained in this work (Tables B1.1-B1.3) and (ii) reported by Landesmann & Camotim (2016) (Tables B2.1-B.2.3). Each individual table provides, for the various lipped channel beams analyzed, (i) the distortional slenderness value ($\lambda_{D.T}$), (ii) the ratio between the failure and yield moments ($M_{u.T}/M_{y.T}$ – Tables B1.1 and B2.1), and (iii) the numerical-to-predicted failure moment ratios obtained with Eqs. (4) and (5), namely $M_{u.T}/M_{nD.T}$ (Tables B1.2 and B2.2) and $M_{u.T}/M_{nD.T*}$ (Tables B1.3 and B2.3).

Table B1.1: Data ($\lambda_{D.T}$ vs $M_{u.T}/M_{y.T}$) of the SCA lipped channel beams at room and elevated temperatures analysed in this work.
(*to be continued*)

Beam	100°C		200°C		300°C		400°C		500°C		600°C		700°C		800°C	
	$\lambda_{D.T}$	$\dfrac{M_{u.T}}{M_{y.T}}$	$\lambda_{D.T}$	$\dfrac{M_{u.T}}{M_{y.T}}$	$\lambda_{D.T}$	$\dfrac{M_{u.T}}{M_{y.T}}$	$\lambda_{D.T}$	$\dfrac{M_{u.T}}{M_{y.T}}$	$\lambda_{D.T}$	$\dfrac{M_{u.T}}{M_{y.T}}$	$\lambda_{D.T}$	$\dfrac{M_{u.T}}{M_{y.T}}$	$\lambda_{D.T}$	$\dfrac{M_{u.T}}{M_{y.T}}$	$\lambda_{D.T}$	$\dfrac{M_{u.T}}{M_{y.T}}$
LC 1	0.300	1.021	0.298	0.976	0.296	0.924	0.289	0.906	0.282	0.909	0.295	0.912	0.300	0.874	0.265	0.925
	0.800	0.945	0.796	0.886	0.790	0.810	0.771	0.732	0.752	0.757	0.787	0.700	0.800	0.683	0.706	0.791
	1.300	0.590	1.293	0.585	1.284	0.572	1.253	0.550	1.222	0.576	1.279	0.521	1.300	0.503	1.146	0.626
	1.800	0.316	1.790	0.326	1.777	0.337	1.735	0.348	1.692	0.366	1.771	0.333	1.800	0.322	1.587	0.408
	2.300	0.216	2.287	0.224	2.271	0.230	2.216	0.236	2.162	0.247	2.263	0.226	2.300	0.219	2.028	0.276
LC 2	0.350	1.014	0.348	0.970	0.346	0.922	0.337	0.895	0.329	0.891	0.344	0.837	0.350	0.806	0.309	0.895
	0.850	0.938	0.845	0.873	0.839	0.790	0.819	0.699	0.799	0.727	0.836	0.665	0.850	0.646	0.750	0.762
	1.350	0.549	1.342	0.548	1.333	0.539	1.301	0.529	1.269	0.555	1.328	0.503	1.350	0.486	1.191	0.610
	1.850	0.327	1.840	0.327	1.827	0.325	1.783	0.328	1.739	0.344	1.820	0.313	1.850	0.303	1.632	0.384
	2.350	0.229	2.337	0.231	2.320	0.231	2.265	0.231	2.209	0.242	2.312	0.221	2.350	0.214	2.073	0.267
LC 3	0.400	1.011	0.398	0.963	0.395	0.915	0.385	0.871	0.376	0.882	0.393	0.865	0.400	0.873	0.353	0.899
	0.900	0.923	0.895	0.857	0.889	0.766	0.867	0.664	0.846	0.693	0.885	0.626	0.900	0.606	0.794	0.730
	1.400	0.523	1.392	0.521	1.382	0.517	1.349	0.514	1.316	0.540	1.377	0.488	1.400	0.472	1.235	0.595
	1.900	0.311	1.889	0.312	1.876	0.310	1.831	0.314	1.786	0.330	1.869	0.301	1.900	0.291	1.676	0.370
	2.400	0.215	2.387	0.215	2.370	0.214	2.313	0.217	2.256	0.227	2.361	0.208	2.400	0.201	2.117	0.252
LC 4	0.450	1.009	0.447	0.951	0.444	0.900	0.434	0.851	0.423	0.863	0.443	0.834	0.450	0.821	0.397	0.879
	0.950	0.900	0.945	0.846	0.938	0.766	0.915	0.678	0.893	0.706	0.935	0.642	0.950	0.623	0.838	0.742
	1.450	0.498	1.442	0.497	1.432	0.494	1.397	0.494	1.363	0.519	1.426	0.471	1.450	0.455	1.279	0.576
	1.950	0.307	1.939	0.306	1.925	0.304	1.879	0.307	1.833	0.322	1.918	0.294	1.950	0.285	1.720	0.359
	2.450	0.215	2.436	0.215	2.419	0.214	2.361	0.216	2.303	0.226	2.410	0.208	2.450	0.201	2.161	0.251
LC 5	0.500	1.008	0.497	0.946	0.494	0.915	0.482	0.866	0.470	0.887	0.492	0.832	0.500	0.747	0.441	0.909
	1.000	0.861	0.994	0.820	0.987	0.753	0.964	0.676	0.940	0.704	0.984	0.642	1.000	0.623	0.882	0.742
	1.500	0.490	1.492	0.489	1.481	0.481	1.445	0.478	1.410	0.501	1.476	0.455	1.500	0.440	1.323	0.555
	2.000	0.313	1.989	0.313	1.975	0.310	1.927	0.311	1.880	0.326	1.967	0.298	2.000	0.288	1.764	0.362
	2.500	0.221	2.486	0.221	2.469	0.220	2.409	0.223	2.350	0.234	2.459	0.214	2.500	0.207	2.205	0.259
LC 6	0.550	1.004	0.547	0.933	0.543	0.860	0.530	0.797	0.517	0.814	0.541	0.773	0.550	0.762	0.485	0.834
	1.050	0.830	1.044	0.796	1.037	0.734	1.012	0.652	0.987	0.681	1.033	0.616	1.050	0.596	0.926	0.720
	1.550	0.445	1.541	0.444	1.531	0.442	1.494	0.446	1.457	0.469	1.525	0.426	1.550	0.412	1.367	0.523
	2.050	0.285	2.039	0.284	2.024	0.282	1.975	0.283	1.927	0.297	2.017	0.271	2.050	0.263	1.808	0.330
	2.550	0.203	2.536	0.204	2.518	0.203	2.457	0.205	2.397	0.214	2.509	0.196	2.550	0.190	2.249	0.237
LC 7	0.600	0.993	0.597	0.929	0.592	0.850	0.578	0.770	0.564	0.803	0.590	0.732	0.600	0.712	0.529	0.824
	1.100	0.769	1.094	0.747	1.086	0.696	1.060	0.618	1.034	0.648	1.082	0.582	1.100	0.563	0.970	0.690
	1.600	0.413	1.591	0.414	1.580	0.412	1.542	0.417	1.504	0.438	1.574	0.398	1.600	0.385	1.411	0.488
	2.100	0.256	2.088	0.261	2.074	0.263	2.024	0.267	1.974	0.280	2.066	0.256	2.100	0.248	1.852	0.312
	2.600	0.189	2.586	0.189	2.567	0.189	2.505	0.192	2.444	0.201	2.558	0.184	2.600	0.179	2.293	0.223
LC 8	0.650	0.995	0.646	0.928	0.642	0.849	0.626	0.769	0.611	0.803	0.639	0.728	0.650	0.704	0.573	0.830
	1.150	0.726	1.144	0.714	1.136	0.680	1.108	0.620	1.081	0.649	1.131	0.586	1.150	0.567	1.014	0.693
	1.650	0.401	1.641	0.400	1.629	0.397	1.590	0.402	1.551	0.422	1.623	0.384	1.650	0.371	1.455	0.471
	2.150	0.262	2.138	0.261	2.123	0.259	2.072	0.262	2.021	0.275	2.115	0.251	2.150	0.243	1.896	0.306
	2.650	0.187	2.635	0.187	2.617	0.186	2.554	0.189	2.491	0.198	2.607	0.182	2.650	0.176	2.337	0.220
LC 9	0.700	0.992	0.696	0.925	0.691	0.854	0.675	0.780	0.658	0.811	0.689	0.742	0.700	0.721	0.617	0.836
	1.200	0.684	1.193	0.672	1.185	0.643	1.156	0.595	1.128	0.624	1.180	0.562	1.200	0.543	1.058	0.670
	1.700	0.390	1.691	0.389	1.679	0.385	1.638	0.387	1.598	0.407	1.672	0.370	1.700	0.358	1.499	0.453
	2.200	0.256	2.188	0.255	2.172	0.254	2.120	0.258	2.068	0.270	2.164	0.247	2.200	0.239	1.940	0.301
	2.700	0.179	2.685	0.180	2.666	0.180	2.602	0.184	2.538	0.193	2.656	0.176	2.700	0.171	2.381	0.216
LC 10	0.750	0.977	0.746	0.906	0.741	0.823	0.723	0.741	0.705	0.769	0.738	0.705	0.750	0.686	0.661	0.809
	1.250	0.641	1.243	0.633	1.234	0.615	1.205	0.576	1.175	0.604	1.230	0.543	1.250	0.525	1.102	0.652
	1.750	0.370	1.740	0.369	1.728	0.366	1.686	0.369	1.645	0.387	1.722	0.352	1.750	0.341	1.543	0.431
	2.250	0.246	2.237	0.246	2.222	0.244	2.168	0.248	2.115	0.260	2.213	0.237	2.250	0.230	1.984	0.289
	2.750	0.175	2.735	0.175	2.715	0.175	2.650	0.179	2.585	0.188	2.705	0.171	2.750	0.166	2.425	0.209
LC 11	0.800	0.953	0.796	0.887	0.790	0.807	0.771	0.728	0.752	0.754	0.787	0.695	0.800	0.676	0.706	0.787
	1.300	0.594	1.293	0.588	1.284	0.575	1.253	0.552	1.222	0.579	1.279	0.522	1.300	0.504	1.146	0.628
	1.800	0.351	1.790	0.350	1.777	0.347	1.735	0.350	1.692	0.367	1.771	0.334	1.800	0.324	1.587	0.409
	2.300	0.235	2.287	0.235	2.271	0.234	2.216	0.238	2.162	0.249	2.263	0.228	2.300	0.221	2.028	0.278
	2.800	0.167	2.784	0.168	2.765	0.168	2.698	0.172	2.632	0.181	2.754	0.165	2.800	0.160	2.469	0.202
LC 12	0.850	0.941	0.845	0.884	0.839	0.808	0.819	0.730	0.799	0.757	0.836	0.697	0.850	0.679	0.750	0.794
	1.350	0.568	1.342	0.562	1.333	0.550	1.301	0.533	1.269	0.559	1.328	0.505	1.350	0.488	1.191	0.611
	1.850	0.342	1.840	0.341	1.827	0.339	1.783	0.341	1.739	0.358	1.820	0.326	1.850	0.315	1.632	0.398
	2.350	0.229	2.337	0.229	2.320	0.229	2.265	0.233	2.209	0.244	2.312	0.223	2.350	0.216	2.073	0.273
	2.850	0.162	2.834	0.162	2.814	0.163	2.746	0.168	2.679	0.176	2.804	0.161	2.850	0.155	2.513	0.198
LC 13	0.900	0.907	0.895	0.845	0.889	0.758	0.867	0.667	0.846	0.694	0.885	0.634	0.900	0.615	0.794	0.730
	1.400	0.510	1.392	0.509	1.382	0.506	1.349	0.504	1.316	0.529	1.377	0.479	1.400	0.463	1.235	0.583
	1.900	0.303	1.889	0.303	1.876	0.302	1.831	0.308	1.786	0.323	1.869	0.294	1.900	0.285	1.676	0.361
	2.400	0.208	2.387	0.208	2.370	0.207	2.313	0.211	2.256	0.221	2.361	0.202	2.400	0.196	2.117	0.245
	2.900	0.153	2.884	0.153	2.864	0.153	2.795	0.157	2.726	0.164	2.853	0.150	2.900	0.146	2.558	0.182
LC 14	0.950	0.894	0.945	0.840	0.938	0.759	0.915	0.669	0.893	0.698	0.935	0.633	0.950	0.613	0.838	0.736
	1.450	0.504	1.442	0.502	1.432	0.495	1.397	0.491	1.363	0.515	1.426	0.466	1.450	0.451	1.279	0.570
	1.950	0.311	1.939	0.310	1.925	0.307	1.879	0.310	1.833	0.325	1.918	0.297	1.950	0.288	1.720	0.363
	2.450	0.215	2.436	0.214	2.419	0.213	2.361	0.216	2.303	0.227	2.410	0.207	2.450	0.201	2.161	0.252
	2.950	0.156	2.934	0.156	2.913	0.156	2.843	0.160	2.773	0.167	2.902	0.153	2.950	0.148	2.602	0.187
LC 15	1.000	0.860	0.994	0.815	0.987	0.740	0.964	0.647	0.940	0.677	0.984	0.610	1.000	0.590	0.882	0.716
	1.500	0.470	1.492	0.468	1.481	0.465	1.445	0.465	1.410	0.488	1.476	0.443	1.500	0.428	1.323	0.543
	2.000	0.294	1.989	0.293	1.975	0.291	1.927	0.294	1.880	0.308	1.967	0.281	2.000	0.272	1.764	0.343
	2.500	0.206	2.486	0.206	2.469	0.205	2.409	0.208	2.350	0.217	2.459	0.199	2.500	0.193	2.205	0.241
	3.000	0.152	2.983	0.153	2.962	0.152	2.891	0.155	2.820	0.163	2.951	0.149	3.000	0.144	2.646	0.181
LC 16	1.050	0.804	1.044	0.770	1.037	0.711	1.012	0.636	0.987	0.664	1.033	0.602	1.050	0.583	0.926	0.704
	1.550	0.440	1.541	0.439	1.531	0.436	1.494	0.437	1.457	0.459	1.525	0.417	1.550	0.403	1.367	0.510
	2.050	0.277	2.039	0.277	2.024	0.276	1.975	0.280	1.927	0.293	2.017	0.268	2.050	0.259	1.808	0.327
	2.550	0.193	2.536	0.193	2.518	0.193	2.457	0.197	2.397	0.206	2.509	0.188	2.550	0.183	2.249	0.230
	3.050	0.141	3.033	0.141	3.012	0.142	2.939	0.146	2.867	0.153	3.000	0.140	3.050	0.135	2.690	0.171

Table B1.1: Data ($\lambda_{D,T}$ vs $M_{u,T}/M_{y,T}$) of the SCA lipped channel beams at room and elevated temperatures analysed in this work.
(*continuation*)

Beam	100°C		200°C		300°C		400°C		500°C		600°C		700°C		800°C	
	$\lambda_{D.T}$	$\dfrac{M_{u.T}}{M_{y.T}}$	$\lambda_{D.T}$	$\dfrac{M_{u.T}}{M_{y.T}}$	$\lambda_{D.T}$	$\dfrac{M_{u.T}}{M_{y.T}}$	$\lambda_{D.T}$	$\dfrac{M_{u.T}}{M_{y.T}}$	$\lambda_{D.T}$	$\dfrac{M_{u.T}}{M_{y.T}}$	$\lambda_{D.T}$	$\dfrac{M_{u.T}}{M_{y.T}}$	$\lambda_{D.T}$	$\dfrac{M_{u.T}}{M_{y.T}}$	$\lambda_{D.T}$	$\dfrac{M_{u.T}}{M_{y.T}}$
LC 17	1.100	0.769	1.094	0.744	1.086	0.696	1.060	0.626	1.034	0.655	1.082	0.592	1.100	0.572	0.970	0.698
	1.600	0.428	1.591	0.426	1.580	0.422	1.542	0.423	1.504	0.444	1.574	0.403	1.600	0.390	1.411	0.494
	2.100	0.274	2.088	0.274	2.074	0.272	2.024	0.276	1.974	0.289	2.066	0.264	2.100	0.256	1.852	0.322
	2.600	0.191	2.586	0.191	2.567	0.191	2.505	0.195	2.444	0.204	2.558	0.187	2.600	0.181	2.293	0.228
	3.100	0.139	3.083	0.140	3.061	0.140	2.987	0.144	2.914	0.152	3.050	0.138	3.100	0.134	2.734	0.170
LC 18	1.150	0.715	1.144	0.698	1.136	0.667	1.108	0.613	1.081	0.643	1.131	0.579	1.150	0.559	1.014	0.689
	1.650	0.406	1.641	0.404	1.629	0.401	1.590	0.401	1.551	0.421	1.623	0.383	1.650	0.370	1.455	0.468
	2.150	0.261	2.138	0.261	2.123	0.259	2.072	0.264	2.021	0.277	2.115	0.252	2.150	0.244	1.896	0.309
	2.650	0.178	2.635	0.179	2.617	0.180	2.554	0.185	2.491	0.194	2.607	0.177	2.650	0.171	2.337	0.218
	3.150	0.126	3.132	0.128	3.110	0.130	3.035	0.135	2.961	0.142	3.099	0.129	3.150	0.125	2.778	0.160
LC 19	1.200	0.665	1.193	0.656	1.185	0.633	1.156	0.585	1.128	0.613	1.180	0.554	1.200	0.536	1.058	0.658
	1.700	0.371	1.691	0.370	1.679	0.369	1.638	0.375	1.598	0.393	1.672	0.358	1.700	0.346	1.499	0.439
	2.200	0.242	2.188	0.242	2.172	0.242	2.120	0.246	2.068	0.258	2.164	0.236	2.200	0.228	1.940	0.287
	2.700	0.172	2.685	0.172	2.666	0.173	2.602	0.177	2.538	0.185	2.656	0.169	2.700	0.164	2.381	0.206
	3.200	0.127	3.182	0.128	3.160	0.129	3.084	0.133	3.008	0.139	3.148	0.127	3.200	0.123	2.822	0.156
LC 20	1.250	0.628	1.243	0.622	1.234	0.606	1.205	0.571	1.175	0.599	1.230	0.539	1.250	0.521	1.102	0.646
	1.750	0.360	1.740	0.359	1.728	0.357	1.686	0.362	1.645	0.379	1.722	0.346	1.750	0.334	1.543	0.424
	2.250	0.240	2.237	0.240	2.222	0.239	2.168	0.243	2.115	0.254	2.213	0.232	2.250	0.225	1.984	0.283
	2.750	0.172	2.735	0.173	2.715	0.173	2.650	0.176	2.585	0.184	2.705	0.169	2.750	0.164	2.425	0.206
	3.250	0.128	3.232	0.129	3.209	0.130	3.132	0.133	3.055	0.140	3.197	0.128	3.250	0.124	2.866	0.156
LC 21	1.300	0.601	1.293	0.594	1.284	0.580	1.253	0.555	1.222	0.583	1.279	0.525	1.300	0.507	1.146	0.633
	1.800	0.357	1.790	0.356	1.777	0.352	1.735	0.354	1.692	0.372	1.771	0.338	1.800	0.327	1.587	0.414
	2.300	0.239	2.287	0.239	2.271	0.238	2.216	0.241	2.162	0.253	2.263	0.231	2.300	0.224	2.028	0.282
	2.800	0.170	2.784	0.171	2.765	0.171	2.698	0.175	2.632	0.183	2.754	0.167	2.800	0.162	2.469	0.205
	3.300	0.125	3.282	0.126	3.258	0.127	3.180	0.131	3.102	0.138	3.246	0.126	3.300	0.121	2.910	0.155
LC 22	1.350	0.544	1.342	0.541	1.333	0.534	1.301	0.524	1.269	0.550	1.328	0.497	1.350	0.480	1.191	0.601
	1.850	0.320	1.840	0.320	1.827	0.319	1.783	0.324	1.739	0.340	1.820	0.310	1.850	0.300	1.632	0.380
	2.350	0.217	2.337	0.217	2.320	0.217	2.265	0.221	2.209	0.231	2.312	0.212	2.350	0.205	2.073	0.257
	2.850	0.157	2.834	0.158	2.814	0.158	2.746	0.162	2.679	0.169	2.804	0.155	2.850	0.150	2.513	0.189
	3.350	0.118	3.331	0.118	3.308	0.119	3.228	0.123	3.149	0.129	3.296	0.118	3.350	0.114	2.954	0.145
LC 23	1.400	0.532	1.392	0.528	1.382	0.518	1.349	0.507	1.316	0.532	1.377	0.482	1.400	0.466	1.235	0.585
	1.900	0.325	1.889	0.324	1.876	0.322	1.831	0.325	1.786	0.341	1.869	0.310	1.900	0.300	1.676	0.380
	2.400	0.219	2.387	0.219	2.370	0.219	2.313	0.223	2.256	0.234	2.361	0.214	2.400	0.207	2.117	0.261
	2.900	0.155	2.884	0.156	2.864	0.157	2.795	0.161	2.726	0.170	2.853	0.155	2.900	0.150	2.558	0.190
	3.400	0.114	3.381	0.115	3.357	0.116	3.276	0.121	3.196	0.127	3.345	0.116	3.400	0.112	2.999	0.143
LC 24	1.450	0.495	1.442	0.494	1.432	0.490	1.397	0.488	1.363	0.512	1.426	0.464	1.450	0.449	1.279	0.567
	1.950	0.304	1.939	0.303	1.925	0.301	1.879	0.305	1.833	0.319	1.918	0.292	1.950	0.282	1.720	0.357
	2.450	0.211	2.436	0.211	2.419	0.210	2.361	0.213	2.303	0.223	2.410	0.205	2.450	0.198	2.161	0.248
	2.950	0.156	2.934	0.156	2.913	0.156	2.843	0.159	2.773	0.166	2.902	0.153	2.950	0.148	2.602	0.185
	3.450	0.118	3.431	0.119	3.407	0.119	3.325	0.123	3.243	0.128	3.394	0.117	3.450	0.114	3.043	0.144
LC 25	1.500	0.472	1.492	0.470	1.481	0.467	1.445	0.467	1.410	0.490	1.476	0.445	1.500	0.430	1.323	0.545
	2.000	0.294	1.989	0.294	1.975	0.292	1.927	0.295	1.880	0.309	1.967	0.283	2.000	0.274	1.764	0.345
	2.500	0.206	2.486	0.206	2.469	0.205	2.409	0.208	2.350	0.218	2.459	0.200	2.500	0.194	2.205	0.242
	3.000	0.152	2.983	0.152	2.962	0.152	2.891	0.155	2.820	0.163	2.951	0.149	3.000	0.144	2.646	0.182
	3.500	0.115	3.481	0.116	3.456	0.116	3.373	0.120	3.290	0.126	3.443	0.115	3.500	0.111	3.087	0.141
LC 26	1.550	0.453	1.541	0.451	1.531	0.448	1.494	0.448	1.457	0.471	1.525	0.427	1.550	0.413	1.367	0.524
	2.050	0.290	2.039	0.289	2.024	0.287	1.975	0.289	1.927	0.303	2.017	0.277	2.050	0.268	1.808	0.337
	2.550	0.206	2.536	0.206	2.518	0.205	2.457	0.208	2.397	0.217	2.509	0.199	2.550	0.193	2.249	0.241
	3.050	0.153	3.033	0.154	3.012	0.154	2.939	0.156	2.867	0.164	3.000	0.150	3.050	0.145	2.690	0.183
	3.550	0.117	3.530	0.117	3.505	0.118	3.421	0.121	3.336	0.127	3.492	0.116	3.550	0.113	3.131	0.143
LC 27	1.600	0.429	1.591	0.428	1.580	0.424	1.542	0.427	1.504	0.448	1.574	0.407	1.600	0.394	1.411	0.500
	2.100	0.279	2.088	0.278	2.074	0.276	2.024	0.279	1.974	0.292	2.066	0.267	2.100	0.259	1.852	0.324
	2.600	0.200	2.586	0.200	2.567	0.199	2.505	0.202	2.444	0.211	2.558	0.193	2.600	0.187	2.293	0.234
	3.100	0.149	3.083	0.150	3.061	0.150	2.987	0.152	2.914	0.160	3.050	0.146	3.100	0.142	2.734	0.178
	3.600	0.114	3.580	0.115	3.555	0.115	3.469	0.119	3.383	0.125	3.541	0.114	3.600	0.110	3.175	0.139
LC 28	1.650	0.412	1.641	0.410	1.629	0.407	1.590	0.409	1.551	0.429	1.623	0.390	1.650	0.377	1.455	0.478
	2.150	0.271	2.138	0.270	2.123	0.268	2.072	0.271	2.021	0.284	2.115	0.260	2.150	0.252	1.896	0.315
	2.650	0.194	2.635	0.194	2.617	0.193	2.554	0.196	2.491	0.206	2.607	0.188	2.650	0.182	2.337	0.228
	3.150	0.144	3.132	0.145	3.110	0.145	3.035	0.148	2.961	0.156	3.099	0.142	3.150	0.138	2.778	0.174
	3.650	0.110	3.630	0.111	3.604	0.111	3.517	0.115	3.430	0.121	3.591	0.110	3.650	0.107	3.219	0.136
LC 29	1.700	0.399	1.691	0.397	1.679	0.393	1.638	0.393	1.598	0.412	1.672	0.375	1.700	0.363	1.499	0.459
	2.200	0.267	2.188	0.266	2.172	0.264	2.120	0.267	2.068	0.279	2.164	0.255	2.200	0.247	1.940	0.310
	2.700	0.191	2.685	0.191	2.666	0.191	2.602	0.194	2.538	0.203	2.656	0.186	2.700	0.180	2.381	0.226
	3.200	0.141	3.182	0.142	3.160	0.143	3.084	0.146	3.008	0.154	3.148	0.140	3.200	0.136	2.822	0.172
	3.700	0.107	3.679	0.108	3.653	0.109	3.565	0.113	3.477	0.119	3.640	0.108	3.700	0.105	3.263	0.134
LC 30	1.750	0.372	1.740	0.371	1.728	0.368	1.686	0.371	1.645	0.389	1.722	0.354	1.750	0.343	1.543	0.434
	2.250	0.249	2.237	0.249	2.222	0.248	2.168	0.251	2.115	0.263	2.213	0.240	2.250	0.233	1.984	0.292
	2.750	0.179	2.735	0.180	2.715	0.179	2.650	0.183	2.585	0.191	2.705	0.175	2.750	0.170	2.425	0.213
	3.250	0.133	3.232	0.134	3.209	0.134	3.132	0.138	3.055	0.145	3.197	0.132	3.250	0.128	2.866	0.162
	3.750	0.101	3.729	0.102	3.703	0.103	3.614	0.107	3.524	0.112	3.689	0.102	3.750	0.099	3.307	0.127

Table B1.2: Data ($\lambda_{D,T}$ vs $M_{u,T}/M_{nD,T}$) of the SCA lipped channel beams at room and elevated temperatures analysed in this work.
(*to be continued*)

Beam	100°C		200°C		300°C		400°C		500°C		600°C		700°C		800°C	
	$\lambda_{D,T}$	$\dfrac{M_{u,T}}{M_{nD,T}}$	$\lambda_{D,T}$	$\dfrac{M_{u,T}}{M_{nD,T}}$	$\lambda_{D,T}$	$\dfrac{M_{u,T}}{M_{nD,T}}$	$\lambda_{D,T}$	$\dfrac{M_{u,T}}{M_{nD,T}}$	$\lambda_{D,T}$	$\dfrac{M_{u,T}}{M_{nD,T}}$	$\lambda_{D,T}$	$\dfrac{M_{u,T}}{M_{nD,T}}$	$\lambda_{D,T}$	$\dfrac{M_{u,T}}{M_{nD,T}}$	$\lambda_{D,T}$	$\dfrac{M_{u,T}}{M_{nD,T}}$
LC 1	0.300	0.966	0.298	0.922	0.296	0.873	0.289	0.855	0.282	0.858	0.295	0.862	0.300	0.826	0.265	0.870
	0.800	1.013	0.796	0.946	0.790	0.861	0.771	0.765	0.752	0.781	0.787	0.742	0.800	0.732	0.706	0.796
	1.300	1.099	1.293	1.082	1.284	1.047	1.253	0.973	1.222	0.986	1.279	0.948	1.300	0.938	1.146	0.983
	1.800	0.955	1.790	0.979	1.777	0.999	1.735	0.995	1.692	1.005	1.771	0.982	1.800	0.975	1.587	1.017
	2.300	0.967	2.287	0.994	2.271	1.005	2.216	0.994	2.162	1.000	2.263	0.984	2.300	0.978	2.028	1.007
LC 2	0.350	0.974	0.348	0.932	0.346	0.885	0.337	0.859	0.329	0.854	0.344	0.804	0.350	0.775	0.309	0.855
	0.850	1.054	0.845	0.977	0.839	0.879	0.819	0.763	0.799	0.778	0.836	0.737	0.850	0.727	0.750	0.784
	1.350	1.079	1.342	1.068	1.333	1.040	1.301	0.987	1.269	1.000	1.328	0.965	1.350	0.955	1.191	1.007
	1.850	1.034	1.840	1.023	1.827	1.007	1.783	0.978	1.739	0.987	1.820	0.965	1.850	0.958	1.632	0.999
	2.350	1.060	2.337	1.061	2.320	1.047	2.265	1.007	2.209	1.012	2.312	0.997	2.350	0.993	2.073	1.009
LC 3	0.400	0.971	0.398	0.924	0.395	0.878	0.385	0.834	0.376	0.844	0.393	0.829	0.400	0.838	0.353	0.857
	0.900	1.095	0.895	1.011	0.889	0.897	0.867	0.760	0.846	0.776	0.885	0.731	0.900	0.719	0.794	0.778
	1.400	1.082	1.392	1.071	1.382	1.051	1.349	1.010	1.316	1.024	1.377	0.988	1.400	0.977	1.235	1.033
	1.900	1.024	1.889	1.018	1.876	1.001	1.831	0.977	1.786	0.986	1.869	0.966	1.900	0.959	1.676	1.001
	2.400	1.031	2.387	1.020	2.370	1.003	2.313	0.977	2.256	0.982	2.361	0.969	2.400	0.965	2.117	0.986
LC 4	0.450	0.970	0.447	0.914	0.444	0.864	0.434	0.816	0.423	0.826	0.443	0.801	0.450	0.790	0.397	0.838
	0.950	1.129	0.945	1.054	0.938	0.948	0.915	0.817	0.893	0.830	0.935	0.791	0.950	0.781	0.838	0.824
	1.450	1.086	1.442	1.075	1.432	1.057	1.397	1.021	1.363	1.034	1.426	1.002	1.450	0.992	1.279	1.049
	1.950	1.055	1.939	1.042	1.925	1.023	1.879	0.994	1.833	1.001	1.918	0.982	1.950	0.977	1.720	1.012
	2.450	1.067	2.436	1.057	2.419	1.040	2.361	1.010	2.303	1.014	2.410	1.001	2.450	0.997	2.161	1.014
LC 5	0.500	0.968	0.497	0.909	0.494	0.878	0.482	0.829	0.470	0.847	0.492	0.798	0.500	0.718	0.441	0.862
	1.000	1.144	0.994	1.082	0.987	0.985	0.964	0.861	0.940	0.872	0.984	0.837	1.000	0.827	0.882	0.863
	1.500	1.122	1.492	1.110	1.481	1.083	1.445	1.036	1.410	1.049	1.476	1.017	1.500	1.008	1.323	1.059
	2.000	1.119	1.989	1.107	1.975	1.086	1.927	1.048	1.880	1.055	1.967	1.036	2.000	1.030	1.764	1.060
	2.500	1.131	2.486	1.121	2.469	1.103	2.409	1.076	2.350	1.081	2.459	1.066	2.500	1.061	2.205	1.082
LC 6	0.550	0.983	0.547	0.913	0.543	0.841	0.530	0.778	0.517	0.793	0.541	0.756	0.550	0.746	0.485	0.808
	1.050	1.167	1.044	1.113	1.037	1.016	1.012	0.877	0.987	0.890	1.033	0.849	1.050	0.838	0.926	0.879
	1.550	1.071	1.541	1.060	1.531	1.043	1.494	1.016	1.457	1.029	1.525	1.000	1.550	0.992	1.367	1.046
	2.050	1.060	2.039	1.047	2.024	1.025	1.975	0.992	1.927	0.999	2.017	0.981	2.050	0.976	1.808	1.006
	2.550	1.076	2.536	1.070	2.518	1.051	2.457	1.019	2.397	1.023	2.509	1.011	2.550	1.007	2.249	1.021
LC 7	0.600	0.982	0.597	0.918	0.592	0.840	0.578	0.760	0.564	0.790	0.590	0.723	0.600	0.704	0.529	0.806
	1.100	1.145	1.094	1.105	1.086	1.021	1.060	0.880	1.034	0.894	1.082	0.850	1.100	0.839	0.970	0.885
	1.600	1.043	1.591	1.036	1.580	1.020	1.542	0.995	1.504	1.007	1.574	0.980	1.600	0.971	1.411	1.023
	2.100	0.990	2.088	0.999	2.074	0.996	2.024	0.973	1.974	0.979	2.066	0.963	2.100	0.958	1.852	0.988
	2.600	1.033	2.586	1.024	2.567	1.010	2.505	0.986	2.444	0.990	2.558	0.979	2.600	0.975	2.293	0.992
LC 8	0.650	0.992	0.646	0.924	0.642	0.845	0.626	0.764	0.611	0.796	0.639	0.725	0.650	0.702	0.573	0.818
	1.150	1.145	1.144	1.118	1.136	1.055	1.108	0.933	1.081	0.946	1.131	0.905	1.150	0.894	1.014	0.935
	1.650	1.061	1.641	1.049	1.629	1.031	1.590	1.005	1.551	1.016	1.623	0.991	1.650	0.982	1.455	1.032
	2.150	1.050	2.138	1.037	2.123	1.019	2.072	0.991	2.021	0.997	2.115	0.981	2.150	0.976	1.896	1.004
	2.650	1.054	2.635	1.045	2.617	1.029	2.554	1.004	2.491	1.009	2.607	0.996	2.650	0.992	2.337	1.011
LC 9	0.700	0.996	0.696	0.928	0.691	0.856	0.675	0.780	0.658	0.809	0.689	0.743	0.700	0.724	0.617	0.828
	1.200	1.142	1.193	1.114	1.185	1.056	1.156	0.945	1.128	0.959	1.180	0.917	1.200	0.906	1.058	0.952
	1.700	1.080	1.691	1.067	1.679	1.047	1.638	1.014	1.598	1.024	1.672	0.999	1.700	0.991	1.499	1.037
	2.200	1.064	2.188	1.053	2.172	1.036	2.120	1.010	2.068	1.017	2.164	1.000	2.200	0.994	1.940	1.025
	2.700	1.040	2.685	1.035	2.666	1.025	2.602	1.007	2.538	1.014	2.656	0.997	2.700	0.992	2.381	1.022
LC 10	0.750	1.006	0.746	0.931	0.741	0.842	0.723	0.751	0.705	0.773	0.738	0.720	0.750	0.707	0.661	0.807
	1.250	1.131	1.243	1.109	1.234	1.066	1.205	0.966	1.175	0.981	1.230	0.938	1.250	0.926	1.102	0.974
	1.750	1.072	1.740	1.058	1.728	1.039	1.686	1.009	1.645	1.019	1.722	0.995	1.750	0.987	1.543	1.031
	2.250	1.061	2.237	1.050	2.222	1.033	2.168	1.007	2.115	1.013	2.213	0.997	2.250	0.992	1.984	1.020
	2.750	1.046	2.735	1.041	2.715	1.029	2.650	1.008	2.585	1.015	2.705	0.999	2.750	0.994	2.425	1.021
LC 11	0.800	1.022	0.796	0.947	0.790	0.857	0.771	0.761	0.752	0.777	0.787	0.737	0.800	0.725	0.706	0.791
	1.300	1.107	1.293	1.088	1.284	1.052	1.253	0.976	1.222	0.990	1.279	0.951	1.300	0.940	1.146	0.987
	1.800	1.061	1.790	1.049	1.777	1.030	1.735	1.000	1.692	1.009	1.771	0.986	1.800	0.979	1.587	1.021
	2.300	1.050	2.287	1.040	2.271	1.025	2.216	1.002	2.162	1.008	2.263	0.992	2.300	0.987	2.028	1.014
	2.800	1.030	2.784	1.027	2.765	1.017	2.698	0.999	2.632	1.006	2.754	0.990	2.800	0.985	2.469	1.013
LC 12	0.850	1.059	0.845	0.989	0.839	0.900	0.819	0.797	0.799	0.811	0.836	0.773	0.850	0.763	0.750	0.818
	1.350	1.116	1.342	1.097	1.333	1.062	1.301	0.994	1.269	1.007	1.328	0.970	1.350	0.960	1.191	1.009
	1.850	1.080	1.840	1.068	1.827	1.048	1.783	1.017	1.739	1.026	1.820	1.003	1.850	0.996	1.632	1.036
	2.350	1.058	2.337	1.051	2.320	1.037	2.265	1.015	2.209	1.022	2.312	1.004	2.350	0.999	2.073	1.031
	2.850	1.026	2.834	1.023	2.814	1.015	2.746	1.002	2.679	1.010	2.804	0.993	2.850	0.987	2.513	1.021
LC 13	0.900	1.075	0.895	0.996	0.889	0.887	0.867	0.764	0.846	0.777	0.885	0.740	0.900	0.730	0.794	0.778
	1.400	1.056	1.392	1.047	1.382	1.028	1.349	0.989	1.316	1.003	1.377	0.969	1.400	0.958	1.235	1.012
	1.900	0.999	1.889	0.989	1.876	0.975	1.831	0.956	1.786	0.964	1.869	0.945	1.900	0.939	1.676	0.979
	2.400	0.995	2.387	0.987	2.370	0.973	2.313	0.951	2.256	0.955	2.361	0.943	2.400	0.940	2.117	0.959
	2.900	1.000	2.884	0.993	2.864	0.982	2.795	0.963	2.726	0.967	2.853	0.957	2.900	0.953	2.558	0.968
LC 14	0.950	1.121	0.945	1.047	0.938	0.939	0.915	0.807	0.893	0.821	0.935	0.780	0.950	0.769	0.838	0.818
	1.450	1.099	1.442	1.084	1.432	1.058	1.397	1.013	1.363	1.027	1.426	0.992	1.450	0.982	1.279	1.037
	1.950	1.068	1.939	1.054	1.925	1.034	1.879	1.005	1.833	1.013	1.918	0.993	1.950	0.986	1.720	1.024
	2.450	1.063	2.436	1.052	2.419	1.035	2.361	1.009	2.303	1.015	2.410	1.000	2.450	0.995	2.161	1.020
	2.950	1.047	2.934	1.042	2.913	1.030	2.843	1.010	2.773	1.016	2.902	1.001	2.950	0.996	2.602	1.023
LC 15	1.000	1.142	0.994	1.075	0.987	0.968	0.964	0.825	0.940	0.839	0.984	0.795	1.000	0.783	0.882	0.833
	1.500	1.077	1.492	1.064	1.481	1.045	1.445	1.008	1.410	1.021	1.476	0.990	1.500	0.980	1.323	1.036
	2.000	1.049	1.989	1.036	1.975	1.018	1.927	0.989	1.880	0.997	1.967	0.978	2.000	0.972	1.764	1.007
	2.500	1.054	2.486	1.043	2.469	1.026	2.409	1.000	2.350	1.005	2.459	0.992	2.500	0.988	2.205	1.008
	3.000	1.054	2.983	1.046	2.962	1.032	2.891	1.011	2.820	1.015	2.951	1.003	3.000	0.999	2.646	1.018
LC 16	1.050	1.131	1.044	1.076	1.037	0.985	1.012	0.856	0.987	0.868	1.033	0.830	1.050	0.820	0.926	0.859
	1.550	1.058	1.541	1.047	1.531	1.029	1.494	0.996	1.457	1.007	1.525	0.979	1.550	0.971	1.367	1.021
	2.050	1.030	2.039	1.020	2.024	1.004	1.975	0.980	1.927	0.987	2.017	0.969	2.050	0.964	1.808	0.997
	2.550	1.020	2.536	1.013	2.518	1.000	2.457	0.979	2.397	0.985	2.509	0.971	2.550	0.966	2.249	0.991
	3.050	0.999	3.033	0.996	3.012	0.989	2.939	0.975	2.867	0.981	3.000	0.966	3.050	0.961	2.690	0.989

Table B1.2: Data ($\lambda_{D.T}$ vs $M_{u.T}/M_{nD.T}$) of the SCA lipped channel beams at room and elevated temperatures analysed in this work. (*continuation*)

Beam	100°C $\lambda_{D.T}$	100°C $\frac{M_{u.T}}{M_{nD.T}}$	200°C $\lambda_{D.T}$	200°C $\frac{M_{u.T}}{M_{nD.T}}$	300°C $\lambda_{D.T}$	300°C $\frac{M_{u.T}}{M_{nD.T}}$	400°C $\lambda_{D.T}$	400°C $\frac{M_{u.T}}{M_{nD.T}}$	500°C $\lambda_{D.T}$	500°C $\frac{M_{u.T}}{M_{nD.T}}$	600°C $\lambda_{D.T}$	600°C $\frac{M_{u.T}}{M_{nD.T}}$	700°C $\lambda_{D.T}$	700°C $\frac{M_{u.T}}{M_{nD.T}}$	800°C $\lambda_{D.T}$	800°C $\frac{M_{u.T}}{M_{nD.T}}$
	1.100	1.146	1.094	1.100	1.086	1.020	1.060	0.891	1.034	0.904	1.082	0.864	1.100	0.853	0.970	0.896
	1.600	1.080	1.591	1.067	1.580	1.046	1.542	1.010	1.504	1.021	1.574	0.993	1.600	0.985	1.411	1.034
LC 17	2.100	1.060	2.088	1.048	2.074	1.030	2.024	1.003	1.974	1.011	2.066	0.993	2.100	0.987	1.852	1.020
	2.600	1.040	2.586	1.035	2.567	1.023	2.505	1.002	2.444	1.009	2.558	0.992	2.600	0.987	2.293	1.016
	3.100	1.015	3.083	1.010	3.061	1.003	2.987	0.992	2.914	0.999	3.050	0.983	3.100	0.977	2.734	1.009
	1.150	1.127	1.144	1.093	1.136	1.034	1.108	0.922	1.081	0.937	1.131	0.894	1.150	0.882	1.014	0.930
	1.650	1.075	1.641	1.061	1.629	1.040	1.590	1.003	1.551	1.014	1.623	0.988	1.650	0.980	1.455	1.026
LC 18	2.150	1.046	2.138	1.035	2.123	1.019	2.072	0.997	2.021	1.005	2.115	0.986	2.150	0.980	1.896	1.016
	2.650	1.003	2.635	1.000	2.617	0.992	2.554	0.978	2.491	0.986	2.607	0.968	2.650	0.963	2.337	0.999
	3.150	0.948	3.132	0.950	3.110	0.952	3.035	0.951	2.961	0.959	3.099	0.942	3.150	0.936	2.778	0.974
	1.200	1.110	1.193	1.087	1.185	1.038	1.156	0.930	1.128	0.943	1.180	0.904	1.200	0.894	1.058	0.934
	1.700	1.026	1.691	1.017	1.679	1.003	1.638	0.980	1.598	0.990	1.672	0.967	1.700	0.960	1.499	1.005
LC 19	2.200	1.006	2.188	0.998	2.172	0.985	2.120	0.964	2.068	0.970	2.164	0.955	2.200	0.950	1.940	0.978
	2.700	0.999	2.685	0.993	2.666	0.984	2.602	0.966	2.538	0.971	2.656	0.958	2.700	0.954	2.381	0.976
	3.200	0.979	3.182	0.975	3.160	0.971	3.084	0.960	3.008	0.966	3.148	0.952	3.200	0.947	2.822	0.973
	1.250	1.109	1.243	1.089	1.234	1.050	1.205	0.958	1.175	0.972	1.230	0.930	1.250	0.919	1.102	0.964
	1.750	1.043	1.740	1.032	1.728	1.015	1.686	0.989	1.645	0.999	1.722	0.976	1.750	0.968	1.543	1.013
LC 20	2.250	1.034	2.237	1.025	2.222	1.010	2.168	0.986	2.115	0.991	2.213	0.976	2.250	0.972	1.984	0.997
	2.750	1.032	2.735	1.025	2.715	1.013	2.650	0.993	2.585	0.998	2.705	0.985	2.750	0.981	2.425	1.002
	3.250	1.013	3.232	1.011	3.209	1.004	3.132	0.990	3.055	0.996	3.197	0.982	3.250	0.977	2.866	1.003
	1.300	1.120	1.293	1.099	1.284	1.062	1.253	0.982	1.222	0.996	1.279	0.956	1.300	0.945	1.146	0.995
	1.800	1.082	1.790	1.067	1.777	1.045	1.735	1.012	1.692	1.022	1.771	0.998	1.800	0.991	1.587	1.032
LC 21	2.300	1.071	2.287	1.060	2.271	1.042	2.216	1.015	2.162	1.022	2.263	1.005	2.300	1.000	2.028	1.029
	2.800	1.047	2.784	1.043	2.765	1.032	2.698	1.013	2.632	1.020	2.754	1.003	2.800	0.998	2.469	1.028
	3.300	1.017	3.282	1.014	3.258	1.009	3.180	0.999	3.102	1.007	3.246	0.990	3.300	0.985	2.910	1.018
	1.350	1.068	1.342	1.056	1.333	1.030	1.301	0.977	1.269	0.990	1.328	0.955	1.350	0.944	1.191	0.993
	1.850	1.012	1.840	1.003	1.827	0.989	1.783	0.966	1.739	0.975	1.820	0.955	1.850	0.948	1.632	0.988
LC 22	2.350	1.003	2.337	0.996	2.320	0.984	2.265	0.962	2.209	0.968	2.312	0.954	2.350	0.949	2.073	0.973
	2.850	0.998	2.834	0.993	2.814	0.984	2.746	0.967	2.679	0.972	2.804	0.959	2.850	0.955	2.513	0.976
	3.350	0.979	3.331	0.975	3.308	0.971	3.228	0.961	3.149	0.967	3.296	0.953	3.350	0.948	2.954	0.975
	1.400	1.102	1.392	1.084	1.382	1.054	1.349	0.996	1.316	1.009	1.377	0.975	1.400	0.964	1.235	1.015
	1.900	1.070	1.889	1.059	1.876	1.039	1.831	1.009	1.786	1.018	1.869	0.996	1.900	0.989	1.676	1.028
LC 23	2.400	1.048	2.387	1.041	2.370	1.028	2.313	1.007	2.256	1.014	2.361	0.996	2.400	0.991	2.117	1.022
	2.900	1.016	2.884	1.012	2.864	1.005	2.795	0.993	2.726	1.001	2.853	0.984	2.900	0.978	2.558	1.011
	3.400	0.973	3.381	0.974	3.357	0.972	3.276	0.968	3.196	0.976	3.345	0.960	3.400	0.955	2.999	0.990
	1.450	1.080	1.442	1.068	1.432	1.048	1.397	1.008	1.363	1.021	1.426	0.988	1.450	0.978	1.279	1.033
	1.950	1.041	1.939	1.030	1.925	1.012	1.879	0.986	1.833	0.994	1.918	0.975	1.950	0.969	1.720	1.006
LC 24	2.450	1.045	2.436	1.036	2.419	1.020	2.361	0.995	2.303	1.000	2.410	0.987	2.450	0.983	2.161	1.002
	2.950	1.047	2.934	1.039	2.913	1.027	2.843	1.006	2.773	1.011	2.902	0.999	2.950	0.995	2.602	1.013
	3.450	1.031	3.431	1.029	3.407	1.021	3.325	1.006	3.243	1.012	3.394	0.998	3.450	0.993	3.043	1.018
	1.500	1.081	1.492	1.069	1.481	1.050	1.445	1.013	1.410	1.026	1.476	0.995	1.500	0.985	1.323	1.040
	2.000	1.051	1.989	1.039	1.975	1.021	1.927	0.995	1.880	1.002	1.967	0.983	2.000	0.978	1.764	1.012
LC 25	2.500	1.054	2.486	1.045	2.469	1.028	2.409	1.004	2.350	1.009	2.459	0.996	2.500	0.991	2.205	1.012
	3.000	1.049	2.983	1.043	2.962	1.032	2.891	1.011	2.820	1.016	2.951	1.003	3.000	0.999	2.646	1.020
	3.500	1.029	3.481	1.025	3.456	1.020	3.373	1.007	3.290	1.013	3.443	0.999	3.500	0.994	3.087	1.021
	1.550	1.090	1.541	1.077	1.531	1.057	1.494	1.021	1.457	1.033	1.525	1.003	1.550	0.994	1.367	1.049
	2.050	1.077	2.039	1.065	2.024	1.045	1.975	1.014	1.927	1.021	2.017	1.003	2.050	0.997	1.808	1.027
LC 26	2.550	1.089	2.536	1.079	2.518	1.061	2.457	1.035	2.397	1.039	2.509	1.026	2.550	1.022	2.249	1.040
	3.050	1.089	3.033	1.082	3.012	1.070	2.939	1.046	2.867	1.051	3.000	1.038	3.050	1.034	2.690	1.054
	3.550	1.071	3.530	1.065	3.505	1.058	3.421	1.045	3.336	1.052	3.492	1.036	3.550	1.031	3.131	1.059
	1.600	1.083	1.591	1.070	1.580	1.051	1.542	1.019	1.504	1.031	1.574	1.003	1.600	0.994	1.411	1.046
	2.100	1.077	2.088	1.064	2.074	1.045	2.024	1.014	1.974	1.020	2.066	1.004	2.100	0.998	1.852	1.026
LC 27	2.600	1.090	2.586	1.080	2.567	1.062	2.505	1.036	2.444	1.040	2.558	1.028	2.600	1.024	2.293	1.041
	3.100	1.089	3.083	1.083	3.061	1.071	2.987	1.047	2.914	1.052	3.050	1.039	3.100	1.035	2.734	1.055
	3.600	1.072	3.580	1.066	3.555	1.059	3.469	1.047	3.383	1.053	3.541	1.038	3.600	1.033	3.175	1.060
	1.650	1.089	1.641	1.076	1.629	1.055	1.590	1.022	1.551	1.034	1.623	1.007	1.650	0.998	1.455	1.047
	2.150	1.087	2.138	1.074	2.123	1.055	2.072	1.024	2.021	1.030	2.115	1.014	2.150	1.008	1.896	1.035
LC 28	2.650	1.095	2.635	1.085	2.617	1.067	2.554	1.041	2.491	1.046	2.607	1.032	2.650	1.028	2.337	1.048
	3.150	1.082	3.132	1.077	3.110	1.067	3.035	1.046	2.961	1.052	3.099	1.038	3.150	1.033	2.778	1.057
	3.650	1.058	3.630	1.055	3.604	1.047	3.517	1.039	3.430	1.046	3.591	1.030	3.650	1.025	3.219	1.056
	1.700	1.105	1.691	1.091	1.679	1.067	1.638	1.028	1.598	1.039	1.672	1.012	1.700	1.004	1.499	1.050
	2.200	1.109	2.188	1.096	2.172	1.078	2.120	1.045	2.068	1.051	2.164	1.033	2.200	1.028	1.940	1.054
LC 29	2.700	1.109	2.685	1.102	2.666	1.086	2.602	1.062	2.538	1.067	2.656	1.052	2.700	1.047	2.381	1.071
	3.200	1.088	3.182	1.084	3.160	1.077	3.084	1.060	3.008	1.067	3.148	1.051	3.200	1.046	2.822	1.074
	3.700	1.055	3.679	1.055	3.653	1.050	3.565	1.047	3.477	1.053	3.640	1.036	3.700	1.031	3.263	1.066
	1.750	1.077	1.740	1.065	1.728	1.045	1.686	1.015	1.645	1.025	1.722	1.001	1.750	0.993	1.543	1.038
	2.250	1.075	2.237	1.065	2.222	1.047	2.168	1.020	2.115	1.026	2.213	1.010	2.250	1.005	1.984	1.030
LC 30	2.750	1.073	2.735	1.066	2.715	1.052	2.650	1.030	2.585	1.035	2.705	1.021	2.750	1.017	2.425	1.039
	3.250	1.052	3.232	1.047	3.209	1.041	3.132	1.027	3.055	1.033	3.197	1.018	3.250	1.013	2.866	1.041
	3.750	1.017	3.729	1.018	3.703	1.014	3.614	1.010	3.524	1.017	3.689	1.002	3.750	0.997	3.307	1.030

35

Table B1.3: Data ($\lambda_{D.T}$ vs $M_{u.T}/M_{nD.T*}$) of the SCA lipped channel beams at room and elevated temperatures analysed in this work.
(*to be continued*)

Beam	100°C $\lambda_{D.T}$	$M_{u.T}/M_{nD.T*}$	200°C $\lambda_{D.T}$	$M_{u.T}/M_{nD.T*}$	300°C $\lambda_{D.T}$	$M_{u.T}/M_{nD.T*}$	400°C $\lambda_{D.T}$	$M_{u.T}/M_{nD.T*}$	500°C $\lambda_{D.T}$	$M_{u.T}/M_{nD.T*}$	600°C $\lambda_{D.T}$	$M_{u.T}/M_{nD.T*}$	700°C $\lambda_{D.T}$	$M_{u.T}/M_{nD.T*}$	800°C $\lambda_{D.T}$	$M_{u.T}/M_{nD.T*}$
	0.300	0.966	0.298	0.990	0.296	1.021	0.289	1.057	0.282	1.050	0.295	1.063	0.300	1.015	0.265	1.050
	0.800	1.013	0.796	1.007	0.790	1.028	0.771	1.056	0.752	1.049	0.787	1.050	0.800	1.051	0.706	1.045
LC 1	1.300	1.099	1.293	1.103	1.284	1.104	1.253	1.092	1.222	1.094	1.279	1.086	1.300	1.084	1.146	1.088
	1.800	0.955	1.790	0.989	1.777	1.027	1.735	1.055	1.692	1.059	1.771	1.052	1.800	1.049	1.587	1.069
	2.300	0.967	2.287	1.000	2.271	1.022	2.216	1.030	2.162	1.033	2.263	1.026	2.300	1.024	2.028	1.039
	0.350	0.974	0.348	1.007	0.346	1.054	0.337	1.110	0.329	1.086	0.344	1.052	0.350	1.017	0.309	1.064
	0.850	1.054	0.845	1.030	0.839	1.019	0.819	1.042	0.799	1.034	0.836	1.040	0.850	1.044	0.750	1.030
LC 2	1.350	1.079	1.342	1.087	1.333	1.092	1.301	1.098	1.269	1.101	1.328	1.094	1.350	1.092	1.191	1.106
	1.850	1.034	1.840	1.033	1.827	1.033	1.783	1.033	1.739	1.037	1.820	1.029	1.850	1.027	1.632	1.047
	2.350	1.060	2.337	1.068	2.320	1.064	2.265	1.043	2.209	1.044	2.312	1.038	2.350	1.037	2.073	1.040
	0.400	0.971	0.398	0.996	0.395	1.039	0.385	1.059	0.376	1.056	0.393	1.058	0.400	1.070	0.353	1.052
	0.900	1.095	0.895	1.058	0.889	1.018	0.867	1.005	0.846	1.000	0.885	0.997	0.900	0.998	0.794	0.997
LC 3	1.400	1.082	1.392	1.089	1.382	1.100	1.349	1.114	1.316	1.119	1.377	1.109	1.400	1.105	1.235	1.125
	1.900	1.024	1.889	1.028	1.876	1.025	1.831	1.029	1.786	1.034	1.869	1.027	1.900	1.024	1.676	1.047
	2.400	1.031	2.387	1.026	2.370	1.019	2.313	1.010	2.256	1.012	2.361	1.008	2.400	1.006	2.117	1.015
	0.450	0.970	0.447	0.984	0.444	1.019	0.434	1.020	0.423	1.021	0.443	1.002	0.450	0.986	0.397	1.017
	0.950	1.129	0.945	1.097	0.938	1.058	0.915	1.050	0.893	1.043	0.935	1.051	0.950	1.059	0.838	1.029
LC 4	1.450	1.086	1.442	1.092	1.432	1.102	1.397	1.118	1.363	1.123	1.426	1.116	1.450	1.113	1.279	1.135
	1.950	1.055	1.939	1.051	1.925	1.047	1.879	1.044	1.833	1.047	1.918	1.042	1.950	1.039	1.720	1.057
	2.450	1.067	2.436	1.062	2.419	1.055	2.361	1.043	2.303	1.044	2.410	1.040	2.450	1.038	2.161	1.043
	0.500	0.968	0.497	0.974	0.494	1.021	0.482	0.999	0.470	1.014	0.492	0.950	0.500	0.849	0.441	1.018
	1.000	1.144	0.994	1.121	0.987	1.085	0.964	1.071	0.940	1.063	0.984	1.082	1.000	1.088	0.882	1.050
LC 5	1.500	1.122	1.492	1.126	1.481	1.126	1.445	1.128	1.410	1.132	1.476	1.124	1.500	1.121	1.323	1.140
	2.000	1.119	1.989	1.116	1.975	1.110	1.927	1.099	1.880	1.102	1.967	1.095	2.000	1.093	1.764	1.105
	2.500	1.131	2.486	1.127	2.469	1.120	2.409	1.110	2.350	1.112	2.459	1.105	2.500	1.103	2.205	1.111
	0.550	0.983	0.547	0.988	0.543	1.007	0.530	1.007	0.517	1.008	0.541	0.989	0.550	0.980	0.485	1.003
	1.050	1.167	1.044	1.148	1.037	1.107	1.012	1.063	0.987	1.059	1.033	1.065	1.050	1.067	0.926	1.044
LC 6	1.550	1.071	1.541	1.074	1.531	1.082	1.494	1.100	1.457	1.105	1.525	1.098	1.550	1.095	1.367	1.121
	2.050	1.060	2.039	1.055	2.024	1.047	1.975	1.038	1.927	1.040	2.017	1.034	2.050	1.032	1.808	1.046
	2.550	1.076	2.536	1.075	2.518	1.066	2.457	1.050	2.397	1.051	2.509	1.047	2.550	1.045	2.249	1.048
	0.600	0.982	0.597	0.998	0.592	1.020	0.578	1.018	0.564	1.033	0.590	0.989	0.600	0.973	0.529	1.024
	1.100	1.145	1.094	1.136	1.086	1.103	1.060	1.044	1.034	1.044	1.082	1.040	1.100	1.040	0.970	1.030
LC 7	1.600	1.043	1.591	1.050	1.580	1.056	1.542	1.071	1.504	1.076	1.574	1.069	1.600	1.066	1.411	1.091
	2.100	0.990	2.088	1.006	2.074	1.016	2.024	1.016	1.974	1.018	2.066	1.013	2.100	1.011	1.852	1.025
	2.600	1.033	2.586	1.030	2.567	1.024	2.505	1.015	2.444	1.016	2.558	1.012	2.600	1.010	2.293	1.017
	0.650	0.992	0.646	1.007	0.642	1.034	0.626	1.044	0.611	1.056	0.639	1.016	0.650	0.998	0.573	1.051
	1.150	1.145	1.144	1.146	1.136	1.131	1.108	1.087	1.081	1.086	1.131	1.084	1.150	1.084	1.014	1.070
LC 8	1.650	1.061	1.641	1.062	1.629	1.065	1.590	1.078	1.551	1.082	1.623	1.075	1.650	1.072	1.455	1.096
	2.150	1.050	2.138	1.045	2.123	1.039	2.072	1.033	2.021	1.035	2.115	1.030	2.150	1.028	1.896	1.040
	2.650	1.054	2.635	1.050	2.617	1.042	2.554	1.032	2.491	1.034	2.607	1.029	2.650	1.027	2.337	1.036
	0.700	0.996	0.696	1.012	0.691	1.048	0.675	1.055	0.658	1.064	0.689	1.028	0.700	1.015	0.617	1.054
	1.200	1.142	1.193	1.140	1.185	1.125	1.156	1.086	1.128	1.088	1.180	1.080	1.200	1.078	1.058	1.076
LC 9	1.700	1.080	1.691	1.079	1.679	1.079	1.638	1.082	1.598	1.087	1.672	1.079	1.700	1.076	1.499	1.097
	2.200	1.064	2.188	1.060	2.172	1.055	2.120	1.051	2.068	1.054	2.164	1.047	2.200	1.045	1.940	1.061
	2.700	1.040	2.685	1.040	2.666	1.038	2.602	1.034	2.538	1.038	2.656	1.029	2.700	1.026	2.381	1.045
	0.750	1.006	0.746	1.003	0.741	1.027	0.723	1.034	0.705	1.035	0.738	1.014	0.750	1.007	0.661	1.043
	1.250	1.131	1.243	1.132	1.234	1.129	1.205	1.096	1.175	1.099	1.230	1.088	1.250	1.085	1.102	1.088
LC 10	1.750	1.072	1.740	1.070	1.728	1.069	1.686	1.073	1.645	1.078	1.722	1.070	1.750	1.067	1.543	1.088
	2.250	1.061	2.237	1.057	2.222	1.051	2.168	1.045	2.115	1.048	2.213	1.042	2.250	1.040	1.984	1.053
	2.750	1.046	2.735	1.046	2.715	1.041	2.650	1.035	2.585	1.038	2.705	1.030	2.750	1.027	2.425	1.044
	0.800	1.022	0.796	1.008	0.790	1.024	0.771	1.049	0.752	1.043	0.787	1.042	0.800	1.040	0.706	1.038
	1.300	1.107	1.293	1.109	1.284	1.109	1.253	1.096	1.222	1.099	1.279	1.089	1.300	1.087	1.146	1.092
LC 11	1.800	1.061	1.790	1.060	1.777	1.059	1.735	1.060	1.692	1.064	1.771	1.056	1.800	1.053	1.587	1.073
	2.300	1.050	2.287	1.047	2.271	1.043	2.216	1.039	2.162	1.041	2.263	1.035	2.300	1.033	2.028	1.046
	2.800	1.030	2.784	1.031	2.765	1.029	2.698	1.024	2.632	1.029	2.754	1.020	2.800	1.017	2.469	1.035
	0.850	1.059	0.845	1.043	0.839	1.043	0.819	1.079	0.799	1.070	0.836	1.076	0.850	1.079	0.750	1.066
	1.350	1.116	1.342	1.116	1.333	1.116	1.301	1.106	1.269	1.109	1.328	1.100	1.350	1.097	1.191	1.107
LC 12	1.850	1.080	1.840	1.078	1.827	1.076	1.783	1.074	1.739	1.078	1.820	1.070	1.850	1.067	1.632	1.086
	2.350	1.058	2.337	1.057	2.320	1.054	2.265	1.051	2.209	1.055	2.312	1.046	2.350	1.043	2.073	1.062
	2.850	1.026	2.834	1.027	2.814	1.027	2.746	1.027	2.679	1.032	2.804	1.021	2.850	1.017	2.513	1.042
	0.900	1.075	0.895	1.042	0.889	1.007	0.867	1.011	0.846	1.002	0.885	1.010	0.900	1.014	0.794	0.997
	1.400	1.056	1.392	1.064	1.382	1.076	1.349	1.091	1.316	1.096	1.377	1.087	1.400	1.084	1.235	1.102
LC 13	1.900	0.999	1.889	0.998	1.876	0.999	1.831	1.007	1.786	1.011	1.869	1.005	1.900	1.002	1.676	1.025
	2.400	0.995	2.387	0.992	2.370	0.989	2.313	0.983	2.256	0.984	2.361	0.981	2.400	0.980	2.117	0.987
	2.900	1.000	2.884	0.997	2.864	0.993	2.795	0.986	2.726	0.988	2.853	0.983	2.900	0.981	2.558	0.988
	0.950	1.121	0.945	1.089	0.938	1.048	0.915	1.037	0.893	1.031	0.935	1.039	0.950	1.045	0.838	1.022
	1.450	1.099	1.442	1.101	1.432	1.104	1.397	1.110	1.363	1.114	1.426	1.105	1.450	1.101	1.279	1.123
LC 14	1.950	1.068	1.939	1.063	1.925	1.058	1.879	1.056	1.833	1.059	1.918	1.053	1.950	1.050	1.720	1.069
	2.450	1.063	2.436	1.058	2.419	1.050	2.361	1.042	2.303	1.045	2.410	1.038	2.450	1.036	2.161	1.049
	2.950	1.047	2.934	1.046	2.913	1.041	2.843	1.033	2.773	1.037	2.902	1.028	2.950	1.025	2.602	1.043
	1.000	1.142	0.994	1.113	0.987	1.066	0.964	1.025	0.940	1.023	0.984	1.028	1.000	1.031	0.882	1.013
	1.500	1.077	1.492	1.080	1.481	1.087	1.445	1.097	1.410	1.102	1.476	1.094	1.500	1.090	1.323	1.116
LC 15	2.000	1.049	1.989	1.045	1.975	1.040	1.927	1.037	1.880	1.040	1.967	1.034	2.000	1.032	1.764	1.049
	2.500	1.054	2.486	1.048	2.469	1.041	2.409	1.031	2.350	1.033	2.459	1.028	2.500	1.027	2.205	1.035
	3.000	1.054	2.983	1.050	2.962	1.043	2.891	1.033	2.820	1.036	2.951	1.029	3.000	1.027	2.646	1.038
	1.050	1.131	1.044	1.109	1.037	1.073	1.012	1.037	0.987	1.033	1.033	1.041	1.050	1.044	0.926	1.020
	1.550	1.058	1.541	1.061	1.531	1.067	1.494	1.077	1.457	1.082	1.525	1.075	1.550	1.072	1.367	1.094
LC 16	2.050	1.030	2.039	1.028	2.024	1.025	1.975	1.025	1.927	1.028	2.017	1.022	2.050	1.020	1.808	1.036
	2.550	1.020	2.536	1.018	2.518	1.014	2.457	1.009	2.397	1.012	2.509	1.005	2.550	1.003	2.249	1.017
	3.050	0.999	3.033	0.999	3.012	0.999	2.939	0.996	2.867	1.000	3.000	0.991	3.050	0.987	2.690	1.007

Table B1.3: Data ($\lambda_{D.T}$ vs $M_{u.T}/M_{nD.T*}$) of the SCA lipped channel beams at room and elevated temperatures analysed in this work. (*continuation*)

Beam	100°C		200°C		300°C		400°C		500°C		600°C		700°C		800°C	
	$\lambda_{D.T}$	$\dfrac{M_{u.T}}{M_{nD.T*}}$	$\lambda_{D.T}$	$\dfrac{M_{u.T}}{M_{nD.T*}}$	$\lambda_{D.T}$	$\dfrac{M_{u.T}}{M_{nD.T*}}$	$\lambda_{D.T}$	$\dfrac{M_{u.T}}{M_{nD.T*}}$	$\lambda_{D.T}$	$\dfrac{M_{u.T}}{M_{nD.T*}}$	$\lambda_{D.T}$	$\dfrac{M_{u.T}}{M_{nD.T*}}$	$\lambda_{D.T}$	$\dfrac{M_{u.T}}{M_{nD.T*}}$	$\lambda_{D.T}$	$\dfrac{M_{u.T}}{M_{nD.T*}}$
LC 17	1.100	1.146	1.094	1.131	1.086	1.102	1.060	1.057	1.034	1.055	1.082	1.056	1.100	1.057	0.970	1.042
	1.600	1.080	1.591	1.081	1.580	1.082	1.542	1.087	1.504	1.092	1.574	1.084	1.600	1.081	1.411	1.103
	2.100	1.060	2.088	1.056	2.074	1.051	2.024	1.048	1.974	1.051	2.066	1.044	2.100	1.042	1.852	1.058
	2.600	1.040	2.586	1.041	2.567	1.037	2.505	1.031	2.444	1.035	2.558	1.026	2.600	1.023	2.293	1.041
	3.100	1.015	3.083	1.014	3.061	1.013	2.987	1.012	2.914	1.017	3.050	1.007	3.100	1.003	2.734	1.027
LC 18	1.150	1.127	1.144	1.121	1.136	1.109	1.108	1.075	1.081	1.076	1.131	1.071	1.150	1.070	1.014	1.065
	1.650	1.075	1.641	1.074	1.629	1.074	1.590	1.076	1.551	1.080	1.623	1.072	1.650	1.069	1.455	1.090
	2.150	1.046	2.138	1.043	2.123	1.039	2.072	1.039	2.021	1.043	2.115	1.035	2.150	1.032	1.896	1.053
	2.650	1.003	2.635	1.005	2.617	1.005	2.554	1.006	2.491	1.011	2.607	1.000	2.650	0.997	2.337	1.023
	3.150	0.948	3.132	0.953	3.110	0.961	3.035	0.970	2.961	0.976	3.099	0.965	3.150	0.960	2.778	0.991
LC 19	1.200	1.110	1.193	1.112	1.185	1.106	1.156	1.069	1.128	1.069	1.180	1.065	1.200	1.064	1.058	1.056
	1.700	1.026	1.691	1.029	1.679	1.034	1.638	1.047	1.598	1.051	1.672	1.044	1.700	1.042	1.499	1.064
	2.200	1.006	2.188	1.005	2.172	1.004	2.120	1.003	2.068	1.005	2.164	1.000	2.200	0.998	1.940	1.012
	2.700	0.999	2.685	0.998	2.666	0.996	2.602	0.992	2.538	0.994	2.656	0.988	2.700	0.986	2.381	0.998
	3.200	0.979	3.182	0.979	3.160	0.980	3.084	0.979	3.008	0.983	3.148	0.974	3.200	0.971	2.822	0.990
LC 20	1.250	1.109	1.243	1.112	1.234	1.113	1.205	1.087	1.175	1.089	1.230	1.079	1.250	1.077	1.102	1.078
	1.750	1.043	1.740	1.043	1.728	1.044	1.686	1.052	1.645	1.056	1.722	1.049	1.750	1.046	1.543	1.069
	2.250	1.034	2.237	1.032	2.222	1.028	2.168	1.023	2.115	1.026	2.213	1.020	2.250	1.019	1.984	1.030
	2.750	1.032	2.735	1.030	2.715	1.026	2.650	1.019	2.585	1.021	2.705	1.016	2.750	1.013	2.425	1.024
	3.250	1.013	3.232	1.015	3.209	1.013	3.132	1.009	3.055	1.013	3.197	1.004	3.250	1.001	2.866	1.020
LC 21	1.300	1.120	1.293	1.120	1.284	1.120	1.253	1.103	1.222	1.106	1.279	1.095	1.300	1.092	1.146	1.101
	1.800	1.082	1.790	1.078	1.777	1.074	1.735	1.073	1.692	1.077	1.771	1.069	1.800	1.066	1.587	1.085
	2.300	1.071	2.287	1.067	2.271	1.060	2.216	1.053	2.162	1.056	2.263	1.049	2.300	1.046	2.028	1.061
	2.800	1.047	2.784	1.047	2.765	1.045	2.698	1.039	2.632	1.043	2.754	1.033	2.800	1.030	2.469	1.051
	3.300	1.017	3.282	1.018	3.258	1.017	3.180	1.018	3.102	1.023	3.246	1.012	3.300	1.008	2.910	1.034
LC 22	1.350	1.068	1.342	1.075	1.333	1.082	1.301	1.086	1.269	1.090	1.328	1.082	1.350	1.079	1.191	1.090
	1.850	1.012	1.840	1.012	1.827	1.014	1.783	1.021	1.739	1.025	1.820	1.019	1.850	1.016	1.632	1.037
	2.350	1.003	2.337	1.002	2.320	1.000	2.265	0.996	2.209	0.998	2.312	0.993	2.350	0.992	2.073	1.002
	2.850	0.998	2.834	0.998	2.814	0.996	2.746	0.991	2.679	0.993	2.804	0.987	2.850	0.984	2.513	0.996
	3.350	0.979	3.331	0.978	3.308	0.979	3.228	0.978	3.149	0.983	3.296	0.973	3.350	0.970	2.954	0.990
LC 23	1.400	1.102	1.392	1.103	1.382	1.103	1.349	1.099	1.316	1.103	1.377	1.094	1.400	1.091	1.235	1.106
	1.900	1.070	1.889	1.068	1.876	1.065	1.831	1.064	1.786	1.067	1.869	1.060	1.900	1.057	1.676	1.076
	2.400	1.048	2.387	1.047	2.370	1.045	2.313	1.041	2.256	1.045	2.361	1.036	2.400	1.033	2.117	1.052
	2.900	1.016	2.884	1.016	2.864	1.016	2.795	1.017	2.726	1.022	2.853	1.011	2.900	1.007	2.558	1.032
	3.400	0.973	3.381	0.977	3.357	0.980	3.276	0.985	3.196	0.991	3.345	0.980	3.400	0.976	2.999	1.005
LC 24	1.450	1.080	1.442	1.085	1.432	1.093	1.397	1.104	1.363	1.108	1.426	1.100	1.450	1.097	1.279	1.119
	1.950	1.041	1.939	1.039	1.925	1.036	1.879	1.036	1.833	1.040	1.918	1.034	1.950	1.031	1.720	1.050
	2.450	1.045	2.436	1.042	2.419	1.036	2.361	1.028	2.303	1.029	2.410	1.025	2.450	1.023	2.161	1.030
	2.950	1.047	2.934	1.044	2.913	1.038	2.843	1.029	2.773	1.032	2.902	1.025	2.950	1.023	2.602	1.033
	3.450	1.031	3.431	1.032	3.407	1.029	3.325	1.023	3.243	1.027	3.394	1.018	3.450	1.015	3.043	1.032
LC 25	1.500	1.081	1.492	1.085	1.481	1.092	1.445	1.102	1.410	1.107	1.476	1.099	1.500	1.096	1.323	1.120
	2.000	1.051	1.989	1.048	1.975	1.044	1.927	1.043	1.880	1.046	1.967	1.040	2.000	1.037	1.764	1.054
	2.500	1.054	2.486	1.050	2.469	1.043	2.409	1.035	2.350	1.037	2.459	1.032	2.500	1.031	2.205	1.039
	3.000	1.049	2.983	1.047	2.962	1.043	2.891	1.033	2.820	1.036	2.951	1.029	3.000	1.027	2.646	1.040
	3.500	1.029	3.481	1.028	3.456	1.028	3.373	1.024	3.290	1.029	3.443	1.018	3.500	1.015	3.087	1.036
LC 26	1.550	1.090	1.541	1.092	1.531	1.097	1.494	1.105	1.457	1.110	1.525	1.101	1.550	1.098	1.367	1.124
	2.050	1.077	2.039	1.073	2.024	1.068	1.975	1.061	1.927	1.063	2.017	1.057	2.050	1.055	1.808	1.068
	2.550	1.089	2.536	1.084	2.518	1.076	2.457	1.066	2.397	1.067	2.509	1.063	2.550	1.061	2.249	1.067
	3.050	1.089	3.033	1.086	3.012	1.080	2.939	1.069	2.867	1.072	3.000	1.065	3.050	1.062	2.690	1.073
	3.550	1.071	3.530	1.068	3.505	1.066	3.421	1.062	3.336	1.067	3.492	1.056	3.550	1.052	3.131	1.074
LC 27	1.600	1.083	1.591	1.084	1.580	1.088	1.542	1.098	1.504	1.102	1.574	1.094	1.600	1.091	1.411	1.116
	2.100	1.077	2.088	1.072	2.074	1.067	2.024	1.059	1.974	1.061	2.066	1.056	2.100	1.054	1.852	1.064
	2.600	1.090	2.586	1.085	2.567	1.077	2.505	1.066	2.444	1.067	2.558	1.063	2.600	1.061	2.293	1.067
	3.100	1.089	3.083	1.087	3.061	1.081	2.987	1.069	2.914	1.072	3.050	1.065	3.100	1.063	2.734	1.074
	3.600	1.072	3.580	1.069	3.555	1.067	3.469	1.063	3.383	1.068	3.541	1.057	3.600	1.053	3.175	1.075
LC 28	1.650	1.089	1.641	1.089	1.629	1.090	1.590	1.096	1.551	1.101	1.623	1.092	1.650	1.089	1.455	1.112
	2.150	1.087	2.138	1.082	2.123	1.075	2.072	1.067	2.021	1.069	2.115	1.064	2.150	1.062	1.896	1.072
	2.650	1.095	2.635	1.090	2.617	1.081	2.554	1.070	2.491	1.072	2.607	1.066	2.650	1.064	2.337	1.073
	3.150	1.082	3.132	1.080	3.110	1.077	3.035	1.068	2.961	1.072	3.099	1.062	3.150	1.059	2.778	1.076
	3.650	1.058	3.630	1.057	3.604	1.055	3.517	1.055	3.430	1.061	3.591	1.049	3.650	1.045	3.219	1.070
LC 29	1.700	1.105	1.691	1.103	1.679	1.100	1.638	1.098	1.598	1.102	1.672	1.093	1.700	1.090	1.499	1.112
	2.200	1.109	2.188	1.104	2.172	1.098	2.120	1.087	2.068	1.089	2.164	1.082	2.200	1.080	1.940	1.091
	2.700	1.109	2.685	1.107	2.666	1.100	2.602	1.090	2.538	1.093	2.656	1.086	2.700	1.083	2.381	1.096
	3.200	1.088	3.182	1.087	3.160	1.087	3.084	1.081	3.008	1.086	3.148	1.075	3.200	1.072	2.822	1.093
	3.700	1.055	3.679	1.057	3.653	1.057	3.565	1.061	3.477	1.067	3.640	1.055	3.700	1.050	3.263	1.079
LC 30	1.750	1.077	1.740	1.076	1.728	1.075	1.686	1.079	1.645	1.084	1.722	1.076	1.750	1.073	1.543	1.095
	2.250	1.075	2.237	1.072	2.222	1.066	2.168	1.059	2.115	1.061	2.213	1.056	2.250	1.054	1.984	1.064
	2.750	1.073	2.735	1.071	2.715	1.065	2.650	1.057	2.585	1.059	2.705	1.053	2.750	1.050	2.425	1.062
	3.250	1.052	3.232	1.050	3.209	1.050	3.132	1.046	3.055	1.051	3.197	1.041	3.250	1.037	2.866	1.058
	3.750	1.017	3.729	1.021	3.703	1.021	3.614	1.024	3.524	1.030	3.689	1.019	3.750	1.015	3.307	1.043

Table B2.1: Data ($\lambda_{D.T}$ vs $M_{u.T}/M_{y.T}$) of the SCA lipped channel beams at room and elevated temperatures reported by Landesmann & Camotim (2016).

100°C		200°C		300°C		400°C		500°C		600°C		700°C		800°C	
$\lambda_{D.T}$	$\dfrac{M_{u.T}}{M_{y.T}}$	$\lambda_{D.T}$	$\dfrac{M_{u.T}}{M_{y.T}}$	$\lambda_{D.T}$	$\dfrac{M_{u.T}}{M_{y.T}}$	$\lambda_{D.T}$	$\dfrac{M_{u.T}}{M_{y.T}}$	$\lambda_{D.T}$	$\dfrac{M_{u.T}}{M_{y.T}}$	$\lambda_{D.T}$	$\dfrac{M_{u.T}}{M_{y.T}}$	$\lambda_{D.T}$	$\dfrac{M_{u.T}}{M_{y.T}}$	$\lambda_{D.T}$	$\dfrac{M_{u.T}}{M_{y.T}}$
0.250	1.026	0.497	0.948	0.494	0.882	0.482	0.827	0.470	0.850	0.492	0.791	0.500	0.772	0.441	0.861
0.500	1.008	1.015	0.776	1.008	0.722	0.983	0.664	0.959	0.688	1.004	0.635	1.020	0.618	0.900	0.726
0.750	0.963	1.572	0.418	1.561	0.416	1.523	0.421	1.486	0.441	1.555	0.403	1.581	0.391	1.394	0.489
1.020	0.809	2.029	0.274	2.015	0.276	1.967	0.283	1.918	0.296	2.008	0.273	2.041	0.266	1.800	0.329
1.250	0.617	2.486	0.196	2.468	0.196	2.409	0.202	2.349	0.212	2.459	0.196	2.500	0.191	2.204	0.236
1.581	0.418	3.010	0.138	2.989	0.141	2.917	0.146	2.845	0.153	2.978	0.141	3.027	0.136	2.670	0.172
1.750	0.354	3.486	0.106	3.461	0.107	3.378	0.113	3.294	0.117	3.448	0.107	3.505	0.104	3.091	0.131
2.041	0.273	0.542	0.933	0.538	0.857	0.525	0.765	0.512	0.797	0.536	0.732	0.545	0.719	0.480	0.823
2.250	0.232	1.024	0.779	1.016	0.719	0.992	0.637	0.967	0.665	1.013	0.602	1.029	0.583	0.908	0.703
2.500	0.194	1.713	0.360	1.701	0.358	1.660	0.362	1.619	0.379	1.694	0.346	1.722	0.335	1.519	0.423
2.749	0.165	2.242	0.240	2.227	0.239	2.173	0.242	2.119	0.252	2.218	0.233	2.255	0.226	1.989	0.279
3.027	0.138	2.589	0.194	2.571	0.194	2.509	0.197	2.447	0.206	2.561	0.190	2.604	0.185	2.296	0.226
3.249	0.122	3.237	0.132	3.214	0.131	3.136	0.140	3.059	0.147	3.202	0.134	3.255	0.130	2.870	0.162
3.505	0.105	3.775	0.101	3.748	0.101	3.658	0.105	3.567	0.110	3.734	0.101	3.796	0.101	3.347	0.133
0.252	1.020	0.502	0.924	0.499	0.833	0.487	0.745	0.475	0.769	0.497	0.727	0.505	0.718	0.445	0.805
0.797	0.956	0.990	0.813	0.983	0.737	0.959	0.643	0.936	0.672	0.979	0.606	0.996	0.586	0.878	0.710
1.350	0.540	1.497	0.455	1.486	0.452	1.451	0.459	1.415	0.482	1.481	0.439	1.505	0.426	1.328	0.541
1.887	0.314	1.980	0.283	1.966	0.282	1.919	0.288	1.872	0.301	1.959	0.275	1.991	0.267	1.756	0.334
2.427	0.215	2.482	0.199	2.465	0.198	2.405	0.201	2.346	0.211	2.456	0.195	2.496	0.189	2.201	0.236
2.969	0.157	2.994	0.145	2.973	0.146	2.901	0.150	2.830	0.157	2.962	0.145	3.011	0.141	2.655	0.174
3.509	0.116	3.511	0.112	3.486	0.113	3.402	0.116	3.318	0.122	3.473	0.112	3.530	0.108	3.113	0.135
0.545	1.002	0.503	0.922	0.499	0.837	0.487	0.759	0.475	0.777	0.497	0.734	0.505	0.724	0.446	0.798
1.029	0.810	1.005	0.808	0.998	0.735	0.974	0.643	0.950	0.672	0.995	0.606	1.011	0.587	0.892	0.711
1.722	0.361	1.508	0.450	1.497	0.448	1.461	0.452	1.425	0.475	1.492	0.432	1.516	0.417	1.337	0.529
2.255	0.240	2.011	0.284	1.996	0.281	1.948	0.286	1.900	0.351	1.989	0.275	2.022	0.267	1.783	0.336
2.604	0.193	2.513	0.200	2.496	0.200	2.435	0.204	2.375	0.213	2.486	0.196	2.527	0.191	2.229	0.237
3.255	0.131	3.016	0.150	2.995	0.150	2.923	0.154	2.850	0.161	2.984	0.148	3.033	0.145	2.675	0.179
3.796	0.100	3.519	0.116	3.494	0.116	3.410	0.120	3.326	0.125	3.481	0.116	3.538	0.112	3.121	0.140
0.238	1.019	0.491	0.936	0.487	0.867	0.475	0.805	0.464	0.816	0.485	0.788	0.493	0.785	0.435	0.855
0.734	0.979	0.996	0.812	0.989	0.743	0.965	0.667	0.942	0.694	0.986	0.638	1.002	0.625	0.884	0.742
1.248	0.655	1.502	0.472	1.491	0.469	1.456	0.468	1.420	0.490	1.486	0.447	1.510	0.439	1.332	0.550
1.749	0.353	1.978	0.306	1.964	0.305	1.916	0.310	1.869	0.323	1.956	0.297	1.989	0.289	1.754	0.361
2.245	0.235	2.483	0.214	2.466	0.214	2.406	0.219	2.347	0.229	2.457	0.211	2.497	0.205	2.202	0.255
2.745	0.170	3.004	0.156	2.983	0.157	2.911	0.162	2.839	0.169	2.972	0.156	3.021	0.151	2.664	0.189
3.246	0.131	3.512	0.121	3.487	0.119	3.403	0.124	3.319	0.130	3.474	0.119	3.532	0.116	3.115	0.145
0.505	1.004														
0.996	0.859														
1.505	0.455														
1.991	0.284														
2.496	0.198														
3.011	0.145														
3.530	0.111														
0.226	1.025														
0.750	0.977														
1.248	0.634														
1.744	0.359														
2.249	0.240														
2.745	0.175														
3.248	0.133														
0.505	1.001														
1.011	0.849														
1.516	0.451														
2.022	0.283														
2.527	0.200														
3.033	0.149														
3.538	0.115														
0.247	1.029														
0.740	0.980														
1.246	0.645														
1.748	0.376														
2.247	0.253														
2.749	0.182														
3.249	0.137														
0.493	1.004														
1.002	0.870														
1.510	0.475														
1.989	0.307														
2.497	0.214														
3.021	0.155														
3.532	0.118														

100°C		200°C		300°C		400°C		500°C		600°C		700°C		800°C	
$\lambda_{D.T}$	$\dfrac{M_{u.T}}{M_{nD.T}}$	$\lambda_{D.T}$	$\dfrac{M_{u.T}}{M_{nD.T}}$	$\lambda_{D.T}$	$\dfrac{M_{u.T}}{M_{nD.T}}$	$\lambda_{D.T}$	$\dfrac{M_{u.T}}{M_{nD.T}}$	$\lambda_{D.T}$	$\dfrac{M_{u.T}}{M_{nD.T}}$	$\lambda_{D.T}$	$\dfrac{M_{u.T}}{M_{nD.T}}$	$\lambda_{D.T}$	$\dfrac{M_{u.T}}{M_{nD.T}}$	$\lambda_{D.T}$	$\dfrac{M_{u.T}}{M_{nD.T}}$
0.250	0.963	0.497	0.923	0.494	0.858	0.482	0.803	0.470	0.825	0.492	0.769	0.500	0.752	0.441	0.832
0.500	0.982	1.015	1.048	1.008	0.966	0.983	0.865	0.959	0.872	1.004	0.847	1.020	0.840	0.900	0.861
0.750	0.991	1.572	1.027	1.561	1.012	1.523	0.987	1.486	0.996	1.555	0.976	1.581	0.970	1.394	1.006
1.020	1.100	2.029	1.003	2.015	0.996	1.967	0.985	1.918	0.989	2.008	0.981	2.041	0.980	1.800	0.994
1.250	1.089	2.486	0.993	2.468	0.985	2.409	0.974	2.349	0.980	2.459	0.976	2.500	0.978	2.204	0.987
1.581	1.035	3.010	0.963	2.989	0.967	2.917	0.967	2.845	0.972	2.978	0.963	3.027	0.952	2.670	0.979
1.750	1.026	3.486	0.939	3.461	0.940	3.378	0.950	3.294	0.948	3.448	0.931	3.505	0.933	3.091	0.956
2.041	1.008	0.542	0.918	0.538	0.842	0.525	0.751	0.512	0.781	0.536	0.720	0.545	0.708	0.480	0.804
2.250	1.001	1.024	1.062	1.016	0.973	0.992	0.838	0.967	0.851	1.013	0.811	1.029	0.801	0.908	0.841
2.500	0.992	1.713	1.009	1.701	0.991	1.660	0.965	1.619	0.974	1.694	0.954	1.722	0.948	1.519	0.987
2.749	0.986	2.242	1.030	2.227	1.014	2.173	0.987	2.119	0.988	2.218	0.981	2.255	0.980	1.989	0.986
3.027	0.972	2.589	1.050	2.571	1.039	2.509	1.017	2.447	1.017	2.561	1.015	2.604	1.015	2.296	1.009
3.249	0.966	3.237	1.038	3.214	1.018	3.136	1.040	3.059	1.048	3.202	1.034	3.255	1.030	2.870	1.040
3.505	0.943	3.775	1.024	3.748	1.016	3.658	1.014	3.567	1.016	3.734	1.008	3.796	1.035	3.347	1.103
0.252	0.968	0.502	0.901	0.499	0.812	0.487	0.725	0.475	0.746	0.497	0.708	0.505	0.700	0.445	0.778
0.797	1.022	0.990	1.067	0.983	0.960	0.959	0.815	0.936	0.829	0.979	0.786	0.996	0.775	0.878	0.823
1.350	1.062	1.497	1.040	1.486	1.022	1.451	1.001	1.415	1.013	1.481	0.987	1.505	0.981	1.328	1.037
1.887	1.024	1.980	0.996	1.966	0.981	1.919	0.962	1.872	0.967	1.959	0.950	1.991	0.947	1.756	0.972
2.427	1.051	2.482	1.006	2.465	0.990	2.405	0.969	2.346	0.972	2.456	0.969	2.496	0.965	2.201	0.981
2.969	1.065	2.994	1.003	2.973	0.995	2.901	0.983	2.830	0.985	2.962	0.981	3.011	0.980	2.655	0.984
3.509	1.038	3.511	1.007	3.486	1.001	3.402	0.988	3.318	0.997	3.473	0.987	3.530	0.982	3.113	0.997
0.545	0.986	0.503	0.895	0.499	0.811	0.487	0.735	0.475	0.750	0.497	0.712	0.505	0.703	0.446	0.767
1.029	1.112	1.005	1.079	0.998	0.974	0.974	0.828	0.950	0.842	0.995	0.800	1.011	0.789	0.892	0.835
1.722	1.021	1.508	1.040	1.497	1.024	1.461	0.997	1.425	0.981	1.492	0.981	1.516	0.972	1.337	1.026
2.255	1.040	2.011	1.022	1.996	1.002	1.948	0.979	1.900	1.155	1.989	0.975	2.022	0.971	1.783	1.002
2.604	1.058	2.513	1.035	2.496	1.022	2.435	0.999	2.375	1.002	2.486	0.994	2.527	0.993	2.229	1.007
3.255	1.039	3.016	1.046	2.995	1.035	2.923	1.022	2.850	1.024	2.984	1.017	3.033	1.018	2.675	1.021
3.796	1.027	3.519	1.044	3.494	1.037	3.410	1.027	3.326	1.029	3.481	1.024	3.538	1.024	3.121	1.035
0.238	0.955	0.487	0.897	0.487	0.830	0.475	0.770	0.464	0.778	0.485	0.755	0.493	0.753	0.435	0.810
0.734	0.998	0.989	1.074	0.989	0.974	0.965	0.851	0.942	0.862	0.986	0.833	1.002	0.831	0.884	0.865
1.248	1.153	1.491	1.084	1.491	1.066	1.456	1.025	1.420	1.035	1.486	1.010	1.510	1.016	1.332	1.060
1.749	1.022	1.964	1.074	1.964	1.058	1.916	1.035	1.869	1.037	1.956	1.024	1.989	1.023	1.754	1.049
2.245	1.010	2.466	1.082	2.466	1.072	2.406	1.053	2.347	1.057	2.457	1.049	2.497	1.050	2.202	1.061
2.745	1.017	2.983	1.081	2.983	1.077	2.911	1.063	2.839	1.065	2.972	1.065	3.021	1.058	2.664	1.076
3.246	1.031	3.487	1.086	3.487	1.061	3.403	1.056	3.319	1.061	3.474	1.050	3.532	1.049	3.115	1.070
0.505	0.978														
0.996	1.135														
1.505	1.049														
1.991	1.006														
2.496	1.009														
3.011	1.009														
3.530	1.005														
0.226	0.950														
0.750	1.006														
1.248	1.117														
1.744	1.034														
2.249	1.034														
2.745	1.048														
3.248	1.053														
0.505	0.972														
1.011	1.142														
1.516	1.050														
2.022	1.028														
2.527	1.044														
3.033	1.050														
3.538	1.044														
0.247	0.936														
0.740	1.003														
1.246	1.133														
1.748	1.087														
2.247	1.087														
2.749	1.091														
3.249	1.080														
0.493	0.963														
1.002	1.158														
1.510	1.101														
1.989	1.085														
2.497	1.092														
3.021	1.084														
3.532	1.070														

Table B2.3: Data ($\lambda_{D.T}$ vs $M_{u.T}/M_{nD.T*}$) of the SCA lipped channel beams at room and elevated temperatures reported by Landesmann & Camotim (2016).

100°C		200°C		300°C		400°C		500°C		600°C		700°C		800°C	
$\lambda_{D.T}$	$\dfrac{M_{u.T}}{M_{nD.T*}}$	$\lambda_{D.T}$	$\dfrac{M_{u.T}}{M_{nD.T*}}$	$\lambda_{D.T}$	$\dfrac{M_{u.T}}{M_{nD.T*}}$	$\lambda_{D.T}$	$\dfrac{M_{u.T}}{M_{nD.T*}}$	$\lambda_{D.T}$	$\dfrac{M_{u.T}}{M_{nD.T*}}$	$\lambda_{D.T}$	$\dfrac{M_{u.T}}{M_{nD.T*}}$	$\lambda_{D.T}$	$\dfrac{M_{u.T}}{M_{nD.T*}}$	$\lambda_{D.T}$	$\dfrac{M_{u.T}}{M_{nD.T*}}$
0.250	0.963	0.497	0.999	0.494	1.027	0.482	1.045	0.470	1.052	0.492	1.012	0.500	0.995	0.441	1.036
0.500	0.982	1.015	1.084	1.008	1.059	0.983	1.063	0.959	1.052	1.004	1.081	1.020	1.090	0.900	1.036
0.750	0.991	1.572	1.040	1.561	1.049	1.523	1.065	1.486	1.066	1.555	1.067	1.581	1.067	1.394	1.074
1.020	1.100	2.029	1.011	2.015	1.018	1.967	1.031	1.918	1.030	2.008	1.035	2.041	1.037	1.800	1.034
1.250	1.089	2.486	0.999	2.468	1.000	2.409	1.004	2.349	1.007	2.459	1.012	2.500	1.016	2.204	1.013
1.581	1.035	3.010	0.966	2.989	0.977	2.917	0.988	2.845	0.991	2.978	0.988	3.027	0.978	2.670	0.997
1.750	1.026	3.486	0.941	3.461	0.948	3.378	0.966	3.294	0.962	3.448	0.950	3.505	0.953	3.091	0.970
2.041	1.008	0.542	0.998	0.538	1.024	0.525	1.016	0.512	1.029	0.536	0.997	0.545	0.992	0.480	1.028
2.250	1.001	1.024	1.098	1.016	1.065	0.992	1.025	0.967	1.022	1.013	1.030	1.029	1.033	0.908	1.008
2.500	0.992	1.713	1.021	1.701	1.021	1.660	1.029	1.619	1.032	1.694	1.028	1.722	1.027	1.519	1.043
2.749	0.986	2.242	1.036	2.227	1.032	2.173	1.024	2.119	1.022	2.218	1.026	2.255	1.027	1.989	1.018
3.027	0.972	2.589	1.056	2.571	1.053	2.509	1.046	2.447	1.043	2.561	1.049	2.604	1.052	2.296	1.034
3.249	0.966	3.237	1.042	3.214	1.027	3.136	1.060	3.059	1.066	3.202	1.057	3.255	1.054	2.870	1.057
3.505	0.943	3.775	1.027	3.748	1.023	3.658	1.029	3.567	1.029	3.734	1.025	3.796	1.054	3.347	1.117
0.252	0.968	0.502	0.975	0.499	0.973	0.487	0.945	0.475	0.955	0.497	0.935	0.505	0.930	0.445	0.971
0.797	1.022	0.990	1.105	0.983	1.058	0.959	1.016	0.936	1.013	0.979	1.020	0.996	1.023	0.878	1.003
1.350	1.062	1.497	1.055	1.486	1.063	1.451	1.088	1.415	1.093	1.481	1.089	1.505	1.091	1.328	1.116
1.887	1.024	1.980	1.004	1.966	1.004	1.919	1.009	1.872	1.010	1.959	1.005	1.991	1.005	1.756	1.013
2.427	1.051	2.482	1.011	2.465	1.004	2.405	0.999	2.346	1.000	2.456	1.005	2.496	1.003	2.201	1.008
2.969	1.065	2.994	1.007	2.973	1.005	2.901	1.005	2.830	1.004	2.962	1.006	3.011	1.007	2.655	1.002
3.509	1.038	3.511	1.010	3.486	1.009	3.402	1.004	3.318	1.012	3.473	1.006	3.530	1.002	3.113	1.011
0.545	0.986	0.503	0.965	0.499	0.964	0.487	0.934	0.475	0.939	0.497	0.909	0.505	0.899	0.446	0.941
1.029	1.112	1.005	1.116	0.998	1.070	0.974	1.024	0.950	1.021	0.995	1.027	1.011	1.030	0.892	1.010
1.722	1.021	1.508	1.055	1.497	1.064	1.461	1.083	1.425	1.088	1.492	1.081	1.516	1.079	1.337	1.103
2.255	1.040	2.011	1.030	1.996	1.024	1.948	1.026	1.900	1.204	1.989	1.029	2.022	1.029	1.783	1.043
2.604	1.058	2.513	1.041	2.496	1.037	2.435	1.030	2.375	1.030	2.486	1.030	2.527	1.032	2.229	1.033
3.255	1.039	3.016	1.050	2.995	1.045	2.923	1.044	2.850	1.044	2.984	1.043	3.033	1.046	2.675	1.040
3.796	1.027	3.519	1.047	3.494	1.045	3.410	1.044	3.326	1.044	3.481	1.044	3.538	1.045	3.121	1.050
0.238	0.955	0.487	0.961	0.487	0.965	0.475	0.925	0.464	0.929	0.485	0.896	0.493	0.887	0.435	0.956
0.734	0.998	0.989	1.112	0.989	1.072	0.965	1.058	0.942	1.049	0.986	1.076	1.002	1.093	0.884	1.051
1.248	1.153	1.491	1.100	1.491	1.108	1.456	1.114	1.420	1.116	1.486	1.114	1.510	1.128	1.332	1.140
1.749	1.022	1.964	1.083	1.964	1.082	1.916	1.085	1.869	1.083	1.956	1.083	1.989	1.086	1.754	1.093
2.245	1.010	2.466	1.088	2.466	1.088	2.406	1.086	2.347	1.087	2.457	1.088	2.497	1.091	2.202	1.089
2.745	1.017	2.983	1.085	2.983	1.088	2.911	1.086	2.839	1.086	2.972	1.092	3.021	1.087	2.664	1.096
3.246	1.031	3.487	1.089	3.487	1.070	3.403	1.073	3.319	1.077	3.474	1.070	3.532	1.071	3.115	1.085
0.505	0.979														
0.996	1.135														
1.505	1.049														
1.991	1.006														
2.496	1.009														
3.011	1.009														
3.530	1.005														
0.226	0.950														
0.750	1.006														
1.248	1.117														
1.744	1.034														
2.249	1.034														
2.745	1.048														
3.248	1.053														
0.505	0.972														
1.011	1.142														
1.516	1.050														
2.022	1.028														
2.527	1.044														
3.033	1.050														
3.538	1.044														
0.247	0.936														
0.740	1.003														
1.246	1.133														
1.748	1.087														
2.247	1.087														
2.749	1.091														
3.249	1.080														
0.493	0.963														
1.002	1.158														
1.510	1.101														
1.989	1.085														
2.497	1.092														
3.021	1.084														
3.532	1.070														

Annex C: Data Concerning the SCB Lipped Channel Beams at Room and Elevated Temperatures

This annex includes two table sets (C1 and C2), concerning SCB lipped channel beams at room and elevated temperatures, and displays the whole set of numerical failure moments (i) obtained in this work (Tables C1.1-C1.3) and (ii) reported in Landesmann and Camotim (2016) (Tables C2.1-C.2.3). Each individual table provides, for the various lipped channel beams analyzed, (i) the distortional slenderness value ($\lambda_{D.T}$), (ii) the ratio between the failure and yield moments ($M_{u.T}/M_{y.T}$ – Tables C1.1 and C2.1), and (iii) the numerical-to-predicted failure moment ratios obtained with Eqs. (4) and (5), namely $M_{u.T}/M_{nD.T}$ (Tables C1.2 and C2.2) and $M_{u.T}/M_{nD.T*}$ (Tables C1.3 and C2.3).

Table C1.1: Data ($\lambda_{D.T}$ vs $M_{u.T}/M_{y.T}$) of the SCB lipped channel beams at room and elevated temperatures analysed in this work.
(*to be continued*)

Beam	100°C		200°C		300°C		400°C		500°C		600°C		700°C		800°C	
	$\lambda_{D.T}$	$\dfrac{M_{u.T}}{M_{y.T}}$	$\lambda_{D.T}$	$\dfrac{M_{u.T}}{M_{y.T}}$	$\lambda_{D.T}$	$\dfrac{M_{u.T}}{M_{y.T}}$	$\lambda_{D.T}$	$\dfrac{M_{u.T}}{M_{y.T}}$	λD	$\lambda_{D.T}$	$\dfrac{M_{u.T}}{M_{y.T}}$	$\lambda_{D.T}$	$\dfrac{M_{u.T}}{M_{y.T}}$	$\lambda_{D.T}$	$\dfrac{M_{u.T}}{M_{y.T}}$	$\lambda_{D.T}$
LC 1	0.300	1.093	0.298	1.025	0.296	0.952	0.289	0.883	0.282	0.900	0.295	0.860	0.300	0.848	0.265	0.919
	0.800	0.939	0.796	0.887	0.790	0.817	0.771	0.746	0.752	0.771	0.787	0.715	0.800	0.697	0.706	0.807
	1.300	0.567	1.293	0.560	1.284	0.546	1.253	0.532	1.222	0.556	1.279	0.506	1.300	0.490	1.146	0.608
	1.800	0.361	1.790	0.361	1.777	0.354	1.735	0.355	1.692	0.370	1.771	0.348	1.800	0.340	1.587	0.401
	2.300	0.269	2.287	0.274	2.271	0.275	2.216	0.281	2.162	0.292	2.263	0.274	2.300	0.268	2.028	0.313
LC 2	0.350	1.077	0.348	1.009	0.346	0.939	0.337	0.880	0.329	0.898	0.344	0.857	0.350	0.843	0.309	0.922
	0.850	0.903	0.845	0.854	0.839	0.780	0.819	0.698	0.799	0.725	0.836	0.664	0.850	0.644	0.750	0.762
	1.350	0.524	1.342	0.514	1.333	0.499	1.301	0.487	1.269	0.510	1.328	0.464	1.350	0.450	1.191	0.560
	1.850	0.404	1.840	0.406	1.827	0.407	1.783	0.399	1.739	0.411	1.820	0.311	1.850	0.341	1.632	0.372
	2.350	0.253	2.337	0.276	2.320	0.293	2.265	0.309	2.209	0.331	2.312	0.273	2.350	0.261	2.073	0.275
LC 3	0.400	1.088	0.398	1.013	0.395	0.923	0.385	0.833	0.376	0.856	0.393	0.802	0.400	0.785	0.353	0.882
	0.900	0.895	0.895	0.847	0.889	0.774	0.867	0.692	0.846	0.720	0.885	0.658	0.900	0.637	0.794	0.757
	1.400	0.502	1.392	0.497	1.382	0.489	1.349	0.484	1.316	0.508	1.377	0.462	1.400	0.447	1.235	0.558
	1.900	0.371	1.889	0.368	1.876	0.362	1.831	0.356	1.786	0.366	1.869	0.344	1.900	0.337	1.676	0.385
	2.400	0.302	2.387	0.300	2.370	0.298	2.313	0.297	2.256	0.306	2.361	0.288	2.400	0.282	2.117	0.324
LC 4	0.450	1.088	0.447	1.016	0.444	0.939	0.434	0.851	0.423	0.874	0.443	0.820	0.450	0.802	0.397	0.900
	0.950	0.860	0.945	0.823	0.938	0.760	0.915	0.683	0.893	0.711	0.935	0.649	0.950	0.629	0.838	0.751
	1.450	0.488	1.442	0.482	1.432	0.474	1.397	0.469	1.363	0.491	1.426	0.447	1.450	0.432	1.279	0.539
	1.950	0.367	1.939	0.364	1.925	0.360	1.879	0.356	1.833	0.366	1.918	0.345	1.950	0.337	1.720	0.386
	2.450	0.299	2.436	0.298	2.419	0.297	2.361	0.296	2.303	0.304	2.410	0.287	2.450	0.281	2.161	0.323
LC 5	0.500	1.059	0.497	1.012	0.494	0.925	0.482	0.829	0.470	0.867	0.492	0.791	0.500	0.815	0.441	0.848
	1.000	0.832	0.994	0.800	0.987	0.748	0.964	0.685	0.940	0.713	0.984	0.653	1.000	0.634	0.882	0.755
	1.500	0.497	1.492	0.492	1.481	0.481	1.445	0.470	1.410	0.492	1.476	0.448	1.500	0.434	1.323	0.539
	2.000	0.340	1.989	0.337	1.975	0.332	1.927	0.334	1.880	0.344	1.967	0.324	2.000	0.317	1.764	0.374
	2.500	0.264	2.486	0.263	2.469	0.262	2.409	0.266	2.350	0.275	2.459	0.258	2.500	0.252	2.205	0.295
LC 6	0.550	1.048	0.547	0.983	0.543	0.893	0.530	0.792	0.517	0.819	0.541	0.757	0.550	0.738	0.485	0.849
	1.050	0.764	1.044	0.746	1.037	0.710	1.012	0.646	0.987	0.674	1.033	0.611	1.050	0.591	0.926	0.717
	1.550	0.440	1.541	0.435	1.531	0.427	1.494	0.424	1.457	0.444	1.525	0.405	1.550	0.392	1.367	0.491
	2.050	0.353	2.039	0.350	2.024	0.345	1.975	0.340	1.927	0.350	2.017	0.330	2.050	0.322	1.808	0.370
	2.550	0.286	2.536	0.287	2.518	0.279	2.457	0.282	2.397	0.294	2.509	0.277	2.550	0.271	2.249	0.312
LC 7	0.600	1.021	0.597	0.956	0.592	0.874	0.578	0.781	0.564	0.807	0.590	0.748	0.600	0.730	0.529	0.836
	1.100	0.706	1.094	0.697	1.086	0.670	1.060	0.623	1.034	0.652	1.082	0.590	1.100	0.570	0.970	0.696
	1.600	0.411	1.591	0.408	1.580	0.403	1.542	0.402	1.504	0.421	1.574	0.384	1.600	0.371	1.411	0.466
	2.100	0.323	2.088	0.322	2.074	0.321	2.024	0.321	1.974	0.330	2.066	0.312	2.100	0.306	1.852	0.348
	2.600	0.263	2.586	0.263	2.567	0.264	2.505	0.267	2.444	0.274	2.558	0.259	2.600	0.254	2.293	0.292
LC 8	0.650	1.019	0.646	0.955	0.642	0.873	0.626	0.781	0.611	0.807	0.639	0.746	0.650	0.727	0.573	0.836
	1.150	0.626	1.144	0.615	1.136	0.601	1.108	0.581	1.081	0.607	1.131	0.552	1.150	0.534	1.014	0.654
	1.650	0.386	1.641	0.383	1.629	0.381	1.590	0.375	1.551	0.393	1.623	0.374	1.650	0.366	1.455	0.425
	2.150	0.318	2.138	0.318	2.123	0.317	2.072	0.317	2.021	0.326	2.115	0.308	2.150	0.302	1.896	0.345
	2.650	0.258	2.635	0.260	2.617	0.261	2.554	0.264	2.491	0.272	2.607	0.257	2.650	0.251	2.337	0.289
LC 9	0.700	0.990	0.696	0.928	0.691	0.855	0.675	0.776	0.658	0.801	0.689	0.744	0.700	0.724	0.617	0.833
	1.200	0.639	1.193	0.629	1.185	0.610	1.156	0.584	1.128	0.611	1.180	0.554	1.200	0.536	1.058	0.660
	1.700	0.381	1.691	0.379	1.679	0.376	1.638	0.375	1.598	0.393	1.672	0.358	1.700	0.347	1.499	0.434
	2.200	0.280	2.188	0.280	2.172	0.280	2.120	0.285	2.068	0.294	2.164	0.277	2.200	0.271	1.940	0.313
	2.700	0.221	2.685	0.221	2.666	0.220	2.602	0.225	2.538	0.232	2.656	0.218	2.700	0.213	2.381	0.252
LC 10	0.750	0.971	0.746	0.910	0.741	0.833	0.723	0.755	0.705	0.781	0.738	0.722	0.750	0.702	0.661	0.811
	1.250	0.602	1.243	0.593	1.234	0.578	1.205	0.559	1.175	0.585	1.230	0.531	1.250	0.514	1.102	0.636
	1.750	0.367	1.740	0.365	1.728	0.364	1.686	0.362	1.645	0.375	1.722	0.352	1.750	0.345	1.543	0.414
	2.250	0.288	2.237	0.288	2.222	0.288	2.168	0.291	2.115	0.300	2.213	0.283	2.250	0.277	1.984	0.319
	2.750	0.230	2.735	0.230	2.715	0.230	2.650	0.235	2.585	0.242	2.705	0.228	2.750	0.223	2.425	0.261
LC 11	0.800	0.936	0.796	0.884	0.790	0.812	0.771	0.738	0.752	0.764	0.787	0.706	0.800	0.687	0.706	0.797
	1.300	0.560	1.293	0.554	1.284	0.541	1.253	0.527	1.222	0.552	1.279	0.502	1.300	0.485	1.146	0.602
	1.800	0.368	1.790	0.368	1.777	0.366	1.735	0.365	1.692	0.375	1.771	0.354	1.800	0.346	1.587	0.397
	2.300	0.290	2.287	0.290	2.271	0.291	2.216	0.294	2.162	0.303	2.263	0.285	2.300	0.279	2.028	0.322
	2.800	0.233	2.784	0.234	2.765	0.233	2.698	0.238	2.632	0.245	2.754	0.231	2.800	0.225	2.469	0.264
LC 12	0.850	0.912	0.845	0.864	0.839	0.794	0.819	0.722	0.799	0.748	0.836	0.689	0.850	0.670	0.750	0.783
	1.350	0.534	1.342	0.528	1.333	0.517	1.301	0.506	1.269	0.530	1.328	0.482	1.350	0.466	1.191	0.580
	1.850	0.347	1.840	0.344	1.827	0.344	1.783	0.346	1.739	0.356	1.820	0.336	1.850	0.329	1.632	0.382
	2.350	0.272	2.337	0.272	2.320	0.272	2.265	0.276	2.209	0.285	2.312	0.269	2.350	0.263	2.073	0.305
	2.850	0.217	2.834	0.217	2.814	0.216	2.746	0.221	2.679	0.228	2.804	0.214	2.850	0.209	2.513	0.247
LC 13	0.900	0.884	0.895	0.841	0.889	0.772	0.867	0.693	0.846	0.721	0.885	0.660	0.900	0.640	0.794	0.758
	1.400	0.500	1.392	0.496	1.382	0.488	1.349	0.481	1.316	0.504	1.377	0.459	1.400	0.444	1.235	0.555
	1.900	0.347	1.889	0.346	1.876	0.344	1.831	0.343	1.786	0.352	1.869	0.333	1.900	0.326	1.676	0.371
	2.400	0.279	2.387	0.279	2.370	0.279	2.313	0.282	2.256	0.290	2.361	0.274	2.400	0.268	2.117	0.308
	2.900	0.228	2.884	0.228	2.864	0.229	2.795	0.233	2.726	0.240	2.853	0.226	2.900	0.221	2.558	0.257
LC 14	0.950	0.845	0.945	0.812	0.938	0.752	0.915	0.677	0.893	0.705	0.935	0.643	0.950	0.624	0.838	0.744
	1.450	0.476	1.442	0.472	1.432	0.465	1.397	0.461	1.363	0.483	1.426	0.439	1.450	0.425	1.279	0.531
	1.950	0.337	1.939	0.336	1.925	0.335	1.879	0.334	1.833	0.343	1.918	0.325	1.950	0.318	1.720	0.362
	2.450	0.264	2.436	0.266	2.419	0.269	2.361	0.275	2.303	0.282	2.410	0.267	2.450	0.261	2.161	0.300
	2.950	0.221	2.934	0.221	2.913	0.222	2.843	0.226	2.773	0.233	2.902	0.220	2.950	0.215	2.602	0.250
LC 15	1.000	0.800	0.994	0.776	0.987	0.729	0.964	0.657	0.940	0.685	0.984	0.623	1.000	0.603	0.882	0.727
	1.500	0.448	1.492	0.447	1.481	0.441	1.445	0.438	1.410	0.459	1.476	0.418	1.500	0.405	1.323	0.507
	2.000	0.341	1.989	0.340	1.975	0.339	1.927	0.336	1.880	0.346	1.967	0.327	2.000	0.320	1.764	0.364
	2.500	0.279	2.486	0.280	2.469	0.280	2.409	0.282	2.350	0.289	2.459	0.274	2.500	0.268	2.205	0.306
	3.000	0.232	2.983	0.233	2.962	0.233	2.891	0.236	2.820	0.243	2.951	0.230	3.000	0.224	2.646	0.260
LC 16	1.050	0.746	1.044	0.728	1.037	0.694	1.012	0.638	0.987	0.666	1.033	0.605	1.050	0.586	0.926	0.709
	1.550	0.425	1.541	0.423	1.531	0.418	1.494	0.417	1.457	0.436	1.525	0.398	1.550	0.385	1.367	0.482
	2.050	0.303	2.039	0.303	2.024	0.303	1.975	0.306	1.927	0.314	2.017	0.297	2.050	0.291	1.808	0.334
	2.550	0.239	2.536	0.240	2.518	0.241	2.457	0.246	2.397	0.253	2.509	0.239	2.550	0.234	2.249	0.271
	3.050	0.193	3.033	0.193	3.012	0.193	2.939	0.197	2.867	0.204	3.000	0.191	3.050	0.186	2.690	0.221

Table C1.1: Data ($\lambda_{D,T}$ vs $M_{u,T}/M_{y,T}$) of the SCB lipped channel beams at room and elevated temperatures analysed in this work.
(*continuation*)

Beam	100°C		200°C		300°C		400°C		500°C		600°C		700°C		800°C	
	$\lambda_{D,T}$	$\dfrac{M_{u,T}}{M_{y,T}}$	$\lambda_{D,T}$	$\dfrac{M_{u,T}}{M_{y,T}}$	$\lambda_{D,T}$	$\dfrac{M_{u,T}}{M_{y,T}}$	$\lambda_{D,T}$	$\dfrac{M_{u,T}}{M_{y,T}}$	λD	$\lambda_{D,T}$	$\dfrac{M_{u,T}}{M_{y,T}}$	$\lambda_{D,T}$	$\dfrac{M_{u,T}}{M_{y,T}}$	$\lambda_{D,T}$	$\dfrac{M_{u,T}}{M_{y,T}}$	$\lambda_{D,T}$
LC 17	1.100	0.707	1.094	0.693	1.086	0.666	1.060	0.621	1.034	0.649	1.082	0.589	1.100	0.570	0.970	0.695
	1.600	0.408	1.591	0.406	1.580	0.402	1.542	0.401	1.504	0.420	1.574	0.383	1.600	0.371	1.411	0.464
	2.100	0.300	2.088	0.301	2.074	0.300	2.024	0.303	1.974	0.312	2.066	0.295	2.100	0.289	1.852	0.331
	2.600	0.238	2.586	0.239	2.567	0.239	2.505	0.244	2.444	0.252	2.558	0.238	2.600	0.232	2.293	0.270
	3.100	0.191	3.083	0.192	3.061	0.192	2.987	0.197	2.914	0.204	3.050	0.190	3.100	0.186	2.734	0.221
LC 18	1.150	0.663	1.144	0.652	1.136	0.630	1.108	0.598	1.081	0.626	1.131	0.567	1.150	0.548	1.014	0.672
	1.650	0.389	1.641	0.387	1.629	0.383	1.590	0.382	1.551	0.400	1.623	0.367	1.650	0.359	1.455	0.443
	2.150	0.303	2.138	0.304	2.123	0.304	2.072	0.306	2.021	0.315	2.115	0.297	2.150	0.291	1.896	0.334
	2.650	0.244	2.635	0.244	2.617	0.244	2.554	0.249	2.491	0.256	2.607	0.242	2.650	0.236	2.337	0.274
	3.150	0.199	3.132	0.199	3.110	0.199	3.035	0.203	2.961	0.210	3.099	0.196	3.150	0.191	2.778	0.227
LC 19	1.200	0.633	1.193	0.623	1.185	0.604	1.156	0.580	1.128	0.607	1.180	0.550	1.200	0.532	1.058	0.655
	1.700	0.378	1.691	0.377	1.679	0.373	1.638	0.372	1.598	0.389	1.672	0.355	1.700	0.346	1.499	0.430
	2.200	0.283	2.188	0.283	2.172	0.283	2.120	0.288	2.068	0.296	2.164	0.280	2.200	0.274	1.940	0.316
	2.700	0.224	2.685	0.224	2.666	0.223	2.602	0.228	2.538	0.236	2.656	0.221	2.700	0.216	2.381	0.255
	3.200	0.178	3.182	0.178	3.160	0.178	3.084	0.181	3.008	0.188	3.148	0.174	3.200	0.170	2.822	0.206
LC 20	1.250	0.595	1.243	0.587	1.234	0.572	1.205	0.554	1.175	0.580	1.230	0.526	1.250	0.509	1.102	0.631
	1.750	0.367	1.740	0.363	1.728	0.358	1.686	0.361	1.645	0.374	1.722	0.353	1.750	0.345	1.543	0.411
	2.250	0.287	2.237	0.288	2.222	0.290	2.168	0.294	2.115	0.303	2.213	0.286	2.250	0.280	1.984	0.321
	2.750	0.233	2.735	0.233	2.715	0.234	2.650	0.239	2.585	0.246	2.705	0.232	2.750	0.227	2.425	0.264
	3.250	0.188	3.232	0.189	3.209	0.189	3.132	0.193	3.055	0.200	3.197	0.186	3.250	0.182	2.866	0.218
LC 21	1.300	0.545	1.293	0.537	1.284	0.525	1.253	0.515	1.222	0.538	1.279	0.491	1.300	0.476	1.146	0.587
	1.800	0.361	1.790	0.361	1.777	0.360	1.735	0.358	1.692	0.369	1.771	0.347	1.800	0.340	1.587	0.390
	2.300	0.285	2.287	0.286	2.271	0.286	2.216	0.289	2.162	0.298	2.263	0.281	2.300	0.275	2.028	0.316
	2.800	0.230	2.784	0.230	2.765	0.231	2.698	0.236	2.632	0.243	2.754	0.229	2.800	0.224	2.469	0.261
	3.300	0.187	3.282	0.187	3.258	0.187	3.180	0.191	3.102	0.198	3.246	0.184	3.300	0.180	2.910	0.216
LC 22	1.350	0.527	1.342	0.522	1.333	0.511	1.301	0.501	1.269	0.524	1.328	0.477	1.350	0.462	1.191	0.575
	1.850	0.357	1.840	0.357	1.827	0.356	1.783	0.354	1.739	0.364	1.820	0.344	1.850	0.337	1.632	0.386
	2.350	0.283	2.337	0.283	2.320	0.283	2.265	0.287	2.209	0.295	2.312	0.278	2.350	0.272	2.073	0.314
	2.850	0.229	2.834	0.228	2.814	0.228	2.746	0.232	2.679	0.240	2.804	0.225	2.850	0.220	2.513	0.258
	3.350	0.184	3.331	0.185	3.308	0.184	3.228	0.188	3.149	0.195	3.296	0.181	3.350	0.176	2.954	0.213
LC 23	1.400	0.503	1.392	0.499	1.382	0.490	1.349	0.481	1.316	0.504	1.377	0.459	1.400	0.444	1.235	0.552
	1.900	0.336	1.889	0.336	1.876	0.336	1.831	0.337	1.786	0.346	1.869	0.327	1.900	0.320	1.676	0.367
	2.400	0.265	2.387	0.265	2.370	0.265	2.313	0.270	2.256	0.278	2.361	0.262	2.400	0.256	2.117	0.297
	2.900	0.212	2.884	0.212	2.864	0.212	2.795	0.216	2.726	0.224	2.853	0.210	2.900	0.204	2.558	0.242
	3.400	0.170	3.381	0.170	3.357	0.170	3.276	0.173	3.196	0.180	3.345	0.167	3.400	0.162	2.999	0.198
LC 24	1.450	0.469	1.442	0.462	1.432	0.452	1.397	0.447	1.363	0.467	1.426	0.428	1.450	0.415	1.279	0.512
	1.950	0.339	1.939	0.338	1.925	0.338	1.879	0.338	1.833	0.348	1.918	0.328	1.950	0.321	1.720	0.369
	2.450	0.270	2.436	0.271	2.419	0.271	2.361	0.275	2.303	0.283	2.410	0.267	2.450	0.261	2.161	0.301
	2.950	0.219	2.934	0.219	2.913	0.220	2.843	0.225	2.773	0.232	2.902	0.218	2.950	0.213	2.602	0.249
	3.450	0.180	3.431	0.180	3.407	0.180	3.325	0.183	3.243	0.188	3.394	0.177	3.450	0.172	3.043	0.207
LC 25	1.500	0.460	1.492	0.457	1.481	0.450	1.445	0.446	1.410	0.468	1.476	0.426	1.500	0.411	1.323	0.515
	2.000	0.325	1.989	0.326	1.975	0.325	1.927	0.326	1.880	0.335	1.967	0.317	2.000	0.310	1.764	0.355
	2.500	0.259	2.486	0.260	2.469	0.260	2.409	0.264	2.350	0.272	2.459	0.256	2.500	0.250	2.205	0.290
	3.000	0.210	2.983	0.211	2.962	0.210	2.891	0.215	2.820	0.222	2.951	0.208	3.000	0.203	2.646	0.239
	3.500	0.172	3.481	0.173	3.456	0.172	3.373	0.176	3.290	0.183	3.443	0.169	3.500	0.165	3.087	0.198
LC 26	1.550	0.454	1.541	0.449	1.531	0.442	1.494	0.437	1.457	0.458	1.525	0.417	1.550	0.404	1.367	0.504
	2.050	0.317	2.039	0.316	2.024	0.315	1.975	0.317	1.927	0.327	2.017	0.308	2.050	0.301	1.808	0.347
	2.550	0.253	2.536	0.252	2.518	0.251	2.457	0.255	2.397	0.263	2.509	0.248	2.550	0.235	2.249	0.281
	3.050	0.197	3.033	0.198	3.012	0.201	2.939	0.206	2.867	0.215	3.000	0.201	3.050	0.196	2.690	0.227
	3.550	0.147	3.530	0.149	3.505	0.151	3.421	0.161	3.336	0.173	3.492	0.163	3.550	0.158	3.131	0.192
LC 27	1.600	0.421	1.591	0.413	1.580	0.403	1.542	0.393	1.504	0.406	1.574	0.379	1.600	0.370	1.411	0.441
	2.100	0.325	2.088	0.324	2.074	0.319	2.024	0.314	1.974	0.324	2.066	0.304	2.100	0.297	1.852	0.345
	2.600	0.271	2.586	0.269	2.567	0.264	2.505	0.261	2.444	0.258	2.558	0.253	2.600	0.247	2.293	0.288
	3.100	0.222	3.083	0.225	3.061	0.223	2.987	0.221	2.914	0.228	3.050	0.213	3.100	0.208	2.734	0.245
	3.600	0.191	3.580	0.190	3.555	0.189	3.469	0.188	3.383	0.195	3.541	0.181	3.600	0.176	3.175	0.211
LC 28	1.650	0.399	1.641	0.399	1.629	0.390	1.590	0.386	1.551	0.402	1.623	0.375	1.650	0.366	1.455	0.442
	2.150	0.318	2.138	0.316	2.123	0.313	2.072	0.310	2.021	0.320	2.115	0.300	2.150	0.294	1.896	0.340
	2.650	0.263	2.635	0.262	2.617	0.258	2.554	0.256	2.491	0.265	2.607	0.247	2.650	0.242	2.337	0.283
	3.150	0.192	3.132	0.217	3.110	0.215	3.035	0.214	2.961	0.222	3.099	0.207	3.150	0.202	2.778	0.239
	3.650	0.162	3.630	0.169	3.604	0.175	3.517	0.178	3.430	0.187	3.591	0.172	3.650	0.167	3.219	0.204
LC 29	1.700	0.410	1.691	0.406	1.679	0.399	1.638	0.394	1.598	0.412	1.672	0.376	1.700	0.365	1.499	0.453
	2.200	0.303	2.188	0.301	2.172	0.300	2.120	0.303	2.068	0.312	2.164	0.295	2.200	0.288	1.940	0.333
	2.700	0.240	2.685	0.239	2.666	0.238	2.602	0.241	2.538	0.250	2.656	0.233	2.700	0.228	2.381	0.270
	3.200	0.185	3.182	0.189	3.160	0.189	3.084	0.193	3.008	0.200	3.148	0.186	3.200	0.181	2.822	0.219
	3.700	0.149	3.679	0.152	3.653	0.153	3.565	0.156	3.477	0.163	3.640	0.149	3.700	0.145	3.263	0.180
LC 30	1.750	0.378	1.740	0.375	1.728	0.371	1.686	0.370	1.645	0.387	1.722	0.353	1.750	0.342	1.543	0.425
	2.250	0.275	2.237	0.273	2.222	0.273	2.168	0.277	2.115	0.286	2.213	0.269	2.250	0.263	1.984	0.306
	2.750	0.217	2.735	0.216	2.715	0.215	2.650	0.217	2.585	0.225	2.705	0.210	2.750	0.205	2.425	0.244
	3.250	0.171	3.232	0.171	3.209	0.170	3.132	0.173	3.055	0.180	3.197	0.167	3.250	0.159	2.866	0.198
	3.750	0.136	3.729	0.136	3.703	0.137	3.614	0.139	3.524	0.146	3.689	0.128	3.750	0.130	3.307	0.158

Table C1.2: Data ($\lambda_{D.T}$ vs $M_{u.T}/M_{nD.T}$) of the SCB lipped channel beams at room and elevated temperatures analysed in this work.
(to be continued)

Beam	100°C		200°C		300°C		400°C		500°C		600°C		700°C		800°C	
	$\lambda_{D.T}$	$\dfrac{M_{u.T}}{M_{nD.T}}$	$\lambda_{D.T}$	$\dfrac{M_{u.T}}{M_{nD.T}}$	$\lambda_{D.T}$	$\dfrac{M_{u.T}}{M_{nD.T}}$	$\lambda_{D.T}$	$\dfrac{M_{u.T}}{M_{nD.T}}$	$\lambda_{D.T}$	$\dfrac{M_{u.T}}{M_{nD.T}}$	$\lambda_{D.T}$	$\dfrac{M_{u.T}}{M_{nD.T}}$	$\lambda_{D.T}$	$\dfrac{M_{u.T}}{M_{nD.T}}$	$\lambda_{D.T}$	$\dfrac{M_{u.T}}{M_{nD.T}}$
LC 1	0.300	1.034	0.298	0.969	0.296	0.900	0.289	0.834	0.282	0.849	0.295	0.813	0.300	0.802	0.265	0.865
	0.800	1.029	0.796	0.968	0.790	0.887	0.771	0.798	0.752	0.812	0.787	0.775	0.800	0.764	0.706	0.823
	1.300	1.016	1.293	0.997	1.284	0.964	1.253	0.911	1.222	0.925	1.279	0.888	1.300	0.877	1.146	0.939
	1.800	0.983	1.790	0.975	1.777	0.949	1.735	0.921	1.692	0.927	1.771	0.926	1.800	0.926	1.587	0.923
	2.300	1.026	2.287	1.039	2.271	1.033	2.216	1.019	2.162	1.021	2.263	1.022	2.300	1.022	2.028	1.004
LC 2	0.350	1.034	0.348	0.969	0.346	0.901	0.337	0.844	0.329	0.860	0.344	0.823	0.350	0.810	0.309	0.881
	0.850	1.037	0.845	0.976	0.839	0.886	0.819	0.778	0.799	0.794	0.836	0.752	0.850	0.739	0.750	0.801
	1.350	0.983	1.342	0.958	1.333	0.922	1.301	0.874	1.269	0.888	1.328	0.854	1.350	0.843	1.191	0.903
	1.850	1.142	1.840	1.139	1.827	1.131	1.783	1.074	1.739	1.069	1.820	0.860	1.850	0.964	1.632	0.889
	2.350	0.996	2.337	1.077	2.320	1.134	2.265	1.153	2.209	1.193	2.312	1.050	2.350	1.025	2.073	0.907
LC 3	0.400	1.045	0.398	0.972	0.395	0.885	0.385	0.798	0.376	0.819	0.393	0.769	0.400	0.753	0.353	0.841
	0.900	1.078	0.895	1.016	0.889	0.923	0.867	0.808	0.846	0.823	0.885	0.781	0.900	0.768	0.794	0.826
	1.400	0.985	1.392	0.970	1.382	0.946	1.349	0.908	1.316	0.923	1.377	0.888	1.400	0.877	1.235	0.939
	1.900	1.086	1.889	1.069	1.876	1.044	1.831	0.998	1.786	0.986	1.869	0.987	1.900	0.987	1.676	0.954
	2.400	1.223	2.387	1.208	2.370	1.188	2.313	1.143	2.256	1.136	2.361	1.140	2.400	1.142	2.117	1.102
LC 4	0.450	1.046	0.447	0.976	0.444	0.902	0.434	0.816	0.423	0.837	0.443	0.787	0.450	0.772	0.397	0.857
	0.950	1.090	0.945	1.038	0.938	0.952	0.915	0.836	0.893	0.851	0.935	0.810	0.950	0.797	0.838	0.852
	1.450	1.000	1.442	0.983	1.432	0.956	1.397	0.917	1.363	0.932	1.426	0.898	1.450	0.887	1.279	0.946
	1.950	1.113	1.939	1.097	1.925	1.074	1.879	1.027	1.833	1.021	1.918	1.023	1.950	1.023	1.720	0.988
	2.450	1.249	2.436	1.236	2.419	1.216	2.361	1.171	2.303	1.164	2.410	1.170	2.450	1.172	2.161	1.129
LC 5	0.500	1.017	0.497	0.972	0.494	0.887	0.482	0.794	0.470	0.828	0.492	0.759	0.500	0.783	0.441	0.805
	1.000	1.109	0.994	1.061	0.987	0.985	0.964	0.880	0.940	0.894	0.984	0.856	1.000	0.845	0.882	0.893
	1.500	1.065	1.492	1.046	1.481	1.014	1.445	0.961	1.410	0.975	1.476	0.941	1.500	0.930	1.323	0.986
	2.000	1.070	1.989	1.052	1.975	1.026	1.927	0.998	1.880	0.993	1.967	0.997	2.000	0.998	1.764	0.992
	2.500	1.134	2.486	1.120	2.469	1.105	2.409	1.085	2.350	1.081	2.459	1.084	2.500	1.084	2.205	1.061
LC 6	0.550	1.026	0.547	0.962	0.543	0.874	0.530	0.773	0.517	0.797	0.541	0.740	0.550	0.723	0.485	0.822
	1.050	1.071	1.044	1.040	1.037	0.983	1.012	0.871	0.987	0.887	1.033	0.842	1.050	0.829	0.926	0.887
	1.550	0.982	1.541	0.965	1.531	0.938	1.494	0.903	1.457	0.916	1.525	0.886	1.550	0.876	1.367	0.935
	2.050	1.147	2.039	1.128	2.024	1.102	1.975	1.052	1.927	1.047	2.017	1.049	2.050	1.049	1.808	1.014
	2.550	1.264	2.536	1.256	2.518	1.211	2.457	1.181	2.397	1.188	2.509	1.194	2.550	1.197	2.249	1.153
LC 7	0.600	1.010	0.597	0.945	0.592	0.864	0.578	0.770	0.564	0.793	0.590	0.739	0.600	0.722	0.529	0.819
	1.100	1.042	1.094	1.022	1.086	0.975	1.060	0.883	1.034	0.899	1.082	0.854	1.100	0.841	0.970	0.900
	1.600	0.957	1.591	0.943	1.580	0.923	1.542	0.891	1.504	0.905	1.574	0.874	1.600	0.865	1.411	0.923
	2.100	1.085	2.088	1.076	2.074	1.062	2.024	1.027	1.974	1.019	2.066	1.027	2.100	1.029	1.852	0.986
	2.600	1.194	2.586	1.186	2.567	1.176	2.505	1.150	2.444	1.141	2.558	1.151	2.600	1.153	2.293	1.109
LC 8	0.650	1.016	0.646	0.951	0.642	0.869	0.626	0.776	0.611	0.799	0.639	0.743	0.650	0.725	0.573	0.824
	1.150	0.971	1.144	0.948	1.136	0.918	1.108	0.864	1.081	0.879	1.131	0.840	1.150	0.828	1.014	0.884
	1.650	0.937	1.641	0.922	1.629	0.909	1.590	0.866	1.551	0.879	1.623	0.888	1.650	0.888	1.455	0.876
	2.150	1.105	2.138	1.095	2.123	1.082	2.072	1.047	2.021	1.040	2.115	1.047	2.150	1.049	1.896	1.009
	2.650	1.204	2.635	1.204	2.617	1.195	2.554	1.169	2.491	1.161	2.607	1.171	2.650	1.173	2.337	1.127
LC 9	0.700	1.007	0.696	0.942	0.691	0.866	0.675	0.780	0.658	0.799	0.689	0.752	0.700	0.736	0.617	0.825
	1.200	1.041	1.193	1.018	1.185	0.979	1.156	0.912	1.128	0.927	1.180	0.886	1.200	0.873	1.058	0.934
	1.700	0.962	1.691	0.950	1.679	0.932	1.638	0.901	1.598	0.913	1.672	0.885	1.700	0.875	1.499	0.929
	2.200	1.005	2.188	0.997	2.172	0.988	2.120	0.972	2.068	0.966	2.164	0.973	2.200	0.973	1.940	0.945
	2.700	1.061	2.685	1.051	2.666	1.037	2.602	1.021	2.538	1.020	2.656	1.020	2.700	1.020	2.381	1.009
LC 10	0.750	1.022	0.746	0.954	0.741	0.870	0.723	0.779	0.705	0.796	0.738	0.752	0.750	0.739	0.661	0.809
	1.250	1.028	1.243	1.007	1.234	0.972	1.205	0.914	1.175	0.930	1.230	0.890	1.250	0.878	1.102	0.940
	1.750	0.961	1.740	0.950	1.728	0.938	1.686	0.905	1.645	0.906	1.722	0.903	1.750	0.904	1.543	0.921
	2.250	1.065	2.237	1.058	2.222	1.047	2.168	1.024	2.115	1.018	2.213	1.024	2.250	1.025	1.984	0.992
	2.750	1.131	2.735	1.121	2.715	1.111	2.650	1.095	2.585	1.091	2.705	1.096	2.750	1.096	2.425	1.072
LC 11	0.800	1.027	0.796	0.965	0.790	0.882	0.771	0.789	0.752	0.804	0.787	0.765	0.800	0.754	0.706	0.813
	1.300	1.004	1.293	0.986	1.284	0.954	1.253	0.903	1.222	0.918	1.279	0.881	1.300	0.869	1.146	0.931
	1.800	1.002	1.790	0.994	1.777	0.981	1.735	0.945	1.692	0.940	1.771	0.943	1.800	0.943	1.587	0.915
	2.300	1.109	2.287	1.100	2.271	1.090	2.216	1.066	2.162	1.060	2.263	1.065	2.300	1.066	2.028	1.033
	2.800	1.175	2.784	1.170	2.765	1.157	2.698	1.134	2.632	1.134	2.754	1.137	2.800	1.137	2.469	1.115
LC 12	0.850	1.047	0.845	0.987	0.839	0.902	0.819	0.805	0.799	0.819	0.836	0.781	0.850	0.769	0.750	0.824
	1.350	1.001	1.342	0.985	1.333	0.955	1.301	0.907	1.269	0.921	1.328	0.886	1.350	0.875	1.191	0.936
	1.850	0.981	1.840	0.964	1.827	0.956	1.783	0.931	1.739	0.926	1.820	0.929	1.850	0.929	1.632	0.914
	2.350	1.069	2.337	1.061	2.320	1.051	2.265	1.033	2.209	1.027	2.312	1.033	2.350	1.033	2.073	1.006
	2.850	1.122	2.834	1.113	2.814	1.100	2.746	1.085	2.679	1.083	2.804	1.083	2.850	1.083	2.513	1.070
LC 13	0.900	1.066	0.895	1.008	0.889	0.920	0.867	0.809	0.846	0.824	0.885	0.784	0.900	0.772	0.794	0.826
	1.400	0.982	1.392	0.967	1.382	0.943	1.349	0.902	1.316	0.917	1.377	0.882	1.400	0.871	1.235	0.934
	1.900	1.016	1.889	1.005	1.876	0.992	1.831	0.955	1.786	0.949	1.869	0.954	1.900	0.955	1.676	0.919
	2.400	1.130	2.387	1.123	2.370	1.112	2.313	1.085	2.256	1.077	2.361	1.086	2.400	1.088	2.117	1.046
	2.900	1.210	2.884	1.203	2.864	1.193	2.795	1.166	2.726	1.166	2.853	1.175	2.900	1.176	2.558	1.140
LC 14	0.950	1.071	0.945	1.023	0.938	0.942	0.915	0.828	0.893	0.843	0.935	0.802	0.950	0.790	0.838	0.845
	1.450	0.976	1.442	0.962	1.432	0.939	1.397	0.902	1.363	0.916	1.426	0.882	1.450	0.871	1.279	0.933
	1.950	1.023	1.939	1.012	1.925	1.000	1.879	0.965	1.833	0.958	1.918	0.964	1.950	0.965	1.720	0.929
	2.450	1.102	2.436	1.101	2.419	1.103	2.361	1.088	2.303	1.080	2.410	1.089	2.450	1.090	2.161	1.050
	2.950	1.202	2.934	1.195	2.913	1.185	2.843	1.167	2.773	1.162	2.902	1.168	2.950	1.168	2.602	1.138
LC 15	1.000	1.067	0.994	1.029	0.987	0.959	0.964	0.844	0.940	0.860	0.984	0.816	1.000	0.804	0.882	0.860
	1.500	0.959	1.492	0.952	1.481	0.929	1.445	0.896	1.410	0.910	1.476	0.878	1.500	0.867	1.323	0.928
	2.000	1.074	1.989	1.062	1.975	1.047	1.927	1.006	1.880	0.998	1.967	1.005	2.000	1.007	1.764	0.965
	2.500	1.197	2.486	1.192	2.469	1.179	2.409	1.148	2.350	1.138	2.459	1.149	2.500	1.151	2.205	1.103
	3.000	1.295	2.983	1.287	2.962	1.274	2.891	1.241	2.820	1.241	2.951	1.251	3.000	1.252	2.646	1.210
LC 16	1.050	1.046	1.044	1.015	1.037	0.960	1.012	0.861	0.987	0.876	1.033	0.834	1.050	0.822	0.926	0.877
	1.550	0.951	1.541	0.939	1.531	0.919	1.494	0.888	1.457	0.901	1.525	0.870	1.550	0.860	1.367	0.918
	2.050	0.985	2.039	0.978	2.024	0.969	1.975	0.945	1.927	0.939	2.017	0.944	2.050	0.945	1.808	0.914
	2.550	1.058	2.536	1.051	2.518	1.044	2.457	1.030	2.397	1.024	2.509	1.032	2.550	1.033	2.249	1.002
	3.050	1.102	3.033	1.094	3.012	1.082	2.939	1.068	2.867	1.067	3.000	1.065	3.050	1.064	2.690	1.056

Table C1.2: Data ($\lambda_{D.T}$ vs $M_{u.T}/M_{nD.T}$) of the SCB lipped channel beams at room and elevated temperatures analysed in this work.
(*continuation*)

Beam	100°C		200°C		300°C		400°C		500°C		600°C		700°C		800°C	
	$\lambda_{D.T}$	$\dfrac{M_{u.T}}{M_{nD.T}}$	$\lambda_{D.T}$	$\dfrac{M_{u.T}}{M_{nD.T}}$	$\lambda_{D.T}$	$\dfrac{M_{u.T}}{M_{nD.T}}$	$\lambda_{D.T}$	$\dfrac{M_{u.T}}{M_{nD.T}}$	$\lambda_{D.T}$	$\dfrac{M_{u.T}}{M_{nD.T}}$	$\lambda_{D.T}$	$\dfrac{M_{u.T}}{M_{nD.T}}$	$\lambda_{D.T}$	$\dfrac{M_{u.T}}{M_{nD.T}}$	$\lambda_{D.T}$	$\dfrac{M_{u.T}}{M_{nD.T}}$
LC 17	1.100	1.043	1.094	1.016	1.086	0.970	1.060	0.881	1.034	0.896	1.082	0.853	1.100	0.841	0.970	0.899
	1.600	0.951	1.591	0.940	1.580	0.921	1.542	0.890	1.504	0.903	1.574	0.873	1.600	0.864	1.411	0.920
	2.100	1.010	2.088	1.003	2.074	0.993	2.024	0.970	1.974	0.964	2.066	0.969	2.100	0.971	1.852	0.938
	2.600	1.083	2.586	1.076	2.567	1.068	2.505	1.053	2.444	1.047	2.558	1.055	2.600	1.056	2.293	1.026
	3.100	1.116	3.083	1.115	3.061	1.104	2.987	1.090	2.914	1.089	3.050	1.087	3.100	1.085	2.734	1.079
LC 18	1.150	1.028	1.144	1.004	1.136	0.963	1.108	0.890	1.081	0.905	1.131	0.863	1.150	0.850	1.014	0.909
	1.650	0.944	1.641	0.931	1.629	0.914	1.590	0.883	1.551	0.895	1.623	0.871	1.650	0.872	1.455	0.912
	2.150	1.055	2.138	1.048	2.123	1.036	2.072	1.010	2.021	1.003	2.115	1.009	2.150	1.011	1.896	0.975
	2.650	1.140	2.635	1.131	2.617	1.120	2.554	1.102	2.491	1.095	2.607	1.103	2.650	1.104	2.337	1.071
	3.150	1.191	3.132	1.182	3.110	1.169	3.035	1.149	2.961	1.148	3.099	1.145	3.150	1.143	2.778	1.134
LC 19	1.200	1.030	1.193	1.008	1.185	0.970	1.156	0.905	1.128	0.920	1.180	0.879	1.200	0.867	1.058	0.927
	1.700	0.955	1.691	0.944	1.679	0.925	1.638	0.894	1.598	0.905	1.672	0.878	1.700	0.873	1.499	0.922
	2.200	1.016	2.188	1.007	2.172	0.999	2.120	0.981	2.068	0.976	2.164	0.981	2.200	0.982	1.940	0.953
	2.700	1.074	2.685	1.064	2.666	1.052	2.602	1.037	2.538	1.035	2.656	1.036	2.700	1.035	2.381	1.021
	3.200	1.089	3.182	1.080	3.160	1.068	3.084	1.050	3.008	1.054	3.148	1.043	3.200	1.039	2.822	1.053
LC 20	1.250	1.017	1.243	0.997	1.234	0.962	1.205	0.906	1.175	0.921	1.230	0.882	1.250	0.870	1.102	0.933
	1.750	0.962	1.740	0.945	1.728	0.924	1.686	0.901	1.645	0.904	1.722	0.905	1.750	0.906	1.543	0.913
	2.250	1.064	2.237	1.058	2.222	1.054	2.168	1.034	2.115	1.027	2.213	1.034	2.250	1.035	1.984	1.000
	2.750	1.146	2.735	1.138	2.715	1.129	2.650	1.114	2.585	1.108	2.705	1.115	2.750	1.115	2.425	1.087
	3.250	1.180	3.232	1.174	3.209	1.162	3.132	1.145	3.055	1.146	3.197	1.140	3.250	1.137	2.866	1.137
LC 21	1.300	0.975	1.293	0.956	1.284	0.926	1.253	0.882	1.222	0.896	1.279	0.863	1.300	0.852	1.146	0.907
	1.800	0.983	1.790	0.976	1.777	0.964	1.735	0.928	1.692	0.924	1.771	0.925	1.800	0.926	1.587	0.900
	2.300	1.089	2.287	1.083	2.271	1.073	2.216	1.048	2.162	1.042	2.263	1.049	2.300	1.051	2.028	1.014
	2.800	1.159	2.784	1.152	2.765	1.144	2.698	1.128	2.632	1.123	2.754	1.130	2.800	1.130	2.469	1.101
	3.300	1.197	3.282	1.189	3.258	1.176	3.180	1.158	3.102	1.159	3.246	1.153	3.300	1.150	2.910	1.151
LC 22	1.350	0.988	1.342	0.972	1.333	0.944	1.301	0.898	1.269	0.912	1.328	0.878	1.350	0.867	1.191	0.927
	1.850	1.009	1.840	1.000	1.827	0.988	1.783	0.953	1.739	0.948	1.820	0.951	1.850	0.952	1.632	0.922
	2.350	1.112	2.337	1.104	2.320	1.094	2.265	1.071	2.209	1.064	2.312	1.070	2.350	1.071	2.073	1.038
	2.850	1.184	2.834	1.173	2.814	1.160	2.746	1.140	2.679	1.137	2.804	1.140	2.850	1.140	2.513	1.118
	3.350	1.207	3.331	1.199	3.308	1.185	3.228	1.163	3.149	1.167	3.296	1.155	3.350	1.150	2.954	1.163
LC 23	1.400	0.987	1.392	0.972	1.382	0.946	1.349	0.902	1.316	0.916	1.377	0.882	1.400	0.871	1.235	0.930
	1.900	0.984	1.889	0.977	1.876	0.968	1.831	0.938	1.786	0.934	1.869	0.937	1.900	0.938	1.676	0.909
	2.400	1.072	2.387	1.065	2.370	1.056	2.313	1.038	2.256	1.032	2.361	1.038	2.400	1.039	2.117	1.009
	2.900	1.125	2.884	1.116	2.864	1.103	2.795	1.088	2.726	1.086	2.853	1.087	2.900	1.086	2.558	1.073
	3.400	1.135	3.381	1.127	3.357	1.116	3.276	1.103	3.196	1.103	3.345	1.090	3.400	1.085	2.999	1.102
LC 24	1.450	0.963	1.442	0.942	1.432	0.913	1.397	0.876	1.363	0.887	1.426	0.861	1.450	0.852	1.279	0.899
	1.950	1.028	1.939	1.020	1.925	1.008	1.879	0.977	1.833	0.971	1.918	0.975	1.950	0.975	1.720	0.946
	2.450	1.129	2.436	1.122	2.419	1.112	2.361	1.087	2.303	1.081	2.410	1.087	2.450	1.089	2.161	1.054
	2.950	1.191	2.934	1.184	2.913	1.175	2.843	1.159	2.773	1.154	2.902	1.158	2.950	1.158	2.602	1.134
	3.450	1.233	3.431	1.221	3.407	1.204	3.325	1.186	3.243	1.176	3.394	1.180	3.450	1.177	3.043	1.180
LC 25	1.500	0.986	1.492	0.972	1.481	0.948	1.445	0.912	1.410	0.926	1.476	0.893	1.500	0.882	1.323	0.942
	2.000	1.023	1.989	1.016	1.975	1.004	1.927	0.975	1.880	0.969	1.967	0.974	2.000	0.975	1.764	0.941
	2.500	1.114	2.486	1.107	2.469	1.097	2.409	1.074	2.350	1.068	2.459	1.075	2.500	1.075	2.205	1.044
	3.000	1.171	2.983	1.165	2.962	1.151	2.891	1.135	2.820	1.131	2.951	1.133	3.000	1.133	2.646	1.114
	3.500	1.202	3.481	1.194	3.456	1.180	3.373	1.161	3.290	1.164	3.443	1.154	3.500	1.149	3.087	1.153
LC 26	1.550	1.014	1.541	0.997	1.531	0.972	1.494	0.931	1.457	0.945	1.525	0.913	1.550	0.902	1.367	0.961
	2.050	1.032	2.039	1.020	2.024	1.005	1.975	0.981	1.927	0.976	2.017	0.979	2.050	0.980	1.808	0.951
	2.550	1.119	2.536	1.105	2.518	1.090	2.457	1.068	2.397	1.063	2.509	1.069	2.550	1.038	2.249	1.040
	3.050	1.123	3.033	1.124	3.012	1.126	2.939	1.113	2.867	1.121	3.000	1.120	3.050	1.119	2.690	1.084
	3.550	1.048	3.530	1.051	3.505	1.059	3.421	1.089	3.336	1.126	3.492	1.133	3.550	1.128	3.131	1.141
LC 27	1.600	0.980	1.591	0.955	1.580	0.923	1.542	0.873	1.504	0.873	1.574	0.865	1.600	0.862	1.411	0.875
	2.100	1.092	2.088	1.081	2.074	1.055	2.024	1.003	1.974	1.000	2.066	0.999	2.100	0.999	1.852	0.976
	2.600	1.231	2.586	1.210	2.567	1.180	2.505	1.124	2.444	1.075	2.558	1.121	2.600	1.122	2.293	1.093
	3.100	1.298	3.083	1.304	3.061	1.280	2.987	1.224	2.914	1.221	3.050	1.219	3.100	1.218	2.734	1.196
	3.600	1.386	3.580	1.373	3.555	1.347	3.469	1.295	3.383	1.297	3.541	1.285	3.600	1.280	3.175	1.278
LC 28	1.650	0.967	1.641	0.960	1.629	0.931	1.590	0.891	1.551	0.899	1.623	0.891	1.650	0.889	1.455	0.912
	2.150	1.106	2.138	1.091	2.123	1.068	2.072	1.023	2.021	1.019	2.115	1.019	2.150	1.020	1.896	0.995
	2.650	1.225	2.635	1.211	2.617	1.182	2.554	1.133	2.491	1.130	2.607	1.128	2.650	1.129	2.337	1.105
	3.150	1.147	3.132	1.289	3.110	1.265	3.035	1.217	2.961	1.215	3.099	1.210	3.150	1.208	2.778	1.193
	3.650	1.201	3.630	1.244	3.604	1.277	3.517	1.253	3.430	1.268	3.591	1.249	3.650	1.241	3.219	1.261
LC 29	1.700	1.034	1.691	1.018	1.679	0.991	1.638	0.947	1.598	0.958	1.672	0.929	1.700	0.921	1.499	0.970
	2.200	1.086	2.188	1.072	2.172	1.058	2.120	1.034	2.068	1.028	2.164	1.034	2.200	1.034	1.940	1.005
	2.700	1.150	2.685	1.137	2.666	1.121	2.602	1.096	2.538	1.096	2.656	1.093	2.700	1.092	2.381	1.083
	3.200	1.131	3.182	1.150	3.160	1.136	3.084	1.118	3.008	1.122	3.148	1.112	3.200	1.108	2.822	1.120
	3.700	1.125	3.679	1.138	3.653	1.135	3.565	1.115	3.477	1.123	3.640	1.103	3.700	1.096	3.263	1.132
LC 30	1.750	0.990	1.740	0.977	1.728	0.957	1.686	0.923	1.645	0.934	1.722	0.906	1.750	0.897	1.543	0.945
	2.250	1.018	2.237	1.004	2.222	0.994	2.168	0.974	2.115	0.970	2.213	0.972	2.250	0.972	1.984	0.951
	2.750	1.066	2.735	1.055	2.715	1.038	2.650	1.014	2.585	1.014	2.705	1.012	2.750	1.011	2.425	1.006
	3.250	1.069	3.232	1.061	3.209	1.047	3.132	1.027	3.055	1.030	3.197	1.020	3.250	0.995	2.866	1.032
	3.750	1.046	3.729	1.043	3.703	1.036	3.614	1.019	3.524	1.027	3.689	0.967	3.750	1.001	3.307	1.016

Table C1.3: Data ($\lambda_{D.T}$ vs $M_{u.T}/M_{nD.T*}$) of the SCB lipped channel beams at room and elevated temperatures analysed in this work.
(*to be continued*)

Beam	100°C		200°C		300°C		400°C		500°C		600°C		700°C		800°C	
	$\lambda_{D.T}$	$\dfrac{M_{u.T}}{M_{nD.T*}}$	$\lambda_{D.T}$	$\dfrac{M_{u.T}}{M_{nD.T*}}$	$\lambda_{D.T}$	$\dfrac{M_{u.T}}{M_{nD.T*}}$	$\lambda_{D.T}$	$\dfrac{M_{u.T}}{M_{nD.T*}}$	$\lambda_{D.T}$	$\dfrac{M_{u.T}}{M_{nD.T*}}$	$\lambda_{D.T}$	$\dfrac{M_{u.T}}{M_{nD.T*}}$	$\lambda_{D.T}$	$\dfrac{M_{u.T}}{M_{nD.T*}}$	$\lambda_{D.T}$	$\dfrac{M_{u.T}}{M_{nD.T*}}$
LC 1	0.300	1.034	0.298	1.042	0.296	1.055	0.289	1.037	0.282	1.048	0.295	1.008	0.300	0.989	0.265	1.048
	0.800	1.029	0.796	1.026	0.790	1.045	0.771	1.100	0.752	1.099	0.787	1.091	0.800	1.088	0.706	1.081
	1.300	1.016	1.293	1.018	1.284	1.021	1.253	1.033	1.222	1.036	1.279	1.032	1.300	1.030	1.146	1.046
	1.800	0.983	1.790	0.986	1.777	0.980	1.735	0.987	1.692	0.986	1.771	1.005	1.800	1.011	1.587	0.979
	2.300	1.026	2.287	1.048	2.271	1.056	2.216	1.067	2.162	1.064	2.263	1.079	2.300	1.083	2.028	1.043
LC 2	0.350	1.034	0.348	1.049	0.346	1.076	0.337	1.099	0.329	1.104	0.344	1.082	0.350	1.068	0.309	1.101
	0.850	1.037	0.845	1.027	0.839	1.021	0.819	1.061	0.799	1.059	0.836	1.055	0.850	1.053	0.750	1.044
	1.350	0.983	1.342	0.977	1.333	0.973	1.301	0.982	1.269	0.986	1.328	0.981	1.350	0.979	1.191	0.998
	1.850	1.142	1.840	1.152	1.827	1.167	1.783	1.147	1.739	1.134	1.820	0.930	1.850	1.048	1.632	0.940
	2.350	0.996	2.337	1.086	2.320	1.158	2.265	1.205	2.209	1.241	2.312	1.106	2.350	1.084	2.073	0.941
LC 3	0.400	1.045	0.398	1.050	0.395	1.051	0.385	1.022	0.376	1.037	0.393	0.988	0.400	0.967	0.353	1.039
	0.900	1.078	0.895	1.062	0.889	1.044	0.867	1.071	0.846	1.060	0.885	1.068	0.900	1.068	0.794	1.052
	1.400	0.985	1.392	0.988	1.382	0.995	1.349	1.013	1.316	1.018	1.377	1.011	1.400	1.007	1.235	1.030
	1.900	1.086	1.889	1.081	1.876	1.075	1.831	1.056	1.786	1.044	1.869	1.063	1.900	1.069	1.676	1.006
	2.400	1.223	2.387	1.217	2.370	1.212	2.313	1.192	2.256	1.180	2.361	1.199	2.400	1.205	2.117	1.142
LC 4	0.450	1.046	0.447	1.054	0.444	1.068	0.434	1.033	0.423	1.050	0.443	0.994	0.450	0.971	0.397	1.050
	0.950	1.090	0.945	1.079	0.938	1.062	0.915	1.071	0.893	1.063	0.935	1.088	0.950	1.094	0.838	1.057
	1.450	1.000	1.442	1.000	1.432	1.003	1.397	1.016	1.363	1.021	1.426	1.013	1.450	1.010	1.279	1.032
	1.950	1.113	1.939	1.109	1.925	1.105	1.879	1.091	1.833	1.078	1.918	1.099	1.950	1.104	1.720	1.040
	2.450	1.249	2.436	1.245	2.419	1.240	2.361	1.220	2.303	1.207	2.410	1.228	2.450	1.234	2.161	1.168
LC 5	0.500	1.017	0.497	1.047	0.494	1.039	0.482	0.973	0.470	1.013	0.492	0.915	0.500	0.936	0.441	0.962
	1.000	1.109	0.994	1.099	0.987	1.086	0.964	1.096	0.940	1.089	0.984	1.111	1.000	1.118	0.882	1.081
	1.500	1.065	1.492	1.063	1.481	1.060	1.445	1.058	1.410	1.063	1.476	1.054	1.500	1.051	1.323	1.070
	2.000	1.070	1.989	1.062	1.975	1.054	1.927	1.058	1.880	1.046	1.967	1.068	2.000	1.073	1.764	1.042
	2.500	1.134	2.486	1.127	2.469	1.126	2.409	1.129	2.350	1.120	2.459	1.136	2.500	1.140	2.205	1.097
LC 6	0.550	1.026	0.547	1.045	0.543	1.052	0.530	1.017	0.517	1.033	0.541	0.979	0.550	0.959	0.485	1.032
	1.050	1.071	1.044	1.074	1.037	1.073	1.012	1.060	0.987	1.058	1.033	1.063	1.050	1.065	0.926	1.052
	1.550	0.982	1.541	0.980	1.531	0.979	1.494	0.989	1.457	0.994	1.525	0.986	1.550	0.983	1.367	1.010
	2.050	1.147	2.039	1.139	2.024	1.131	1.975	1.112	1.927	1.100	2.017	1.119	2.050	1.125	1.808	1.062
	2.550	1.264	2.536	1.265	2.518	1.233	2.457	1.228	2.397	1.229	2.509	1.250	2.550	1.257	2.249	1.191
LC 7	0.600	1.010	0.597	1.031	0.592	1.054	0.578	1.048	0.564	1.057	0.590	1.022	0.600	1.007	0.529	1.050
	1.100	1.042	1.094	1.052	1.086	1.056	1.060	1.054	1.034	1.054	1.082	1.055	1.100	1.055	0.970	1.049
	1.600	0.957	1.591	0.957	1.580	0.960	1.542	0.971	1.504	0.976	1.574	0.967	1.600	0.964	1.411	0.993
	2.100	1.085	2.088	1.086	2.074	1.089	2.024	1.083	1.974	1.069	2.066	1.093	2.100	1.100	1.852	1.031
	2.600	1.194	2.586	1.194	2.567	1.197	2.505	1.193	2.444	1.180	2.558	1.203	2.600	1.209	2.293	1.144
LC 8	0.650	1.016	0.646	1.040	0.642	1.069	0.626	1.076	0.611	1.083	0.639	1.054	0.650	1.041	0.573	1.071
	1.150	0.971	1.144	0.974	1.136	0.988	1.108	1.016	1.081	1.016	1.131	1.018	1.150	1.018	1.014	1.016
	1.650	0.937	1.641	0.935	1.629	0.944	1.590	0.939	1.551	0.945	1.623	0.977	1.650	0.984	1.455	0.938
	2.150	1.105	2.138	1.105	2.123	1.109	2.072	1.102	2.021	1.089	2.115	1.112	2.150	1.119	1.896	1.054
	2.650	1.204	2.635	1.211	2.617	1.216	2.554	1.212	2.491	1.199	2.607	1.222	2.650	1.228	2.337	1.161
LC 9	0.700	1.007	0.696	1.021	0.691	1.057	0.675	1.073	0.658	1.080	0.689	1.047	0.700	1.032	0.617	1.066
	1.200	1.041	1.193	1.043	1.185	1.047	1.156	1.057	1.128	1.059	1.180	1.056	1.200	1.055	1.058	1.060
	1.700	0.962	1.691	0.963	1.679	0.966	1.638	0.973	1.598	0.978	1.672	0.969	1.700	0.964	1.499	0.992
	2.200	1.005	2.188	1.005	2.172	1.012	2.120	1.021	2.068	1.010	2.164	1.031	2.200	1.036	1.940	0.985
	2.700	1.061	2.685	1.057	2.666	1.054	2.602	1.058	2.538	1.052	2.656	1.063	2.700	1.066	2.381	1.039
LC 10	0.750	1.022	0.746	1.021	0.741	1.048	0.723	1.077	0.705	1.082	0.738	1.056	0.750	1.045	0.661	1.061
	1.250	1.028	1.243	1.031	1.234	1.035	1.205	1.048	1.175	1.051	1.230	1.046	1.250	1.044	1.102	1.057
	1.750	0.961	1.740	0.962	1.728	0.971	1.686	0.973	1.645	0.967	1.722	0.984	1.750	0.991	1.543	0.979
	2.250	1.065	2.237	1.067	2.222	1.071	2.168	1.074	2.115	1.062	2.213	1.083	2.250	1.088	1.984	1.032
	2.750	1.131	2.735	1.128	2.715	1.129	2.650	1.133	2.585	1.124	2.705	1.141	2.750	1.145	2.425	1.103
LC 11	0.800	1.027	0.796	1.022	0.790	1.039	0.771	1.088	0.752	1.088	0.787	1.077	0.800	1.072	0.706	1.067
	1.300	1.004	1.293	1.007	1.284	1.011	1.253	1.025	1.222	1.028	1.279	1.024	1.300	1.021	1.146	1.036
	1.800	1.002	1.790	1.005	1.777	1.013	1.735	1.013	1.692	1.000	1.771	1.023	1.800	1.030	1.587	0.970
	2.300	1.109	2.287	1.109	2.271	1.113	2.216	1.115	2.162	1.104	2.263	1.124	2.300	1.129	2.028	1.073
	2.800	1.175	2.784	1.177	2.765	1.175	2.698	1.176	2.632	1.168	2.754	1.182	2.800	1.185	2.469	1.146
LC 12	0.850	1.047	0.845	1.038	0.839	1.039	0.819	1.092	0.799	1.090	0.836	1.084	0.850	1.082	0.750	1.068
	1.350	1.001	1.342	1.004	1.333	1.008	1.301	1.020	1.269	1.024	1.328	1.018	1.350	1.016	1.191	1.035
	1.850	0.981	1.840	0.975	1.827	0.986	1.783	0.994	1.739	0.983	1.820	1.005	1.850	1.011	1.632	0.966
	2.350	1.069	2.337	1.069	2.320	1.073	2.265	1.079	2.209	1.068	2.312	1.088	2.350	1.092	2.073	1.043
	2.850	1.122	2.834	1.120	2.814	1.117	2.746	1.120	2.679	1.114	2.804	1.125	2.850	1.127	2.513	1.099
LC 13	0.900	1.066	0.895	1.054	0.889	1.041	0.867	1.073	0.846	1.062	0.885	1.072	0.900	1.074	0.794	1.053
	1.400	0.982	1.392	0.985	1.382	0.992	1.349	1.006	1.316	1.011	1.377	1.004	1.400	1.001	1.235	1.025
	1.900	1.016	1.889	1.016	1.876	1.022	1.831	1.017	1.786	1.004	1.869	1.027	1.900	1.035	1.676	0.970
	2.400	1.130	2.387	1.131	2.370	1.135	2.313	1.132	2.256	1.119	2.361	1.142	2.400	1.148	2.117	1.084
	2.900	1.210	2.884	1.209	2.864	1.210	2.795	1.210	2.726	1.199	2.853	1.219	2.900	1.223	2.558	1.170
LC 14	0.950	1.071	0.945	1.064	0.938	1.051	0.915	1.061	0.893	1.053	0.935	1.077	0.950	1.085	0.838	1.048
	1.450	0.976	1.442	0.979	1.432	0.984	1.397	0.999	1.363	1.004	1.426	0.996	1.450	0.992	1.279	1.018
	1.950	1.023	1.939	1.023	1.925	1.028	1.879	1.025	1.833	1.011	1.918	1.035	1.950	1.042	1.720	0.977
	2.450	1.102	2.436	1.109	2.419	1.125	2.361	1.133	2.303	1.120	2.410	1.143	2.450	1.148	2.161	1.087
	2.950	1.202	2.934	1.201	2.913	1.202	2.843	1.203	2.773	1.194	2.902	1.211	2.950	1.214	2.602	1.167
LC 15	1.000	1.067	0.994	1.066	0.987	1.058	0.964	1.051	0.940	1.047	0.984	1.060	1.000	1.064	0.882	1.040
	1.500	0.959	1.492	0.968	1.481	0.972	1.445	0.986	1.410	0.991	1.476	0.983	1.500	0.980	1.323	1.007
	2.000	1.074	1.989	1.073	1.975	1.076	1.927	1.065	1.880	1.051	1.967	1.076	2.000	1.083	1.764	1.013
	2.500	1.197	2.486	1.200	2.469	1.201	2.409	1.194	2.350	1.180	2.459	1.204	2.500	1.210	2.205	1.140
	3.000	1.295	2.983	1.293	2.962	1.292	2.891	1.287	2.820	1.275	2.951	1.295	3.000	1.299	2.646	1.240
LC 16	1.050	1.046	1.044	1.048	1.037	1.048	1.012	1.048	0.987	1.045	1.033	1.054	1.050	1.056	0.926	1.039
	1.550	0.951	1.541	0.954	1.531	0.959	1.494	0.972	1.457	0.977	1.525	0.968	1.550	0.965	1.367	0.992
	2.050	0.985	2.039	0.988	2.024	0.994	1.975	0.998	1.927	0.987	2.017	1.008	2.050	1.014	1.808	0.958
	2.550	1.058	2.536	1.059	2.518	1.063	2.457	1.070	2.397	1.060	2.509	1.079	2.550	1.084	2.249	1.035
	3.050	1.102	3.033	1.100	3.012	1.097	2.939	1.099	2.867	1.094	3.000	1.102	3.050	1.103	2.690	1.082

Table C1.3: Data ($\lambda_{D,T}$ vs $M_{u,T}/M_{nD,T*}$) of the SCB lipped channel beams at room and elevated temperatures analysed in this work.
(*continuation*)

Beam	100°C $\lambda_{D.T}$	$\dfrac{M_{u.T}}{M_{nD.T*}}$	200°C $\lambda_{D.T}$	$\dfrac{M_{u.T}}{M_{nD.T*}}$	300°C $\lambda_{D.T}$	$\dfrac{M_{u.T}}{M_{nD.T*}}$	400°C $\lambda_{D.T}$	$\dfrac{M_{u.T}}{M_{nD.T*}}$	500°C $\lambda_{D.T}$	$\dfrac{M_{u.T}}{M_{nD.T*}}$	600°C $\lambda_{D.T}$	$\dfrac{M_{u.T}}{M_{nD.T*}}$	700°C $\lambda_{D.T}$	$\dfrac{M_{u.T}}{M_{nD.T*}}$	800°C $\lambda_{D.T}$	$\dfrac{M_{u.T}}{M_{nD.T*}}$
LC 17	1.100	1.043	1.094	1.046	1.086	1.051	1.060	1.051	1.034	1.051	1.082	1.053	1.100	1.054	0.970	1.047
	1.600	0.951	1.591	0.954	1.580	0.958	1.542	0.969	1.504	0.975	1.574	0.966	1.600	0.962	1.411	0.989
	2.100	1.010	2.088	1.012	2.074	1.018	2.024	1.022	1.974	1.010	2.066	1.032	2.100	1.038	1.852	0.980
	2.600	1.083	2.586	1.083	2.567	1.087	2.505	1.093	2.444	1.083	2.558	1.102	2.600	1.107	2.293	1.058
	3.100	1.116	3.083	1.121	3.061	1.119	2.987	1.120	2.914	1.117	3.050	1.123	3.100	1.124	2.734	1.104
LC 18	1.150	1.028	1.144	1.031	1.136	1.037	1.108	1.045	1.081	1.047	1.131	1.046	1.150	1.045	1.014	1.045
	1.650	0.944	1.641	0.944	1.629	0.949	1.590	0.957	1.551	0.962	1.623	0.959	1.650	0.966	1.455	0.977
	2.150	1.055	2.138	1.057	2.123	1.061	2.072	1.063	2.021	1.050	2.115	1.072	2.150	1.079	1.896	1.018
	2.650	1.140	2.635	1.138	2.617	1.140	2.554	1.142	2.491	1.131	2.607	1.151	2.650	1.155	2.337	1.104
	3.150	1.191	3.132	1.188	3.110	1.184	3.035	1.181	2.961	1.177	3.099	1.183	3.150	1.183	2.778	1.160
LC 19	1.200	1.030	1.193	1.033	1.185	1.038	1.156	1.049	1.128	1.051	1.180	1.048	1.200	1.047	1.058	1.052
	1.700	0.955	1.691	0.956	1.679	0.958	1.638	0.965	1.598	0.970	1.672	0.961	1.700	0.962	1.499	0.983
	2.200	1.016	2.188	1.016	2.172	1.022	2.120	1.030	2.068	1.019	2.164	1.040	2.200	1.045	1.940	0.994
	2.700	1.074	2.685	1.071	2.666	1.070	2.602	1.074	2.538	1.068	2.656	1.080	2.700	1.082	2.381	1.052
	3.200	1.089	3.182	1.085	3.160	1.082	3.084	1.078	3.008	1.079	3.148	1.077	3.200	1.074	2.822	1.077
LC 20	1.250	1.017	1.243	1.020	1.234	1.024	1.205	1.038	1.175	1.041	1.230	1.037	1.250	1.034	1.102	1.049
	1.750	0.962	1.740	0.957	1.728	0.956	1.686	0.969	1.645	0.965	1.722	0.987	1.750	0.994	1.543	0.971
	2.250	1.064	2.237	1.067	2.222	1.077	2.168	1.084	2.115	1.072	2.213	1.093	2.250	1.099	1.984	1.040
	2.750	1.146	2.735	1.145	2.715	1.148	2.650	1.152	2.585	1.143	2.705	1.160	2.750	1.164	2.425	1.118
	3.250	1.180	3.232	1.180	3.209	1.176	3.132	1.175	3.055	1.173	3.197	1.176	3.250	1.175	2.866	1.162
LC 21	1.300	0.975	1.293	0.976	1.284	0.982	1.253	1.001	1.222	1.003	1.279	1.002	1.300	1.000	1.146	1.010
	1.800	0.983	1.790	0.988	1.777	0.996	1.735	0.995	1.692	0.983	1.771	1.004	1.800	1.011	1.587	0.955
	2.300	1.089	2.287	1.091	2.271	1.096	2.216	1.097	2.162	1.085	2.263	1.107	2.300	1.113	2.028	1.054
	2.800	1.159	2.784	1.159	2.765	1.162	2.698	1.166	2.632	1.157	2.754	1.174	2.800	1.178	2.469	1.132
	3.300	1.197	3.282	1.194	3.258	1.191	3.180	1.188	3.102	1.186	3.246	1.188	3.300	1.188	2.910	1.175
LC 22	1.350	0.988	1.342	0.992	1.333	0.997	1.301	1.010	1.269	1.013	1.328	1.009	1.350	1.006	1.191	1.025
	1.850	1.009	1.840	1.012	1.827	1.019	1.783	1.018	1.739	1.005	1.820	1.028	1.850	1.035	1.632	0.975
	2.350	1.112	2.337	1.113	2.320	1.117	2.265	1.119	2.209	1.107	2.312	1.127	2.350	1.133	2.073	1.077
	2.850	1.184	2.834	1.180	2.814	1.177	2.746	1.178	2.679	1.170	2.804	1.184	2.850	1.187	2.513	1.148
	3.350	1.207	3.331	1.205	3.308	1.199	3.228	1.192	3.149	1.193	3.296	1.189	3.350	1.186	2.954	1.187
LC 23	1.400	0.987	1.392	0.991	1.382	0.995	1.349	1.006	1.316	1.011	1.377	1.004	1.400	1.001	1.235	1.021
	1.900	0.984	1.889	0.988	1.876	0.997	1.831	0.999	1.786	0.988	1.869	1.009	1.900	1.016	1.676	0.959
	2.400	1.072	2.387	1.073	2.370	1.077	2.313	1.083	2.256	1.072	2.361	1.092	2.400	1.096	2.117	1.046
	2.900	1.125	2.884	1.122	2.864	1.120	2.795	1.122	2.726	1.117	2.853	1.128	2.900	1.130	2.558	1.101
	3.400	1.135	3.381	1.132	3.357	1.129	3.276	1.125	3.196	1.127	3.345	1.122	3.400	1.119	2.999	1.125
LC 24	1.450	0.963	1.442	0.959	1.432	0.957	1.397	0.970	1.363	0.972	1.426	0.971	1.450	0.970	1.279	0.981
	1.950	1.028	1.939	1.030	1.925	1.037	1.879	1.037	1.833	1.025	1.918	1.047	1.950	1.053	1.720	0.995
	2.450	1.129	2.436	1.130	2.419	1.134	2.361	1.133	2.303	1.121	2.410	1.141	2.450	1.147	2.161	1.091
	2.950	1.191	2.934	1.191	2.913	1.192	2.843	1.194	2.773	1.186	2.902	1.201	2.950	1.204	2.602	1.163
	3.450	1.233	3.431	1.226	3.407	1.218	3.325	1.214	3.243	1.201	3.394	1.214	3.450	1.213	3.043	1.204
LC 25	1.500	0.986	1.492	0.988	1.481	0.992	1.445	1.004	1.410	1.009	1.476	1.000	1.500	0.996	1.323	1.022
	2.000	1.023	1.989	1.026	1.975	1.032	1.927	1.033	1.880	1.020	1.967	1.042	2.000	1.049	1.764	0.987
	2.500	1.114	2.486	1.114	2.469	1.117	2.409	1.118	2.350	1.107	2.459	1.126	2.500	1.131	2.205	1.080
	3.000	1.171	2.983	1.171	2.962	1.167	2.891	1.169	2.820	1.162	2.951	1.173	3.000	1.176	2.646	1.142
	3.500	1.202	3.481	1.199	3.456	1.193	3.373	1.188	3.290	1.188	3.443	1.186	3.500	1.183	3.087	1.175
LC 26	1.550	1.014	1.541	1.013	1.531	1.014	1.494	1.020	1.457	1.025	1.525	1.016	1.550	1.012	1.367	1.038
	2.050	1.032	2.039	1.029	2.024	1.032	1.975	1.037	1.927	1.026	2.017	1.046	2.050	1.051	1.808	0.997
	2.550	1.119	2.536	1.113	2.518	1.110	2.457	1.110	2.397	1.100	2.509	1.119	2.550	1.090	2.249	1.074
	3.050	1.123	3.033	1.130	3.012	1.142	2.939	1.146	2.867	1.150	3.000	1.159	3.050	1.161	2.690	1.110
	3.550	1.048	3.530	1.055	3.505	1.071	3.421	1.114	3.336	1.149	3.492	1.163	3.550	1.160	3.131	1.163
LC 27	1.600	0.980	1.591	0.970	1.580	0.960	1.542	0.950	1.504	0.942	1.574	0.957	1.600	0.961	1.411	0.941
	2.100	1.092	2.088	1.091	2.074	1.081	2.024	1.057	1.974	1.048	2.066	1.063	2.100	1.069	1.852	1.021
	2.600	1.231	2.586	1.218	2.567	1.201	2.505	1.167	2.444	1.111	2.558	1.171	2.600	1.176	2.293	1.128
	3.100	1.298	3.083	1.311	3.061	1.297	2.987	1.259	2.914	1.252	3.050	1.260	3.100	1.262	2.734	1.224
	3.600	1.386	3.580	1.378	3.555	1.361	3.469	1.324	3.383	1.322	3.541	1.318	3.600	1.316	3.175	1.301
LC 28	1.650	0.967	1.641	0.973	1.629	0.967	1.590	0.966	1.551	0.967	1.623	0.980	1.650	0.985	1.455	0.976
	2.150	1.106	2.138	1.100	2.123	1.094	2.072	1.077	2.021	1.067	2.115	1.083	2.150	1.088	1.896	1.039
	2.650	1.225	2.635	1.219	2.617	1.203	2.554	1.174	2.491	1.167	2.607	1.177	2.650	1.182	2.337	1.139
	3.150	1.147	3.132	1.295	3.110	1.281	3.035	1.250	2.961	1.245	3.099	1.250	3.150	1.251	2.778	1.221
	3.650	1.201	3.630	1.249	3.604	1.290	3.517	1.280	3.430	1.293	3.591	1.281	3.650	1.276	3.219	1.284
LC 29	1.700	1.034	1.691	1.031	1.679	1.027	1.638	1.022	1.598	1.026	1.672	1.018	1.700	1.015	1.499	1.035
	2.200	1.086	2.188	1.082	2.172	1.083	2.120	1.086	2.068	1.075	2.164	1.095	2.200	1.101	1.940	1.048
	2.700	1.150	2.685	1.144	2.666	1.140	2.602	1.135	2.538	1.131	2.656	1.139	2.700	1.141	2.381	1.116
	3.200	1.131	3.182	1.155	3.160	1.151	3.084	1.148	3.008	1.149	3.148	1.148	3.200	1.146	2.822	1.145
	3.700	1.125	3.679	1.142	3.653	1.146	3.565	1.139	3.477	1.145	3.640	1.131	3.700	1.126	3.263	1.152
LC 30	1.750	0.990	1.740	0.990	1.728	0.990	1.686	0.992	1.645	0.997	1.722	0.988	1.750	0.983	1.543	1.005
	2.250	1.018	2.237	1.012	2.222	1.016	2.168	1.021	2.115	1.012	2.213	1.028	2.250	1.032	1.984	0.989
	2.750	1.066	2.735	1.061	2.715	1.054	2.650	1.049	2.585	1.045	2.705	1.053	2.750	1.055	2.425	1.035
	3.250	1.069	3.232	1.066	3.209	1.060	3.132	1.054	3.055	1.055	3.197	1.052	3.250	1.028	2.866	1.054
	3.750	1.046	3.729	1.047	3.703	1.046	3.614	1.040	3.524	1.046	3.689	0.991	3.750	1.028	3.307	1.034

Table C2.1: Data ($\lambda_{D.T}$ vs $M_{u.T}/M_{y.T}$) of the SCB lipped channel beams at room and elevated temperatures reported by Landesmann & Camotim (2016).

100°C		200°C		300°C		400°C		500°C		600°C		700°C		800°C	
$\lambda_{D.T}$	$\dfrac{M_{u.T}}{M_{y.T}}$	$\lambda_{D.T}$	$\dfrac{M_{u.T}}{M_{y.T}}$	$\lambda_{D.T}$	$\dfrac{M_{u.T}}{M_{y.T}}$	$\lambda_{D.T}$	$\dfrac{M_{u.T}}{M_{y.T}}$	$\lambda_{D.T}$	$\dfrac{M_{u.T}}{M_{y.T}}$	$\lambda_{D.T}$	$\dfrac{M_{u.T}}{M_{y.T}}$	$\lambda_{D.T}$	$\dfrac{M_{u.T}}{M_{y.T}}$	$\lambda_{D.T}$	$\dfrac{M_{u.T}}{M_{y.T}}$
0.510	1.037	0.507	0.977	0.503	0.904	0.491	0.824	0.479	0.845	0.501	0.797	0.510	0.783	0.449	0.869
1.005	0.778	0.999	0.755	0.992	0.713	0.968	0.660	0.945	0.685	0.989	0.630	1.005	0.612	0.886	0.728
1.519	0.439	1.511	0.437	1.500	0.432	1.464	0.432	1.428	0.451	1.495	0.415	1.519	0.403	1.340	0.496
2.010	0.306	1.999	0.305	1.985	0.303	1.937	0.306	1.889	0.315	1.977	0.298	2.010	0.292	1.773	0.339
2.548	0.235	2.534	0.235	2.516	0.235	2.456	0.240	2.395	0.247	2.507	0.232	2.548	0.228	2.247	0.266
3.063	0.182	3.046	0.183	3.024	0.183	2.951	0.189	2.878	0.196	3.013	0.182	3.063	0.178	2.701	0.215
3.398	0.158	3.379	0.159	3.355	0.160	3.274	0.165	3.193	0.172	3.342	0.160	3.398	0.156	2.996	0.188
0.255	1.093	0.529	0.950	0.525	0.860	0.512	0.769	0.500	0.793	0.523	0.737	0.531	0.721	0.469	0.821
0.750	0.959	1.121	0.644	1.113	0.620	1.086	0.589	1.060	0.617	1.109	0.558	1.127	0.540	0.994	0.665
1.248	0.586	1.629	0.436	1.617	0.427	1.578	0.416	1.540	0.427	1.611	0.405	1.638	0.397	1.445	0.448
1.749	0.360	2.147	0.351	2.132	0.347	2.080	0.346	2.029	0.357	2.124	0.335	2.159	0.328	1.904	0.378
2.247	0.271	2.695	0.277	2.676	0.275	2.611	0.278	2.547	0.289	2.666	0.269	2.710	0.263	2.390	0.312
2.752	0.213	3.215	0.244	3.192	0.243	3.115	0.247	3.038	0.255	3.180	0.239	3.233	0.234	2.851	0.274
3.246	0.170	3.774	0.198	3.748	0.199	3.657	0.204	3.567	0.212	3.734	0.197	3.795	0.191	3.347	0.232
0.266	1.076	0.517	0.961	0.513	0.866	0.501	0.765	0.488	0.791	0.511	0.732	0.520	0.715	0.458	0.820
0.806	0.931	0.976	0.785	0.970	0.729	0.946	0.648	0.923	0.678	0.966	0.612	0.982	0.593	0.866	0.719
1.350	0.519	1.513	0.429	1.502	0.423	1.466	0.423	1.430	0.443	1.496	0.404	1.521	0.392	1.342	0.490
1.887	0.398	2.048	0.316	2.034	0.313	1.985	0.313	1.936	0.323	2.026	0.304	2.060	0.298	1.816	0.344
2.430	0.327	2.509	0.268	2.491	0.267	2.431	0.269	2.371	0.278	2.482	0.262	2.523	0.257	2.225	0.295
2.969	0.273	3.025	0.216	3.004	0.215	2.932	0.218	2.859	0.225	2.993	0.211	3.042	0.205	2.683	0.244
3.509	0.230	3.493	0.182	3.469	0.182	3.385	0.186	3.302	0.194	3.456	0.180	3.513	0.175	3.098	0.211
0.531	1.025	0.495	0.981	0.491	0.890	0.479	0.793	0.468	0.817	0.489	0.760	0.498	0.743	0.439	0.846
1.127	0.657	1.024	0.758	1.017	0.715	0.992	0.644	0.968	0.672	1.013	0.610	1.030	0.591	0.908	0.718
1.638	0.441	1.508	0.448	1.497	0.441	1.461	0.437	1.425	0.458	1.491	0.418	1.516	0.406	1.337	0.506
2.159	0.354	2.005	0.339	1.991	0.336	1.943	0.336	1.895	0.345	1.984	0.328	2.016	0.321	1.778	0.364
2.710	0.278	2.509	0.277	2.491	0.276	2.431	0.278	2.371	0.285	2.482	0.271	2.523	0.267	2.225	0.303
3.233	0.244	2.986	0.234	2.965	0.234	2.894	0.237	2.822	0.243	2.954	0.231	3.003	0.226	2.648	0.259
3.795	0.197	3.498	0.198	3.474	0.198	3.390	0.201	3.306	0.207	3.461	0.196	3.518	0.191	3.102	0.222
0.241	1.098	0.506	1.010	0.503	0.936	0.491	0.847	0.479	0.871	0.501	0.813	0.509	0.806	0.449	0.851
0.748	0.973	0.992	0.796	0.985	0.743	0.961	0.681	0.937	0.705	0.981	0.649	0.997	0.634	0.879	0.751
1.242	0.588	1.498	0.482	1.487	0.473	1.452	0.466	1.416	0.487	1.482	0.447	1.506	0.433	1.329	0.535
1.745	0.370	1.988	0.330	1.974	0.327	1.927	0.327	1.879	0.340	1.967	0.317	2.000	0.311	1.763	0.372
2.248	0.301	2.490	0.254	2.472	0.253	2.412	0.257	2.353	0.265	2.463	0.251	2.504	0.246	2.208	0.285
2.749	0.250	2.996	0.202	2.975	0.202	2.903	0.207	2.832	0.214	2.964	0.201	3.013	0.197	2.657	0.232
3.248	0.213	3.490	0.162	3.466	0.163	3.382	0.167	3.299	0.174	3.453	0.161	3.510	0.158	3.095	0.192
0.520	1.036														
0.982	0.811														
1.521	0.431														
2.060	0.319														
2.523	0.269														
3.042	0.217														
3.513	0.182														
0.230	1.116														
0.740	0.982														
1.247	0.600														
1.749	0.383														
2.249	0.311														
2.748	0.256														
3.249	0.216														
0.498	1.055														
1.030	0.779														
1.516	0.453														
2.016	0.341														
2.523	0.278														
3.003	0.235														
3.518	0.198														
0.232	1.154														
0.750	0.983														
1.247	0.631														
1.749	0.396														
2.249	0.289														
2.748	0.228														
3.249	0.182														
0.509	1.073														
0.997	0.828														
1.506	0.487														
2.000	0.332														
2.504	0.255														
3.013	0.203														
3.510	0.161														

Table C2.2: Data ($\lambda_{D.T}$ vs $M_{u.T}/M_{nD.T}$) of the SCB lipped channel beams at room and elevated temperatures reported by Landesmann & Camotim (2016).

100°C		200°C		300°C		400°C		500°C		600°C		700°C		800°C	
$\lambda_{D.T}$	$\dfrac{M_{u.T}}{M_{nD.T}}$	$\lambda_{D.T}$	$\dfrac{M_{u.T}}{M_{nD.T}}$	$\lambda_{D.T}$	$\dfrac{M_{u.T}}{M_{nD.T}}$	$\lambda_{D.T}$	$\dfrac{M_{u.T}}{M_{nD.T}}$	$\lambda_{D.T}$	$\dfrac{M_{u.T}}{M_{nD.T}}$	$\lambda_{D.T}$	$\dfrac{M_{u.T}}{M_{nD.T}}$	$\lambda_{D.T}$	$\dfrac{M_{u.T}}{M_{nD.T}}$	$\lambda_{D.T}$	$\dfrac{M_{u.T}}{M_{nD.T}}$
0.510	1.012	0.507	0.953	0.503	0.881	0.491	0.802	0.479	0.821	0.501	0.777	0.510	0.764	0.449	0.840
1.005	1.042	0.999	1.006	0.992	0.944	0.968	0.852	0.945	0.865	0.989	0.831	1.005	0.820	0.886	0.867
1.519	0.955	1.511	0.943	1.500	0.924	1.464	0.895	1.428	0.905	1.495	0.883	1.519	0.876	1.340	0.920
2.010	0.967	1.999	0.955	1.985	0.939	1.937	0.919	1.889	0.913	1.977	0.920	2.010	0.922	1.773	0.902
2.548	1.033	2.534	1.025	2.516	1.014	2.456	1.001	2.395	0.997	2.507	0.999	2.548	1.003	2.247	0.980
3.063	1.041	3.046	1.038	3.024	1.033	2.951	1.026	2.878	1.029	3.013	1.022	3.063	1.019	2.701	1.028
3.398	1.056	3.379	1.051	3.355	1.047	3.274	1.043	3.193	1.045	3.342	1.041	3.398	1.040	2.996	1.044
0.255	1.026	0.529	0.933	0.525	0.844	0.512	0.754	0.500	0.776	0.523	0.724	0.531	0.708	0.469	0.801
0.750	1.016	1.121	0.969	1.113	0.926	1.086	0.857	1.060	0.873	1.109	0.830	1.127	0.818	0.994	0.882
1.248	0.998	1.629	1.038	1.617	1.007	1.578	0.950	1.540	0.944	1.611	0.951	1.638	0.950	1.445	0.913
1.749	0.942	2.147	1.213	2.132	1.188	2.080	1.146	2.029	1.141	2.124	1.142	2.159	1.145	1.904	1.108
2.247	1.000	2.695	1.322	2.676	1.299	2.611	1.269	2.547	1.270	2.666	1.265	2.710	1.263	2.390	1.255
2.752	1.049	3.215	1.498	3.192	1.478	3.115	1.451	3.038	1.448	3.180	1.449	3.233	1.449	2.851	1.415
3.246	1.059	3.774	1.539	3.748	1.529	3.657	1.514	3.567	1.520	3.734	1.506	3.795	1.500	3.347	1.517
0.266	1.024	0.517	0.938	0.513	0.845	0.501	0.746	0.488	0.769	0.511	0.715	0.520	0.699	0.458	0.794
0.806	1.030	0.976	1.022	0.970	0.943	0.946	0.819	0.923	0.837	0.966	0.789	0.982	0.776	0.866	0.840
1.350	0.971	1.513	0.926	1.502	0.907	1.466	0.878	1.430	0.891	1.496	0.862	1.521	0.853	1.342	0.910
1.887	1.151	2.048	1.025	2.034	1.003	1.985	0.970	1.936	0.967	2.026	0.970	2.060	0.973	1.816	0.946
2.430	1.346	2.509	1.154	2.491	1.137	2.431	1.110	2.371	1.104	2.482	1.113	2.523	1.116	2.225	1.071
2.969	1.495	3.025	1.218	3.004	1.198	2.932	1.171	2.859	1.169	2.993	1.168	3.042	1.167	2.683	1.155
3.509	1.610	3.493	1.265	3.469	1.252	3.385	1.236	3.302	1.240	3.456	1.229	3.513	1.225	3.098	1.230
0.531	1.007	0.495	0.950	0.491	0.862	0.479	0.766	0.468	0.788	0.489	0.736	0.498	0.721	0.439	0.812
1.127	0.994	1.024	1.036	1.017	0.970	0.992	0.852	0.968	0.868	1.013	0.824	1.030	0.812	0.908	0.874
1.638	1.056	1.508	0.964	1.497	0.939	1.461	0.903	1.425	0.916	1.491	0.887	1.516	0.879	1.337	0.936
2.159	1.234	2.005	1.066	1.991	1.046	1.943	1.012	1.895	1.005	1.984	1.016	2.016	1.019	1.778	0.974
2.710	1.337	2.509	1.193	2.491	1.176	2.431	1.146	2.371	1.134	2.482	1.150	2.523	1.157	2.225	1.102
3.233	1.514	2.986	1.296	2.965	1.280	2.894	1.250	2.822	1.240	2.954	1.256	3.003	1.261	2.648	1.204
3.795	1.545	3.498	1.377	3.474	1.363	3.390	1.339	3.306	1.329	3.461	1.342	3.518	1.343	3.102	1.298
0.241	1.030	0.503	0.972	0.503	0.901	0.491	0.813	0.479	0.833	0.501	0.781	0.509	0.776	0.449	0.809
0.748	1.030	0.985	1.052	0.985	0.976	0.961	0.873	0.937	0.883	0.981	0.849	0.997	0.843	0.879	0.889
1.242	0.995	1.487	1.029	1.487	1.000	1.452	0.956	1.416	0.967	1.482	0.940	1.506	0.931	1.329	0.981
1.745	0.965	1.974	1.027	1.974	1.006	1.927	0.974	1.879	0.979	1.967	0.971	2.000	0.976	1.763	0.984
2.248	1.111	2.472	1.081	2.472	1.065	2.412	1.048	2.353	1.041	2.463	1.053	2.504	1.058	2.208	1.025
2.749	1.227	2.975	1.124	2.975	1.112	2.903	1.099	2.832	1.096	2.964	1.102	3.013	1.103	2.657	1.083
3.248	1.331	3.466	1.125	3.466	1.118	3.382	1.106	3.299	1.113	3.453	1.099	3.510	1.103	3.095	1.115
0.520	1.013														
0.982	1.062														
1.521	0.939														
2.060	1.042														
2.523	1.167														
3.042	1.230														
3.513	1.273														
0.230	1.034														
0.740	1.034														
1.247	1.021														
1.749	1.002														
2.249	1.146														
2.748	1.255														
3.249	1.352														
0.498	1.023														
1.030	1.070														
1.516	0.981														
2.016	1.082														
2.523	1.206														
3.003	1.309														
3.518	1.388														
0.232	1.046														
0.750	1.041														
1.247	1.073														
1.749	1.036														
2.249	1.067														
2.748	1.117														
3.249	1.138														
0.509	1.034														
0.997	1.100														
1.506	1.047														
2.000	1.041														
2.504	1.094														
3.013	1.135														
3.510	1.128														

Table C2.3: Data ($\lambda_{D.T}$ vs $M_{u.T}/M_{nD.T*}$) of the SCB lipped channel beams at room and elevated temperatures reported by Landesmann & Camotim (2016).

100°C		200°C		300°C		400°C		500°C		600°C		700°C		800°C	
$\lambda_{D.T}$	$\dfrac{M_{u.T}}{M_{nD.T*}}$	$\lambda_{D.T}$	$\dfrac{M_{u.T}}{M_{nD.T*}}$	$\lambda_{D.T}$	$\dfrac{M_{u.T}}{M_{nD.T*}}$	$\lambda_{D.T}$	$\dfrac{M_{u.T}}{M_{nD.T*}}$	$\lambda_{D.T}$	$\dfrac{M_{u.T}}{M_{nD.T*}}$	$\lambda_{D.T}$	$\dfrac{M_{u.T}}{M_{nD.T*}}$	$\lambda_{D.T}$	$\dfrac{M_{u.T}}{M_{nD.T*}}$	$\lambda_{D.T}$	$\dfrac{M_{u.T}}{M_{nD.T*}}$
0.510	1.014	0.507	1.038	0.503	1.065	0.491	1.059	0.479	1.066	0.501	1.035	0.510	1.022	0.449	1.058
1.005	1.042	0.999	1.042	0.992	1.040	0.968	1.058	0.945	1.050	0.989	1.075	1.005	1.082	0.886	1.045
1.519	0.956	1.511	0.960	1.500	0.967	1.464	0.984	1.428	0.986	1.495	0.988	1.519	0.989	1.340	0.998
2.010	0.969	1.999	0.966	1.985	0.966	1.937	0.974	1.889	0.963	1.977	0.986	2.010	0.993	1.773	0.949
2.548	1.035	2.534	1.033	2.516	1.035	2.456	1.042	2.395	1.033	2.507	1.047	2.548	1.055	2.247	1.014
3.063	1.043	3.046	1.045	3.024	1.048	2.951	1.057	2.878	1.057	3.013	1.058	3.063	1.057	2.701	1.055
3.398	1.057	3.379	1.057	3.355	1.060	3.274	1.070	3.193	1.070	3.342	1.073	3.398	1.073	2.996	1.067
0.255	1.028	0.529	1.019	0.525	1.032	0.512	1.028	0.500	1.035	0.523	1.006	0.531	0.995	0.469	1.029
0.750	1.011	1.121	0.997	1.113	1.001	1.086	1.014	1.060	1.016	1.109	1.014	1.127	1.014	0.994	1.019
1.248	1.000	1.629	1.054	1.617	1.048	1.578	1.033	1.540	1.017	1.611	1.049	1.638	1.056	1.445	0.980
1.749	0.943	2.147	1.226	2.132	1.219	2.080	1.207	2.029	1.196	2.124	1.214	2.159	1.222	1.904	1.158
2.247	1.001	2.695	1.332	2.676	1.323	2.611	1.316	2.547	1.312	2.666	1.319	2.710	1.321	2.390	1.294
2.752	1.051	3.215	1.507	3.192	1.498	3.115	1.492	3.038	1.484	3.180	1.496	3.233	1.499	2.851	1.448
3.246	1.061	3.774	1.547	3.748	1.545	3.657	1.547	3.567	1.549	3.734	1.544	3.795	1.541	3.347	1.544
0.266	1.025	0.517	1.023	0.513	1.023	0.501	0.989	0.488	1.003	0.511	0.958	0.520	0.941	0.458	1.003
0.806	1.027	0.976	1.060	0.970	1.044	0.946	1.029	0.923	1.027	0.966	1.036	0.982	1.040	0.866	1.023
1.350	0.973	1.513	0.943	1.502	0.949	1.466	0.966	1.430	0.971	1.496	0.964	1.521	0.962	1.342	0.986
1.887	1.154	2.048	1.036	2.034	1.031	1.985	1.026	1.936	1.018	2.026	1.037	2.060	1.044	1.816	0.992
2.430	1.348	2.509	1.164	2.491	1.160	2.431	1.156	2.371	1.145	2.482	1.167	2.523	1.174	2.225	1.109
2.969	1.498	3.025	1.226	3.004	1.216	2.932	1.207	2.859	1.202	2.993	1.209	3.042	1.211	2.683	1.185
3.509	1.613	3.493	1.272	3.469	1.268	3.385	1.266	3.302	1.267	3.456	1.264	3.513	1.263	3.098	1.256
0.531	1.009	0.495	1.033	0.491	1.031	0.479	0.985	0.468	1.002	0.489	0.946	0.498	0.926	0.439	1.003
1.127	0.995	1.024	1.071	1.017	1.064	0.992	1.046	0.968	1.044	1.013	1.052	1.030	1.056	0.908	1.043
1.638	1.058	1.508	0.982	1.497	0.983	1.461	0.994	1.425	0.999	1.491	0.993	1.516	0.992	1.337	1.015
2.159	1.236	2.005	1.079	1.991	1.077	1.943	1.073	1.895	1.059	1.984	1.088	2.016	1.097	1.778	1.024
2.710	1.340	2.509	1.203	2.491	1.200	2.431	1.193	2.371	1.177	2.482	1.206	2.523	1.217	2.225	1.140
3.233	1.516	2.986	1.304	2.965	1.300	2.894	1.289	2.822	1.275	2.954	1.302	3.003	1.311	2.648	1.236
3.795	1.547	3.498	1.384	3.474	1.380	3.390	1.371	3.306	1.358	3.461	1.380	3.518	1.384	3.102	1.324
0.241	1.031	0.503	1.052	0.503	1.062	0.491	0.999	0.479	1.022	0.501	0.946	0.509	0.931	0.449	0.969
0.748	1.024	0.985	1.090	0.985	1.077	0.961	1.088	0.937	1.075	0.981	1.104	0.997	1.118	0.879	1.075
1.242	0.997	1.487	1.047	1.487	1.047	1.452	1.053	1.416	1.055	1.482	1.053	1.506	1.053	1.329	1.066
1.745	0.966	1.974	1.040	1.974	1.036	1.927	1.034	1.879	1.033	1.967	1.041	2.000	1.051	1.763	1.035
2.248	1.113	2.472	1.090	2.472	1.087	2.412	1.091	2.353	1.081	2.463	1.104	2.504	1.114	2.208	1.061
2.749	1.229	2.975	1.132	2.975	1.130	2.903	1.133	2.832	1.126	2.964	1.142	3.013	1.146	2.657	1.111
3.248	1.333	3.466	1.131	3.466	1.132	3.382	1.133	3.299	1.137	3.453	1.131	3.510	1.137	3.095	1.139
0.520	1.015														
0.982	1.061														
1.521	0.941														
2.060	1.044														
2.523	1.169														
3.042	1.232														
3.513	1.275														
0.230	1.036														
0.740	1.027														
1.247	1.022														
1.749	1.004														
2.249	1.148														
2.748	1.257														
3.249	1.354														
0.498	1.026														
1.030	1.070														
1.516	0.982														
2.016	1.084														
2.523	1.208														
3.003	1.311														
3.518	1.390														
0.232	1.047														
0.750	1.035														
1.247	1.075														
1.749	1.038														
2.249	1.069														
2.748	1.118														
3.249	1.140														
0.509	1.037														
0.997	1.100														
1.506	1.049														
2.000	1.043														
2.504	1.096														
3.013	1.137														
3.510	1.130														